AD_____

Award Number: DAMD17-97-1-7211

TITLE: Cell-Cell Adhesion and Insulin-Like Growth Factor I Receptor in Breast Cancer

PRINCIPAL INVESTIGATOR: Monica Bartucci, Ph.D.
Ewa Surmacz

CONTRACTING ORGANIZATION: Thomas Jefferson University
Philadelphia, Pennsylvania 19107-5541

REPORT DATE: September 2001

TYPE OF REPORT: Final

PREPARED FOR: U.S. Army Medical Research and Materiel Command
Fort Detrick, Maryland 21702-5012

REPORT DOCUMENTATION PAGE

Form Approved
OMB No. 074-0188

1. AGENCY USE ONLY (Leave blank)	2. REPORT DATE	3. REPORT TYPE AND DATES COVERED
	September 2001	Final (15 Aug 97 - 14 Aug 01)

4. TITLE AND SUBTITLE
Cell-Cell Adhesion and Insulin-Like Growth Factor I Receptor in Breast Cancer

5. FUNDING NUMBERS
DAMD17-97-1-7211

6. AUTHOR(S)
Monica Bartucci, Ph.D.
Ewa Surmacz

7. PERFORMING ORGANIZATION NAME(S) AND ADDRESS(ES)
Thomas Jefferson University
Philadelphia, Pennsylvania 19107 -5541

E-Mail: Monica.Bartucci@mail.tju.edu

8. PERFORMING ORGANIZATION REPORT NUMBER

9. SPONSORING / MONITORING AGENCY NAME(S) AND ADDRESS(ES)
U.S. Army Medical Research and Materiel Command
Fort Detrick, Maryland 21702-5012

10. SPONSORING / MONITORING AGENCY REPORT NUMBER

11. SUPPLEMENTARY NOTES

12a. DISTRIBUTION / AVAILABILITY STATEMENT
Approved for Public Release; Distribution Unlimited

12b. DISTRIBUTION CODE

13. Abstract ***(Maximum 200 Words)*** *(abstract should contain no proprietary or confidential information)*

This is a final report of the research carried out between 8/15/1997 and 8/14/2001. Our goal was to study the role of the insulin-like growth factor I receptor (IGF-IR) in breast cancer. The IGF-IR is a multifunctional tyrosine kinase that has been recently implicated in breast tumor development and progression. The IGF-IR is often overexpressed in estrogen receptor (ER)-positive breast tumors and this feature predicts enhanced tumor drug- and radio-resistance and cancer recurrence at the primary site. Our research demonstrated that the IGF-IR induces cell survival, growth and estrogen-independence in hormone-sensitive cells. We have also shown that IGF-IR transmits non-mitogenic signals, such as stimulation as cell migration and adhesion, which may be critical for metastatic cell spread. The IGF-I-induced cell-cell adhesion in ER-positive cells and IGF-I-mediated cell migration in ER-negative cells involve interactions with cadherin/catenin and integrin systems, respectively. The molecular mechanisms underlying these processes are described in the publications supported by this program.

14. Subject Terms (keywords previously assigned to proposal abstract or terms which apply to this award)	15. NUMBER OF PAGES
Breast cancer, Insulin-Like Growth factor, Adhesion, Motility	75
	16. PRICE CODE

17. SECURITY CLASSIFICATION OF REPORT	18. SECURITY CLASSIFICATION OF THIS PAGE	19. SECURITY CLASSIFICATION OF ABSTRACT	20. LIMITATION OF ABSTRACT
Unclassified	Unclassified	Unclassified	Unlimited

TABLE OF CONTENTS

Appendix : Manuscripts:

Mauro, L., Bartucci, M., Morelli, C., Ando', S., Surmacz, E. IGF-I receptor-induced cell-cell adhesion of MCF-7 breast cancer cells requires the expression of a junction protein ZO-1, revised, J. Biol. Chem.

Bartucci, M., Morelli, C., Mauro, L., Ando', S., Surmacz, E. Differential insulin-like growth factor I receptor signaling and function in estrogen receptor (ER)-positive MCF-7 and ER-negative MDA-MB-231 breast cancer cells. Cancer Research 61: 2001.

Mauro, L., Sisci, D., Bartucci, M., Salerno, M., Kim, J., Tam, T., Guvakova, M., Ando, S., Surmacz, E. SHC-alpha5 beta1 integrin interactions regulate breast cancer cell adhesion and motility. Exp. Cell Res., 252: 439-448, 1999.

Guvakova, M., Surmacz, E. The activated insulin-like growth factor I receptor induces depolarization in breast epithelial cells characterized by actin filament disassembly and tyrosine dephosphorylation of FAK, Cas, and paxillin. Exp. Cell Res., 251: 244-255, 1999.

Salerno, M., Sisci, D., Mauro, L., Guvakova, M., Ando, S., Surmacz, E. Insulin receptor substrate 1 (IRS-1) is a target of a pure antiestrogen ICI 182,780 in breast cancer cells. Int. J. Cancer, 81: 299-304, 1999.

INTRODUCTION

The insulin-like growth factor I (IGF-I) receptor (IGF-IR) is a ubiquitous multifuctional tyrosine kinase. The IGF-IR regulates normal breast development; however, hyperactivation of the same receptor has been implicated in breast cancer (1). In particular, overexpression of either the IGF-IR or its major signaling substrate IRS-1 in estrogen receptor (ER)-positive breast tumors has been linked with cancer recurrence at the primary site. Furthermore, high circulating levels of IGF-I (an IGF-IR ligand) have been associated with increased breast cancer risk in premenopausal women (1-3).

Although current evidence suggests that abnormal activation of the IGF-IR may contribute to the autonomous growth and increased survival of primary ER-positive breast tumors, the function of this receptor in breast cancer metastasis is not clear. For instance, some small clinical studies demonstrated a correlation between IGF-IR expression in node-positive tumors and worse prognosis. Other data linked IGF-IR expression with better clinical outcome, as the IGF-IR was predominantly expressed in a subset of breast tumors with good prognostic characteristics. In the experimental setting, anti-IGF-IR strategies were successfully applied to inhibit the growth and spread of human breast cancer xenografts, which implicated the role of the IGF-IR in metastasis (1).

Using in vitro model systems developed in our laboratory, we asked how the IGF-IR and its different signaling pathways contribute to breast tumor development and progression. We focused on abnormal proliferation and survival, enhanced resistance to anti-tumor treatments, and augmented migration and invasion. Our data strongly suggested that hyperactivation of the IGF-IR in ER-positive breast cancer cells stimulates cell proliferation and survival, and contributes to the development of antiestrogen resistance. Overexpression of the IGF-IR in these cells also improved cell-cell adhesion through an E-cadherin-dependent mechanism. The IGF-I-mediated intercellular adhesion was found to be related to the increased expression of a junction protein, ZO-1. Overexpression of the IGF-IR in ER-negative cells did not influence cell growth and survival, but induced cell migration through PI-3 and p38 kinase pathways.

TECHNICAL REPORT

Administrative Note: This postdoctoral fellowship was originally awarded to Dr. M. Guvakova. After the completion of the second year, Dr. Guvakova transferred to another institution and since then the program has been carried out by Dr. M. Bartucci under the guidance of the same mentor (Dr. E. Surmacz) within the recipient institution. Due to administrative delays caused by this transfer, there was an interruption in funding and research from September 1999 to January 2000. Consequently, a 1 year no-cost extension has been requested and granted till August 2001, and the research plan has been extended into Year 4. This final report encompasses the entire research period August 15, 1997 till August 14, 2001.

Science Report.

A. This proposal stemmed from our initial observations that in ER-positive MCF-7 cells, overexpression of the IGF-IR or treatment of cells with IGF-I promoted cell aggregation

in 3-dimentional culture (4). The most important goal of the proposed program was to understand the mechanism by which the IGF-IR stimulates cell-cell adhesion and to address the biologic significance of this phenomenon in breast cancer cells.

The results indicated that overexpression of the IGF-IR results in increased cell-cell adhesion in E-cadherin-positive, but not in E-cadherin-negative breast cancer cells. However, when E-cadherin was re-introduced into E-cadherin-negative cells, cell aggregation was restored. This suggested that IGF-IR requires the E-cadherin complex to increase intercellular adhesion. Since the phosphorylation status and the amounts of adhesion proteins may affect cell aggregation, we studied whether overexpressed IGF-IR modifies the expression or tyrosine phosphorylation of the proteins in the E-cadherin complex. The experiments indicated that the IGF-IR did not modulate tyrosine phosphorylation or the proteins levels of E-cadherin, alpha-, beta-, and gamma-catenins. IGF-IR, however, did increase the expression of a junction protein, ZO-1 (zonula occludens 1). Further studies provided evidence that ZO-1 expression (on the RNA and protein levels) can be induced by the stimulation of cells with IGF-I. Using cell lines expressing a dominant-negative "dead" IGF-IR, we demonstrated that tyrosine kinase activity of the IGF-IR is critical in the upregulation of ZO-1 expression.

Additional studies demonstrated that ZO-1 associates with the E-cad complex and the IGF-IR. High levels of ZO-1 coincided with an increased IGF-IR/alpha-catenin/ZO-1binding and improved ZO-1/actin association, while downregulation of ZO-1 by the expression of an anti-ZO-1 RNA inhibited IGF-IR-dependent cell-cell adhesion.

Cumulatively, the results suggested that one of the mechanisms by which the activated IGF-IR regulates E-cad-mediated cell-cell adhesion is overexpression of ZO-1 and resulting stronger connections between the E-cad complex and the actin cytoskeleton. We hypothesized that in E-cad-positive cells, the IGF-IR may produce anti-metastatic effects.

The above research data have been reported in detail in *Mauro, L., Bartucci, M., Morelli, C., Ando', S., Surmacz, E. IGF-I receptor-induced cell-cell adhesion of MCF-7 breast cancer cells requires the expression of a junction protein ZO-1, revised, J. Biol. Chem.*, see Appendix.

B. The function of the IGF-IR has also been addressed in E-cadherin-negative, ER-negative breast cancer cells. The role of the IGF-IR in hormone-independent breast cancer is not clear. ER-negative breast cancer cells often express low levels of the IGF-IR and fail to respond to IGF-I with mitogenesis. On the other hand, anti-IGF-IR strategies effectively reduced metastatic potential of different ER-negative cell lines, suggesting a role of this receptor in late stages of the disease.

We examined IGF-IR signaling and function in ER-negative MDA-MB-231 breast cancer cells and their IGF-IR-overexpressing derivatives. We demonstrated that IGF-I acts as a chemoattractant for these cells. The extent of IGF-I-induced migration reflected IGF-IR levels and required the activation of PI-3K and p38 kinases. The same pathways promoted IGF-I-dependent motility in ER-positive MCF-7 cells. In contrast with the positive effects on cell migration, IGF-I was unable to stimulate growth or improve survival in MDA-MB-231 cells, while it induced mitogenic and anti-apoptotic effects in MCF-7 cells. Moreover, IGF-I partially restored growth in ER-positive cells treated with PI-3K and ERK1/ERK2 inhibitors, while it had no protective effects in ER-negative cells. The impaired IGF-I growth response of ER-negative cells was not caused by a low IGF-IR expression, defective IGF-IR tyrosine phosphorylation, or improper tyrosine phosphorylation of IRS-1. Also, the acute (15 min) IGF-I activation of PI-3 and Akt kinases was similar in ER-negative and ER-positive cells.

However, a chronic (2 days) IGF-I exposure induced the PI-3K/Akt pathway only in MCF-7 cells. The reactivation of this pathway in ER-negative cells by overexpression of constitutively active Akt mutants was not sufficient to significantly improve proliferation or survival (with or without IGF-I), which indicated that other pathways are also required to support these functions.

Our results suggested that in breast cancer cells, IGF-IR can control non-mitogenic processes regardless of the ER status, while IGF-IR growth-related functions may depend on ER expression

The research data have been reported in detail in *Bartucci, et al. Differential insulin-like growth factor I receptor signaling and function in estrogen receptor (ER)-positive MCF-7 and ER-negative MDA-MB-231 breast cancer cells. Cancer Research 61: 2001 (in press)*, see Appendix.

C. Cell motility and adhesion may depend on the modifications of the actin cytoskeleton. We addressed this problem in one of our projects. We found that the activated IGF-IR induces depolarization of the cells, which coincides with actin filament disassembly and tyrosine dephosphorylation of several proteins in the focal adhesion complex. This process seemed dependent on a tyrosine phosphatase activity and PI-3 kinase activity.

The research has been reported in detail in *Guvakova and Surmacz. The activated insulin-like growth factor I receptor induces depolarization in breast epithelial cells characterized by actin filament disassembly and tyrosine dephosphorylation of FAK, Cas, and paxillin. Exp. Cell Res., 251: 244-255, 1999,* see Appendix.

D. We studied whether the elements of the IGF-IR signaling interfere with integrins, the proteins that are receptors for different components of the extracellular matrix, and also play a role in cell migration and adhesion. We found that SHC, one of the major signaling substrates of the IGF-IR interacts with the integrin system. The oncogenic SHC proteins are signaling substrates for most receptor and cytoplasmic tyrosine kinases (TKs) and have been implicated in cellular growth, transformation and differentiation. In tumor cells overexpressing TKs, the levels of tyrosine phosphorylated SHC are chronically elevated. The significance of amplified SHC signaling in breast tumorigenesis and metastasis remains unknown. Here we demonstrate that 7-9-fold overexpression of SHC significantly altered interactions of cells with fibronectin (FN). Specifically, in human breast cancer cells overexpressing SHC (MCF-7/SHC) the association of SHC with alpha-5beta-1 integrin (FN receptor) was increased, spreading on FN accelerated, and basal growth on FN reduced. These effects coincided with an early decline of adhesion-dependent MAP kinase activity. Basal motility of MCF-7/SHC cells on FN was inhibited relative to that in several cell lines with normal SHC levels. However, when EGF or IGF-I were used as chemoattractants, the locomotion of MCF-7/SHC cells was greatly (~5-fold) stimulated, while it was only minimally altered in the control cells. These data suggest that SHC is a mediator of the dynamic regulation of cell adhesion and motility on FN in breast cancer cells.

The research has been reported in detail in *Mauro et al. SHC-alpha5 beta1 integrin interactions regulate breast cancer cell adhesion and motility. Exp. Cell Res., 252: 439-448, 1999,* see Appendix.

E. The PI supported by this fellowship grant also participated in studies on the cross-talk between ER and the IGF-IR. We found that antiestrogens interfere with IGF-IR-dependent growth by inhibiting the expression and function of IRS-1, a signaling substrate of the IGF-IR. In addition, we noted that the cytotoxic/cytostatic action of antiestrogens was less effective in breast cancer cells overexpressing IRS-1. Considering that in the clinical setting, IRS-1 is overexpressed in a fraction of ER-positive breast tumors, and this overexpression correlates with cancer recurrance, we concluded that high levels of IRS-1 may contribute to antiestrogen resistance.

The research has been reported in detail in *Salerno et al. Insulin receptor substrate 1 (IRS-1) is a target of a pure antiestrogen ICI 182,780 in breast cancer cells. Int. J. Cancer, 81: 299-304, 1999,* see Appendix.

Key Research Accomplishments:

- Demonstrated that the IGF-IR has different functions in ER-positive and ER-negative cells. In ER-positive non-metastatic cells, the IGF-IR regulates growth and survival, and improves cell-cell adhesion. In ER-negative metastatic cells, only motogenic (migratory) signaling is operative;

- Determined that IGF-I-dependent cell-cell adhesion in ER-positive cells involves a junction protein ZO-1. Overexpression of ZO-1 result in stronger connections between the E-cad complex and the actin cytoskeleton.

- Determined that IGF-I-dependent migration in both ER-positive and ER-negative cells is mediated through p38 kinase and PI-3K pathways, and is inhibited by ERK1/ERK2 pathways.

Reportable Outcomes:

1. Manuscripts, abstracts and scientific presentations:

Manuscripts:

1. Mauro, L., Bartucci, M., Morelli, C., Ando', S., Surmacz, E. IGF-I receptor-induced cell-cell adhesion of MCF-7 breast cancer cells requires the expression of a junction protein ZO-1, revised, J. Biol. Chem.

2. Bartucci, M., Morelli, C., Mauro, L., Ando', S., Surmacz, E. Differential insulin-like growth factor I receptor signaling and function in estrogen receptor (ER)-positive MCF-7 and ER-negative MDA-MB-231 breast cancer cells. Cancer Research 61: 2001.

3. Mauro, L., Sisci, D., Bartucci, M., Salerno, M., Kim, J., Tam, T., Guvakova, M., Ando, S., Surmacz, E. SHC-alpha5 beta1 integrin interactions regulate breast cancer cell adhesion and motility. Exp. Cell Res., 252: 439-448, 1999.

4. Guvakova, M., Surmacz, E. The activated insulin-like growth factor I receptor induces depolarization in breast epithelial cells characterized by actin filament disassembly and tyrosine dephosphorylation of FAK, Cas, and paxillin. Exp. Cell Res., 251: 244-255, 1999.

5. Salerno, M., Sisci, D., Mauro, L., Guvakova, M., Ando, S., Surmacz, E. Insulin receptor substrate 1 (IRS-1) is a target of a pure antiestrogen ICI 182,780 in breast cancer cells. Int. J. Cancer, 81: 299-304, 1999.

Presentations/Abstracts:

1. Morelli, C., Bartucci, M., Mauro, L., Ando' S., Surmacz, E. Insulin-like growth factor I receptor (IGF-IR) signaling in metastatic breast cancer cells. The Endocrine Society Annual Meeting, Toronto, Canada, June 21-24, 2000.

2. Bartucci, M., Mauro, L., Salerno, M., Morelli, C., Ando', Surmacz, E. Function of the insulin-like growth factor I receptor in metastatic breast cancer cells. Era of Hope, Department of Defense Breast Cancer Research Program Meeting, Atlanta, June 8-11, 2000.

3. Bartucci, M., Mauro, L., Salerno, M., Morelli, C., Ando', S., Surmacz, E. Function of the insulin-like growth factor I receptor in metastatic breast cancer cells. 22nd Annual Breast Cancer Symposium. San Antonio, TX, December 8-11, 1999

4. Guvakova, M., Surmacz, E. Tyrosine kinase activity of the IGF-IR is required for the development of breast cancer cell aggregates in three-dimensional culture. AACR Annual Meeting, Philadelphia, PA, April 10-14, 1999

5. Guvakova, M., Surmacz, E. IGF-IR tyrosine kinase is required for breast cancer cell motility. Specificity in Signal Transduction. Keystone Symp.Keystone, CO, April 9-14, 1999

6. Guvakova, M., Surmacz, E. IGF-IR stimulates breast epithelial cell motility via reorganization of the actin cytoskeleton, remodeling of focal contacts, and modulation of the phosphorylation status of focal adhesion proteins: FAK, Cas, and paxillin.14th Annual Symposium on Cellular Endocrinology, Lake Placid, NY, September 24-27, 1998

7. Guvakova, M., Surmacz, E. IGF-IR modulates breast cancer cell motility through the regulation of p125 FAK/p130 CAS. 37th American Society for Cell Biology Annual Meeting, Washington D.C., December 13-17, 1997

8. Surmacz, E., Sisci, D., Salerno, M., Guvakova, M., Ando, S. Insulin receptor substrate 1 (IRS-1) is a target for a pure antiestrogen ICI 182,780. Annual Breast Cancer Meeting, San Antonio, TX, December 3-6, 1997

9. Guvakova, M., Surmacz, E. Molecular mechanisms of tamoxifen effect on IGF-IR signaling in breast cancer cells. The 2nd World Congress on Advances in Oncology, Vouliagmenti, Athens, Greece, October 16-18, 1997

2. Patents and licenses: None

3. Degrees: N/A

4. Development of biologic reagents:

- metastatic breast cancer cell lines overexpressing IGF-IR: MDA-MB-231/IGF-IR cells

5. Databases: None

6. Funding applied for: None

7. Employment applied for: None

Conclusions

The IGF-IR has different functions in ER-positive and ER-negative cells. Targeting the IGF-IR in ER-positive cells will result in the inhibition of cell growth and survival. Blocking the IGF-IR in ER-negative cells will not affect growth properties (at least in vitro), but will inhibit cell migration. Thus, anti-IGF strategies may prove beneficial at different stages of tumor progression.

References

1. Surmacz, E. Function of the IGF-IR in breast cancer. J. Mammary Gland Biol. Neopl., *5*: 95-105, 2000.

2. Hankinson, S. E., Willet, W. C., Colditz, G. A., Hunter, D. J., Michaud, D. S., Deroo, B., Rosner, B., Speitzer, F. E., and Pollak, M. Circulating concentrations of insulin-like growth factor and risk of breast cancer. Lancet , *35*: 1393-1396, 1998.

3. Byrne, C., Colditz, G. A., Willett, W. C., Speizer, F. E., Pollak, M., and Hankinson, S. E. Plasma insulin-like growth factor (IGF) I, IGF-binding protein 3, and mammaographic density. Cancer Res. *60*: 3744-3748, 2000.

4. Guvakova, M. A., and Surmacz, E. Overexpressed IGF-I receptors reduce estrogen growth requirements, enhance survival and promote cell-cell adhesion in human breast cancer cells. Exp. Cell Res., *231*: 149-162, 1997.

IGF-I Receptor-Induced Cell-Cell Adhesion of MCF-7 Breast Cancer Cells Requires the Expression of a Junction Protein ZO-1

Loredana Mauro[1, 2], Monica Bartucci[1, 2], Catia Morelli[1,2], Sebastiano Ando'[2], and Eva Surmacz[1]*

[1]Kimmel Cancer Center, Thomas Jefferson University, Philadelphia, PA 19107, [2]Department of Cellular Biology and Faculty of Pharmacy, University of Calabria, 87030 Rende (Cs) Italy

Running Title: IGF-IR upregulates adhesion through ZO-1

*Corresponding Author: Eva Surmacz, Ph.D.
Kimmel Cancer Center, Thomas Jefferson University
233 S 10th Street, BLSB 631, Philadelphia, Pa 19107
Tel.: 215-503-4512, Fax: 215-923-0249
e-mail: eva.surmacz@mail.tju.edu

SUMMARY

Hyperactivation of the insulin-like growth factor I receptor (IGF-IR) contributes to primary breast cancer development, but the role of the IGF-IR in tumor metastasis is unclear. Here we studied the effects of the IGF-IR on intercellular connections mediated by the major epithelial adhesion protein, E-cadherin (E-cad). We found that IGF-IR overexpression markedly stimulated aggregation in E-cad-positive MCF-7 breast cancer cells, but not in E-cad-negative MDA-MB-231 cells. However, when the IGF-IR and E-cad were co-expressed in MDA-MB-231 cells, cell-cell adhesion was substantially increased. The IGF-IR-dependent cell-cell adhesion of MCF-7 cells was not related to altered expression of E-cad, α-, β-, or γ-catenins, but coincided with the upregulation of another element of the E-cad complex, ZO-1. ZO-1 expression (mRNA and protein) was induced by IGF-I and was blocked in MCF-7 cells with a tyrosine kinase-defective IGF-IR mutant. By co-immunoprecipitation, we found that ZO-1 associates with the E-cad complex and the IGF-IR. High levels of ZO-1 coincided with an increased IGF-IR/α-catenin/ZO-1binding and improved ZO-1/actin association, while downregulation of ZO-1 by the expression of an anti-ZO-1 RNA inhibited IGF-IR-dependent cell-cell adhesion. The results suggested that one of the mechanisms by which the activated IGF-IR regulates E-cad-mediated cell-cell adhesion is overexpression of ZO-1 and resulting stronger connections between the E-cad complex and the actin cytoskeleton. We hypothesize that in E-cad-positive cells, the IGF-IR may produce anti-metastatic effects.

INTRODUCTION

The insulin-like growth factor I (IGF-I) receptor (IGF-IR) is a ubiquitous tyrosine kinase capable of regulating different growth-related and -unrelated processes (1-3).

Recent evidence indicates that the IGF-IR may be involved in breast cancer development. The IGF-IR is significantly (10-14-fold) overexpressed in estrogen receptor (ER)-positive primary breast tumors compared to normal mammary epithelium or benign tumors (1, 4). Moreover, the intrinsic ligand-independent tyrosine kinase activity of the IGF-IR has been found substantially upregulated (~2-4-fold) in breast cancer cells (4). It has been suggested that the increased receptor function coupled with enhanced receptor expression amounts to a 40-fold elevation in IGF-IR activity in ER-positive breast tumors (4). Recent clinical and experimental data indicate that upregulation of IGF-IR signaling in ER-positive breast cancer cells is associated with autonomous cell proliferation, estrogen-independence, and increased resistance to various anti-tumor treatments (1). Consequently, it is believed that hyperactivation of the IGF-IR may induce and sustain the growth of primary breast tumors (1).

The role of the IGF-IR in breast cancer metastasis, however, is unclear. The experimental data suggested that the IGF-IR has a function in cell spreading, as it effectively stimulates the motility of different metastatic breast cancer cell lines lacking the expression of a major adhesion protein E-cadherin (E-cad) (1, 5, 6). On the other hand, we and others have shown that in more differentiated E-cad-positive cells, IGF-I treatment or IGF-IR overexpression upregulates cell-cell adhesion, which correlates with increased cell survival in 3-dimensional (3-D) culture and reduced cell migration in vitro and in organ culture (1, 7-10).

The mechanism of IGF-I-dependent intercellular adhesion and the clinical consequences of this phenomenon have not been fully elucidated. Previously, we demonstrated that in MCF-7 human breast cancer cells, the IGF-IR co-localizes and co-

precipitates with the E-cad complex, and IGF-induced aggregation is blocked with an anti-E-cad antibody (7). In this study we assessed the effects of the IGF-IR on the elements of the E-cad adhesion complex, i.e. E-cad, β-, γ-, and α-catenins and α-catenin-associated proteins (see Fig. 6). The initial results prompted us to focus on an α-catenin-binding element—a junction protein *zonula occludens-1* (ZO-1).

ZO-1 is a ~220 kDa scaffolding protein containing various domains (an SH3 domain, three PDZ domains, a proline-rich region, and a guanylate kinase domain), which allow its interaction with specialized sites of plasma membrane as well as with other proteins (11, 12). ZO-1 is a characteristic element of tight junctions, but recently its presence has also been demonstrated in E-cad adherens junctions (13-15). The role of ZO-1 in adherens junctions is yet unclear, but it is assumed that it may functionally link E-cad with the actin cytoskeleton, as it associates with α-catenin and actin through its N- and C-terminus, respectively (13, see Fig. 6). In addition, as a member of the MAGUK (membrane-associated guanylate kinase homologues) family of putative signaling proteins, ZO-1 may be involved in signal transduction. Indeed, ZO-1 has been found to bind a target of Ras, AF6 (16). Deletions or mutations in the ZO-1 gene produced overgrowth, suggesting that ZO-1 may act as a tumor suppressor (11). In breast cancer, ZO-1 is usually co-expressed with E-cad and is a strong independent marker of a more differentiated phenotype (17).

At present, very little is known about the regulation of ZO-1 by growth factors. However, some recent studies demonstrated that EGF (epidermal growth factor) and VEGF (vascular endothelial growth factor) are able to increase ZO-1 tyrosine phosphorylation, modulate its subcellular localization, and consequently produce increased

permeability (18-20). Here, we present the first evidence that in MCF-7 breast cancer cells 1) the IGF-IR upregulates ZO-1 expression; 2) elevated levels of ZO-1 coincide with enhanced IGF-IR/E-cad-mediated cell-cell adhesion; and 3) ZO-1 expression is required for IGF-IR-increased cell aggregation in E-cad-positive MCF-7 cells.

MATERIALS AND METHODS

Expression Plasmids. E-cad expression plasmid. The pBAT-EM2 plasmid is a derivative of pBR322 and contains the mouse E-cad cDNA cloned under the β-actin promoter in pBR322 (21). As demonstrated previously, transfection of MDA-MB-231cells with pBAT-EM2 results in E-cad overexpression, improved cell aggregation, and reduced metastatic potential of the cells (21, 22).

Antisense ZO-1 RNA vector. The pcDNA3/anti-ZO-1 plasmid encoding the anti-ZO-1 antisense RNA contains a 959 bp BamH1 fragment of the human ZO-1 cDNA (nt 4205-5164) inserted (in the 3'-5' orientation) into the pcDNA3.1/Hygro plasmid (Invitrogen). PcDNA3/sense-ZO-1 is the control vector in which the above 959 bp ZO-1 cDNA fragment was cloned in the 5'-3' orientation.

Cell Lines and Cell Culture Conditions. MCF-7/IGF-IR, clone 12, 15 and 17 are MCF-7-derived clones overexpressing the IGF-IR at the levels $5x10^5$, $3x10^6$, and $1x10^6$ receptors/cell, respectively (7). To avoid clonal variation, in several experiments we used a population of mixed clones 12, 15 and 17. The mixed population is referred to as MCF-7/IGF-IR cells and expresses ~ $0.9x10^6$ IGF-IR receptors/cell (which represents ~18-fold overexpression over the levels in normal cells)(1). MCF-7/IGF-IR/Y3F express an IGF-IR (~$3x10^6$ receptors/cell) with inactivating mutations in the tyrosine kinase domain (Tyr

1131, 1135, 1136 replaced with Phe) (23). MCF-7/IGF-IR/Y3F cells were derived from MCF-7 cells by stable transfection with the pcDNA3/IGF-IR/KR plasmid and subsequent selection in 2 mg/ml G418. The results obtained with the MCF-7/IGF-IR/Y3F clone were verified using a population of MCF-7 cells transiently transfected with the IGF-IR/Y3F vector (see below). MCF-7/IGF-IR/anti-ZO-1 and MCF-7/IGF-IR/sense-ZO-1 cells were derived from MCF-7/IGF-IR clone 15 by stable transfection with the antisense- and sense-ZO-1 vectors, respectively, and subsequent selection in 500 μg/ml Hygromycin B.

MDA-MB-231 is a metastatic breast cancer cell line lacking E-cad and expressing ~ $7x10^3$ IGF-IR receptors/cell (24, Bartucci et al., in revision). MDA-MB-231/IGF-IR clone 31 was derived from MDA-MB-231 cells by stable transfection with the pcDNA3/IGF-IR plasmid. MDA-MB-231/IGF-IR cells express ~ 250,000 IGF-IR/cell (Bartucci et al., in revision).

All cell lines were grown in DMEM:F12 (1:1) containing 5% calf serum (CS). MCF-7- and MDA-MB-231-derived clones transfected with the wild type or mutant IGF-IR were maintained in growth medium with 100 μg/ml G418. MCF-7/IGF-IR/anti-ZO-1 and MCF-7/IGF-IR/sense-ZO-1 cells were cultured in growth medium with 50 μg/ml Hygromycin B. In the experiments requiring serum-free conditions, the cells were cultured in phenol red-free DMEM containing 0.5 mg/ml BSA, 1 uM FeSO4 and 2 mM L-glutamine (referred to as SFM).

Transient Transfection. MDA-MB-231 and MDA-MB-231/IGF-IR cells were transiently transfected using Lipofectamine 2000 (Gibco) (reagent/DNA ratio = 5 μl/1μg). The transfection was carried out in growth medium for 24 h, then, the cells were lysed and processed for E-cad Western blotting (WB). To evaluate the extent of cell-cell adhesion in

the transfected MDA-MB-231 and MDA-MB-231/IGF-IR cells, the cells were trypsinized upon transfection, counted and placed in 3-D suspension culture, as described below. MCF-7 cells were transfected for 6 h in growth medium using Fugene 6 (Roche) (reagent/DNA ratio = 3 μl/1μg). To study IGF-I signaling, the transfected MCF-7 cells were shifted to SFM for 36 h and stimulated with IGF-I for 15 min. The efficiency of transfection (transfected cells/total cell number) was at least 70% for all cell types, and was estimated by scoring fluorescent cells in cultures transfected with the plasmid pCMS (encoding Green Fluorescent Protein) (Invitrogen).

3-D Spheroid Culture. The cells were grown to 70-80% confluence, trypsinized, and plated as single cell suspension in 2%-agar-coated plates containing either normal growth medium or SFM. $2x10^6$ cells were plated per 100 mm culture dish. To generate 3-D spheroids, the plates were rotated for 4 h at 37°C. The spheroids started to assemble at ~1 h after plating and were completely organized after 3-4 h of culture in suspension. The 3-D cultures were photographed using a phase contrast microscope (Nikon or Olympus). The extent of aggregation was scored by measuring the spheroids with an ocular micrometer. For each cell type, the spheroids of 25≤50, 50≤100, and >100 μm (in the smallest cross-section) were counted in 10 different fields under 10x magnification.

IGF Stimulation. 70% confluent cell cultures were synchronized in SFM for 36 h and then stimulated with 20 ng/ml IGF-I for 0-72 h.

Immunoprecipitation and Western Blotting. The expression of different elements of the adhesion complex was assessed in 500 μg of protein lysate by immunoprecipitation (IP) and Western blotting (WB) with appropriate antibodies. The expression of ERK1/ERK2 was tested in 50 μg of total cell lysate. The cell lysis buffer contained 50

mM HEPES pH 7.5, 150 mM NaCl, 1% Triton X-100, 1.5 mM $MgCl_2$, 1 mM $CaCl_2$, 100 mM NaF, 0.2 mM Na_3VO_4, 1% PMSF, 1% aprotinin, as described before (25). The following antibodies were used: anti-ZO-1 polyclonal antibody (pAb) (Zymed Laboratories) for ZO-1 IP (5 μg/ml) and WB (2 μg/ml); anti-E-cad monoclonal antibody (mAB), clone 36 (Transduction Laboratories) for E-cadherin IP (2 μg/ml) and WB (0.1 μg/ml); anti-α-catenin pAb (Sigma or Zymed Laboratories) for α-catenin IP (4 μg/ml) and WB (anti-serum dilution 1:4,000); anti-β-catenin mAb (Transduction Laboratories) for β-catenin IP (4 μg/ml) and WB (0.5 μg/ml); anti-γ catenin pAb (Sigma) for γ-catenin WB (1 μg/ml); anti-actin mAb clone AC-40 (Sigma) for actin WB (0.4 μg/ml); anti-IGF-IR mAb, clone alpha IR-3 (Calbiochem) for IGF-IR IP (3 μg/ml), and anti-IGF-IR pAb C-20 (Santa Cruz) for IGF-IR WB (0.2 μg/ml); anti-p85 pAb (UBI) for p85 subunit of PI-3 kinase WB (0.25 μg/ml); anti-phospho-MAPK mAb (New England Biolabs) for active ERK1/ERK2 WB (0.5 μg/ml); anti-MAPK pAb (New England Biolabs) for total ERK1/ERK2 WB (1 μg/ml). Tyrosine phosphorylation of immunoprecipitated proteins was measured by WB with anti-phosphotyrosine mAb (Transduction Laboratories) (0.03 μg/ml). WBs were developed using an ECL chemiluminescence kit (Amersham). The intensity of bands representing relevant proteins was measured by laser densitometry scanning.

RESULTS

IGF-IR overexpression stimulates cell-cell adhesion through E-cad-dependent mechanism. First, we demonstrated that under 3-D culture conditions, overexpression of the IGF-IR stimulated cell-cell adhesion in E-cad-positive MCF-7 breast cancer cells, but

not in E-cad-negative MDA-MB-231 cells (Fig. 1 A, B, and Tab. 1). However, co-expression of the IGF-IR and E-cad resulted in robust cell-cell adhesion of MDA-MB-231 cells, while the expression of E-cad alone was less efficient in inducing intercellular contacts (Fig. 1 C, D, and Tab. 1). These results together with our previous data that IGF-IR-mediated aggregation in MCF-7 cells is blocked with an anti-E-cad antibody (7) indicated that IGF-IR adhesion signals are transmitted through the E-cad complex.

IGF-IR overexpression upregulates ZO-1. We tested whether high levels of the IGF-IR affect the expression of the proteins within the E-cad complex. We found that in MCF-7 and MCF-7/IGF-IR cells cultured as 3-D spheroids, the levels of E-cad, α-, β-, and γ-catenin were similar, however, the abundance of ZO-1 was significantly increased in MCF-7/IGF-IR cells (Fig. 2). The tyrosine phosphorylation of all these adhesion proteins was undetectable in spheroids, and was not influenced by IGF-IR overexpression (Fig. 5 and data not shown).

To investigate whether the increased expression of ZO-1 in MCF-7/IGF-IR cells depends on IGF-IR tyrosine kinase activity, we generated by stable or transient transfection MCF-7/IGF-IR/Y3F cells expressing high levels of a kinase-defective IGF-IR mutant (IGF-IR/Y3F). The overexpression of the IGF-IR/Y3F mutant resulted in impaired IGF-I response, which was reflected by markedly reduced IGF-IR and IRS-1 tyrosine phosphorylation, decreased IRS-1/p85 binding, and diminished ERK1/ERK2 stimulation (Fig. 3). The basal expression of ZO-1 in MCF-7/IGF-IR/Y3F cells was significantly reduced compared to that in MCF-7/IGF-IR cells, indicating that tyrosine kinase activity of the IGF-IR is required for the upregulation of ZO-1 (Fig. 3). Interestingly, the inhibition of IGF-I response did not affect E-cad expression, suggesting a selective action of the

IGF-IR towards ZO-1 (Fig. 3). The blockade of the IGF-IR signal in MCF-7/IGF-IR/Y3F cells coincided with reduced cell-cell adhesion (Tab. 1).

ZO-1 mRNA and protein expression is regulated by IGF-I. To establish whether the activation of the IGF-IR by IGF produces a similar effect on ZO-1 as that seen with IGF-IR overexpression, we studied ZO-1 mRNA and protein in MCF-7 and MCF-7/IGF-IR cells treated with 20 ng/ml IGF-I for 1-72h (Fig. 4). In MCF-7 cells cultured in SFM, the basal levels of ZO-1 mRNA were low, and were markedly increased between 4 and 36h of IGF-I treatment (Fig. 4A). In contrast, the abundance of ZO-1 mRNA was always elevated in MCF-7/IGF-IR cells, and was only moderately improved by IGF-I (4-72 h) (Fig. 4A). ZO-1 protein levels in IGF-I-treated cells generally reflected the expression of ZO-1 mRNA (Fig. 4B).

Interactions of ZO-1 with the E-cad complex in MCF-7/IGF-IR cells. It has been recently reported that ZO-1 is an element of the E-cad complex (12-14). This complex also contains the IGF-IR, as described in our previous work (7, 8). Here, we analyzed tyrosine phosphorylation status of the IGF-IR, E-cad, and ZO-1, and the interactions among these proteins in MCF-7 and MCF-7/IGF-IR cells cultured as 3-D spheroids (Fig. 5). The autophosphorylation of the IGF-IR was elevated in MCF-7/IGF-IR cells, reflecting the increased responsiveness of the cells to IGF-IR ligands (IGF-I, IGF-II, and insulin) present in serum. However, tyrosine phosphorylation of E-cad and ZO-1 were unaffected by IGF-IR overexpression (Fig. 5A). Similarly, high levels of the IGF-IR did not affect tyrosine phosphorylation of α-, β-, or γ-catenin (data not shown). Next, we asked whether hyperactivation of the IGF-IR and increased expression ZO-1 have consequences on the associations among the proteins within the E-cad complex. Co-

immunoprecipitation experiments demonstrated that IGF-IR overexpression resulted in an increased abundance of IGF-IR/E-cad and IGF-IR/ZO-1 complexes (Fig. 5A). Also, the elevated levels of ZO-1 in MCF-7/IGF-IR cells coincided with an increased association of ZO-1 with either E-cad or the IGF-IR (Fig. 5A). Moreover, the binding of α-catenin (an ZO-1-associated protein) to the IGF-IR or ZO-1, but not to E-cad, was greater in MCF-7/IGF-IR cells than in MCF-7 cells (Fig. 5A). The presence of α-catenin in IGF-IR immunoprecipitates was confirmed with cell lysates in which α-catenin was first removed with a specific antibody. As expected, immunoprecipitation of such depleted lysates with either anti-IGF-IR or anti-E-cad antibodies revealed reduced α-catenin/E-cad and α-catenin/IGF-IR associations (Fig. 5B). Further experiments with α-catenin immunoprecipitates indicated increased abundance of α-catenin/actin and α-catenin/ZO-1 complexes in MCF-7/IGF-IR cells (Fig. 5C). A hypothetical model of possible interactions between adhesion proteins and the IGF-IR is shown in Fig. 6.

Downregulation of ZO-1 results in decreased cell-cell adhesion in MCF-7/IGF-IR cells. Since the results suggested that ZO-1 may be an important intermediate in IGF-IR-stimulated cell-cell adhesion, we set out to confirm this notion using MCF-7/IGF-IR cells in which ZO-1 levels were downregulated by the expression of an anti-ZO-1 RNA (MCF-7/IGF-IR/anti-ZO-1 cells) (Fig. 7). The clones with the best ZO-1 reduction and an intact E-cad and IGF-IR expression were analyzed in 3-D culture. The cell-cell adhesion of MCF-7/IGF-IR/anti-ZO-1 cells was greatly inhibited compared with that in the parental MCF-7/IGF-IR cells (Fig. 7 and Tab. 1). The expression of the anti-ZO-1 plasmid in the parental MCF-7 cells was toxic and no viable clones were obtained. The transfection of the sense-ZO-1 vector had no effect on cell-cell adhesion (data not shown).

DISCUSSION

Cell-cell adhesion is a known factor modulating the motility of tumor cells, and consequently, impacting tumor metastasis (26). The regulation of this process by exogenous growth factors is still not well understood. In E-cad-positive breast cancer cells, the overexpression or activation of the IGF-IR has been shown to stimulate cell-cell adhesion and reduce cell spreading in vitro or in organ culture (7-10). The IGF-IR has also been found co-localized and co-precipitated with the E-cad adhesion complex (7, 8). The mechanism of IGF-IR-stimulated E-cad-dependent cell-cell adhesion is unknown and has been investigated in this work. We found that 1) IGF-IR overexpression increased aggregation in E-cad-positive cells, but not in E-cad-negative cells; 2) high expression of both IGF-IR and E-cad markedly improved cell aggregation in E-cad-negative cells; 3) IGF-IR-dependent cell-cell adhesion in E-cad-positive cells did not affect the expression of E-cad, α-, β-, or γ-catenins, but coincided with upregulation of ZO-1; 4) ZO-1 expression was induced by IGF-I and required IGF-IR tyrosine kinase activity; 5) high levels of ZO-1 coincided with an increased IGF-IR/α-catenin/ZO-1 binding and improved ZO-1/actin association, while downregulation of ZO-1 by the expression of an anti-ZO-1 RNA inhibited IGF-IR-dependent cell-cell adhesion. We hypothesize that the mechanism, or one of the mechanisms, by which the activated IGF-IR stimulates cell-cell adhesion is overexpression of ZO-1 and resultant stronger connections between the E-cad complex and the actin cytoskeleton.

Very little is known about the regulation of ZO-1 by growth factors. Several growth factors (EGF, VEGF) have been demonstrated to increase tyrosine

phosphorylation of ZO-1 in different cellular model systems (18, 19). Hyperphosphorylation of ZO-1 usually coincides with its departure from tight junctions into the cytoplasm and with increased permeability (18, 19). In addition, v-src-increased ZO-1 tyrosine phosphorylation has been linked with decreased cell-cell adhesion (27). IGF-I, on the other hand, has been shown to stabilize ZO-1 in tight junctions and to preserve epithelial barrier in embryonic kidney cells and in pig thyrocytes (28, 29). However, the effects of IGF-I on ZO-1 expression and function in breast cancer cells have never been explored. Our findings provide the first evidence that the activation of the IGF-IR upregulates ZO-1 mRNA and protein levels, without affecting ZO-1 tyrosine phosphorylation. Consistent with the results obtained in other models, we noted increased adhesion in cells overexpressing ZO-1 and reduced aggregation in cells with downregulated ZO-1 levels.

IGF-IR tyrosine phosphorylation was required for the stimulation of ZO-1 expression, as the basal levels of ZO-1 were not increased in MCF-7/IGF-IR/Y3F cells expressing a dominant-negative kinase-defective mutant of the IGF-IR. However, the putative IGF-I signaling pathways leading to ZO-1 expression have yet to be characterized. Our preliminary data with MCF-7/IRS-1 cells, in which the major IGF-IR/IRS-1/PI-3K growth/survival pathway is hyperactivated, suggested that this pathway is not involved in ZO-1 regulation (Surmacz et al., data not shown).

The clinical implications of IGF-induced and ZO-1-mediated cell-cell adhesion on tumor development and progression are unknown. Until now, the data from our and other laboratories suggest that in E-cad-positive breast cancer cells, IGF-IR improves cell-cell adhesion and cell survival in 3-D culture, but at the same, reduces cell spreading (1). Thus,

one consequence of IGF-IR overexpression in breast cancer could be increased growth and survival of the primary tumor, but reduced cell metastasis. This hypothesis is consistent with the observation that the IGF-IR is a good prognostic indicator for breast cancer, as tumors with good prognosis express much higher levels of the IGF-IR than tumors with bad prognosis (1, 30, 31). Notably, independent study has shown that in breast tumors, E-cad and ZO-1 are co-expressed and are markers of a more differentiated phenotype (17). A formal analysis of the correlations between ZO-1 and the IGF-IR is underway in our laboratory and should help in clarifying the role of the IGF-IR in breast cancer progression.

ACKNOWLEDGMENTS

Drs. J. M. Anderson and A. S. Fanning (Yale University, New Haven, CT) generously provided the pSKZO-1 plasmid encoding the human ZO-1 cDNA. The E-cad expression vector pBAT-EM2 was a gift form Drs. M. Takeichi (Kyoto University, Kyoto, Japan) and T. Yoneda (University of Texas, San Antonio, TX). The MCF-7/Y3F clone was developed by Dr. M. Guvakova (University of Pennsylvania, Philadelphia, PA). This work was supported by the following grants and awards: U.S. Department of Defense DAMD17-99-1-9407 and DAMD17-97-1-7211; International Union against Cancer Award ICRETT 1007/1999, and POP 98 grant from Regione Calabria.

REFERENCES

1. Surmacz, E. (2000) J. Mammary Gland Biol. Neopl. **5,** 95-105

2. Werner, H., and Le Roith, D. (2000) Cell. Mol. Life Sci. **57,** 932-42

3. Baserga, R. (1999) Exp. Cell Res. **253,** 1-6

4. Resnik, J. L., Reichart, D. B., Huey, K., Webster, N. J. G., and Seely, B. L. (1998) Cancer Res. **58,** 1159-1164

5. Dunn, S. E., Ehrlich, M., Sharp, N. J. H., Reiss, K., Solomon, G., Hawkins, R., Baserga, R., and Barrett, J. C. (1998) Cancer Res. **58,** 3353-3361

6. Doerr, M., and Jones, J. J. (1996) Biol. Chem. **271,** 2443-2447

7. Guvakova, M. A., and Surmacz, E. (1997) Exp. Cell Res. **231,** 149-162

8. Surmacz, E., Guvakova, M., Nolan, M., Nicosia, R., and Sciacca, L. (1998) Breast Cancer Res. Treat. **47**, 255-267

9. Bracke, M. E., Vyncke B. M., Bruyneel, E.A., Vermeulen, S.J., De Bruyne, G. K., Van Larebeke, N. A., Vleminckx, K., Van Roy F.M., and Mareel, M.M. (1993) Br. J. Cancer **68,** 282-289

10. Bracke, M.E., Van Roy, F.M., and Mareel, M.M. (1996) Curr. Top. Microbiol. Immunol. **213,** 123-61

11. Willott, E., Balda, M. S., Fanning, A. S., Jameson, B., Van Itallie, C, and Anderson, J. M. (1993) Proc. Natl. Acad. Sci. USA **90**, 7834-7838

12. Tsukita, S., Furuse, M.,and Itoh, M. (1997) Soc. Gen. Phys. Series **52**, 69-76

13. Itoh, M., Nagafuchi, A., Moroi, S., and Tsukita, S. J. (1997) Cell Biol. **138,** 181-192

14. Rajasekaran, A.K., Hojo, M., Huima, T., and Rodriguez-Boulan, E. J. (1996) Cell Biol. **132,** 451-463

15. Provost, E., and Rimm DL (1999) Curr. Opin. Cell Biol. **11,** 567-72

16. Yamamoto, T., Harada, N., Kano, K., Taya, S., Canaani, E., Matsuura, Y., Mizoguchi, A., Ide, C., and Kaibuchi, K. J. (1997) Cell Biol. **139,** 785-795

17. Hoover, K. B., Liao, S-Y., and Bryant, P. J. (1998) Amer. J. Pathol. **153,** 1767-17773

18. Van Itallie, C. M., Balda, M. S. and Anderson, J. M. (1995) J. Cell Sci. **108,** 1735-1742

19. Antonetti, D.A., Barber, A.J., Hollinger, L.A., Wolpert, E.B., and Gardner, T.W. (1999) J. Biol. Chem . **274,** 23463-23467

20. Merwin, J.R., Anderson, J.M., Kocher, O., Van Itallie, C.M., and Madri, J.A. (1990) J. Cell. Physiol. **142,** 117-28

21. Nagafuchi, A., Shirayoshi, Y., Okazaki, K., Yasuda, K., and Takeichi, M. (1987) Nature **329,** 341-3

22. Mbalaviele, G., Dunstan, C.R., Sasaki, A., Williams, P.J., Mundy, G.R., and Yoneda, T. (1996) Cancer Res. **56**, 4063-70

23. Kato, H., Faria, T., Stannard, B., Roberts, C. T., Jr., and LeRoith, D. (1994) Mol. Endocrin. **8,** 40-50

24. Peyrat, J. P., Bonneterre, J., Dusanter-Fourt, I., Leroy-Martin, B., Dijane, J., and Demaille, A. (1989) Bull. Cancer **76,** 311-309

25. Mauro, L., Sisci, D., Salerno, M., Kim, J., Tam, T., Guvakova, M., Ando, S., and Surmacz, E. (1999) Exp. Cell Res. **252**, 439-448

26. Christofori, G., and Semb, H. (1999) Trends Biochem. Sci. **24,** 73-6

27. Takeda, H., Nagafuchi, A., Yonemura, S., Tsukita, S., Behrens, J., Birchmeier, W., and Tsukita, S. (1995) J. Cell Biol. **131,** 1839-1847

28. Sakurai, H., Barros, E.J., Tsukamoto, T., Barasch, J., Nigam, S.K. (1997) Proc. Natl. Acad. Sci. USA **94,** 6279-84

29. Ericson, L.E., and Nilsson, M. (1996) Eur. J. Endocrinol . **135,** 118-27

30. Pezzino, V., Papa, V., Milazzo, G., Gliozzo, B., Russo, P., and Scalia, P. L. (1996) Ann. NY Acad. Sci. **784,** 189-201

31. Schnarr, B., Strunz, K., Ohsam, J., Benner, A., Wacker, J., and Mayer, D. (2000) Int. J. Cancer **89**, 506-513

FIGURE LEGENDS

Fig. 1. IGF-IR overexpression stimulates cell-cell adhesion in E-cad-positive but not in E-cad-negative breast cancer cells. A) E-cad-positive MCF-7 and MCF-7/IGF-IR cells and E-cad-negative MDA-MB-231 and MDA-MB-231/IGF-IR cells were cultured in normal growth medium as 3-D spheroids for 24 h, as described in Materials and Methods, and then photographed under phase contrast. a) MCF-7 cells expressing ~ $6x10^4$ IGF-IR/cell/cell (7); b) MCF-7/IGF-IR, clone 12 expressing ~$5x10^5$ IGF-IGF-IR/cell (7); c) MDA-MB-231 cells with ~$7x10^3$ IGF-IGF-IR/cell (24), and d) MDA-MB-231/IGF-IR, clone 31 with ~ $3x10^5$ IGF-IR/cell (Bartucci et al., in revision). The bar in a) equals 50 μm. **B)** IGF-IR levels in cells pictured in Fig. 1 A, a-d were assessed by WB in 50 μg of cell lysate, as described in Materials and Methods. **C)** MDA-MB-231 and MDA-MB-231/IGF-IR cells were transiently transfected with the E-cad expression plasmid (b and d) or a vector alone (a and c) and then cultured in suspension as 3-D spheroids. The bar in a) equals 100 μm. **D)** E-cad levels in cells pictured in Fig. 1 C, a-d were determined by WB in 50 μg of cell lysate, as described in Materials and Methods.

Fig. 2. Expression of adhesion proteins in MCF-7 and MCF-7/IGF-IR cells. The expression of adhesion proteins and the IGF-IR was studied in 50 μg of protein lysates

obtained from cells cultured as 3-D spheroids in normal growth medium. MCF-7/IGF-IR cells are pooled MCF-7/IGF-IR clones 12, 15, and 17 (Materials and Methods). **A)** The levels of the IGF-IR, E-cad, α-, β-, γ-catenin, and ZO-1 detected by WB using specific Abs (Materials and Methods). **B)** The expression of ZO-1 in MCF-7 cells and in MCF-7/IGF-IR clones 12, 17, and 15, expressing ~ $5x10^5$, $1x10^6$, and $3x10^6$ IGF-IR/cell, respectively (7).

Fig. 3. ZO-1 expression is inhibited in MCF-7/IGF-IR/Y3F cells. MCF-7/IGF-IR cells expressing the wild-type IGF-IR (WT) and MCF-7/IGF-IR/Y3F cells stably transfected with a dominant-negative kinase-defective IGF-IR mutant (Y3F) were synchronized in SFM for 36 h and then stimulated for 15 min with 20 ng/ml IGF-I, as described in Materials and Methods. The expression and tyrosine phosphorylation (PY) of the IGF-IR and IRS-1 in the cells were detected by IP and WB in 500 μg of protein lysates. The binding of p85 subunit of PI-3 kinase to IRS-1 (IRS-1/p85) was studied by WB in IRS-1 IPs. The expression of active ERK1/ERK2 (p-ERK1/2), total ERK1/2, ZO-1 and E-cad was evaluated by WB in 50 μg of total protein lysates. The specific Abs used are listed in Materials and Methods. Similar results were obtained with MCF-7 cells transiently transfected with the IGF-IR/Y3F expression vector.

Fig. 4. ZO-1 mRNA and protein are regulated by IGF-I. A) MCF-7 cells and MCF-7/IGF-IR were synchronized in SFM (time 0) and then stimulated with 20 ng/ml IGF-I for different times (1-72 h). The expression of 7.8 kb ZO-1 mRNA in MCF-7 and MCF-7/IGF-IR cells was studied by Northern blotting in 20 μg of total RNA using a ^{32}P-dCTP-

labeled ZO-1 probe (described in Materials and Methods). 28 and 18 S rRNA are shown as a control of RNA loading. **B)** The expression of ZO-1 protein in IGF-I- treated cells was detected by WB as described under Fig. 3.

Fig. 5. Interactions of ZO-1 with the IGF-IR in the E-cad complex. A) The IGF-IR, E-cad, and ZO-1 were immunoprecipitated (IP) from 500 μg of total protein lysates obtained from MCF-7 and MCF-7/IGF-IR cells cultured as 3-D spheroids in normal growth medium. The IPs were then probed by WB for phosphotyrosine (PY), the IGF-IR (~97 kDa) , ZO-1 (~220 kDa), E-cad (~ 120 kDa), and α-catenin (~102 kDa). **B)** To confirm α-catenin presence in IGF-IR immunoprecipitates, the lysates were first treated with anti-α-catenin Ab (Zymed) O/N to deplete α-catenin, and then immunoprecipitated with either anti-E-cad or anti-IGF-IR Abs. The E-cad and IGF-IR IPs were then probed with another anti-α-catenin Ab (Sigma). Note significantly reduced α-catenin associations with IGF-IR and E-cad compared with that seen in A). **C)** 500 μg of protein lysates were precipitated with anti-α-catenin Ab and probed by WB for α-catenin, actin, and ZO-1. The blots presented in **A, B,** and **C** were identically developed with film exposure time 10 sec.

Fig. 6. Possible interactions between ZO-1 and the IGF-IR within the E-cad complex. The well established connections between E-cad, catenins and actin are shown as solid lines. The proposed connections between the IGF-IR , α-catenin, ZO-1, and actin

are drown as broken lines. At present, it is not known whether the IGF-IR interacts with α-catenin directly, or other intermediate proteins are involved.

Fig. 7. Reduced cell-cell adhesion in MCF-7/IGF-IR/anti-ZO-1 cells. MCF-7/IGF-IR/anti-ZO-1 clones were obtained by stable transfection of MCF-7/IGF-IR cells with an anti-ZO-1 RNA expression plasmid (Materials and Methods). The levels of ZO-1, IGF-IR, and E-cad in the parental MCF-7/IGF-IR cells (A) and in the clones (B and C) were studied by WB in 50 μg of protein lysate. The aggregation of cells was studied in 3-D culture, as described in Materials and Methods. The bar in B) represents 50 μm.

TABLES

TABLE 1. Effects of IGF-IR and ZO-1 expression on cell aggregation in E-cad-positive and -negative breast cancer cells.

Cells	*Spheroids*		
	25 ≤ 50 μm	**50 ≤ 100 μm**	**> 100 μm**
MCF-7	21.0±1.9	96.0±6.7	2.7±0.9
MCF-7/IGF-IR	1.7±0.7	22.3±1.4	86.5±3.9
MCF-7/IGF-IR/anti-ZO-1	75.0±3.5	40.7±2.1	0.0±0.0
MCF-7/Y3F	45.0±2.9	39.8±4.6	0.0±0.0
MDA-MB-231	7.0±0.6	0.5±0.2	0.0±0.0
MDA-MB-231/IGF-IR	12.5±0.8	0.5±0.1	0.0±0.0
MDA-MB-231/E-cad	39.8±3.6	15.2±1.1	0.0±0.0
MDA-MB-231/vector	10.0±1.4	0.6±0.4	0.0±0.0
MDA-MB-231/IGF-IR/E-cad	27.0±2.2	68.3±7.2	8.0±1.5
MDA-MB-231/IGF-IR/vector	18.6±2.2	0.9±0.3	0.0±0.0

The stable cell lines (MCF-7, MCF-7/IGF-IR, MCF-7/IGF-IR/anti-ZO-1, MCF-7/Y3F, MDA-MB-231, and MDA-MB-231/IGF-IR) and transiently transfected populations (MDA-MB-231/E-cad, MDA-MB-231/vector, MDA-MB-231/IGF-IR/E-cad, and MDA-MB-231/IGF-IR/vector) were cultured as 3-D spheroids in normal growth medium. The number of spheroids of different sizes was established as described in Materials and Methods. The values represent a sum of spheroids in 10 optical fields under 10x magnification. The results are average ±SE from at least 3 experiments. Representative 3-D cultures are shown in Fig. 1 and 7.

Fig. 1

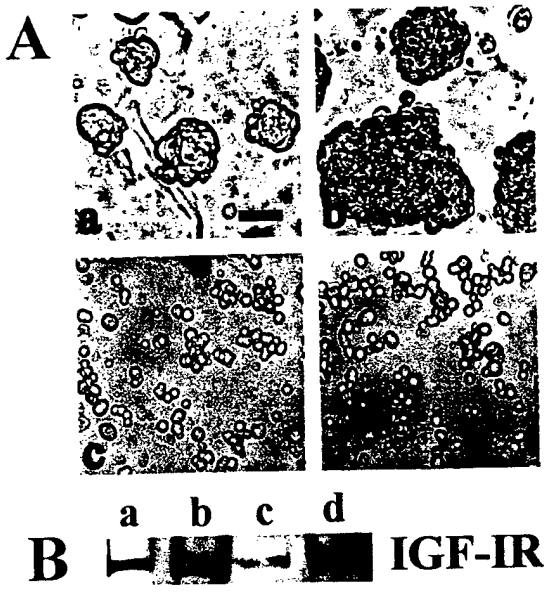

Fig. 1

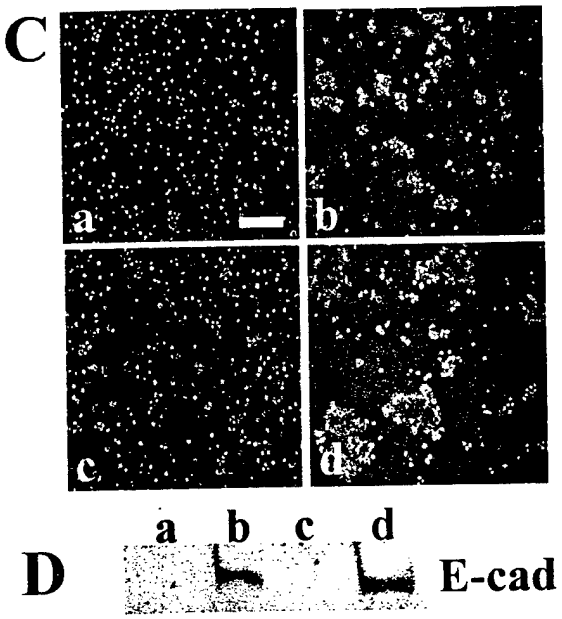

Fig. 2

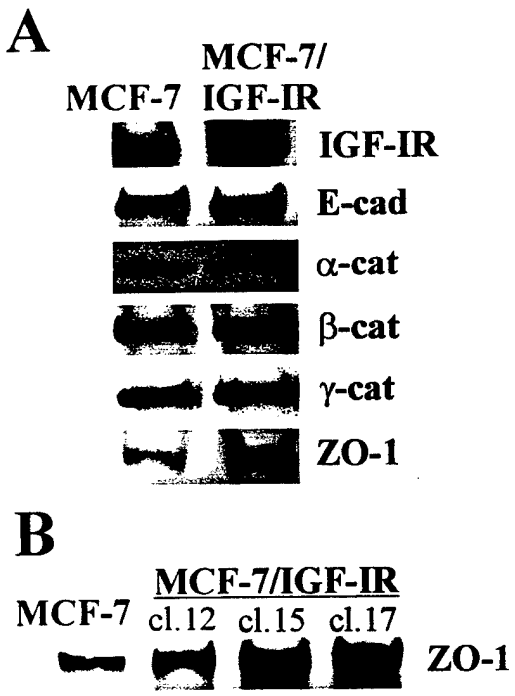
A
MCF-7
MCF-7/
IGF-IR
IGF-IR
E-cad
α-cat
β-cat
γ-cat
ZO-1
B
MCF-7/IGF-IR
MCF-7
cl.12
cl.15
cl.17
ZO-1

Fig. 3

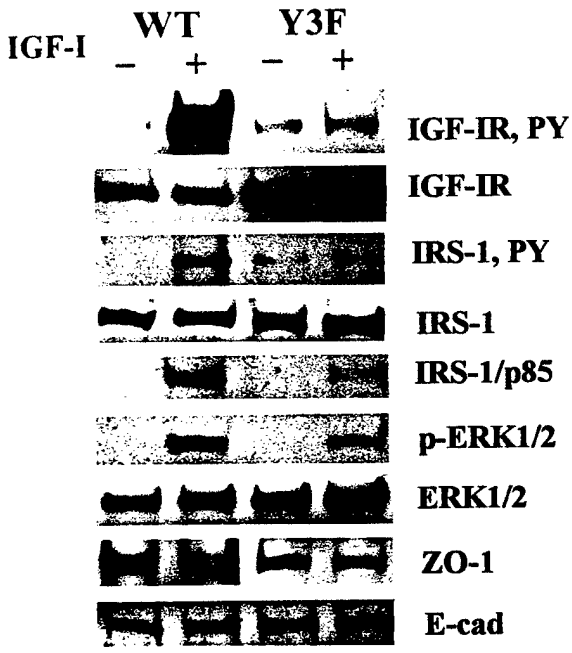
IGF-I
WT
Y3F
–
+
–
+
IGF-IR, PY
IGF-IR
IRS-1, PY
IRS-1
IRS-1/p85
p-ERK1/2
ERK1/2
ZO-1
E-cad

Fig. 4

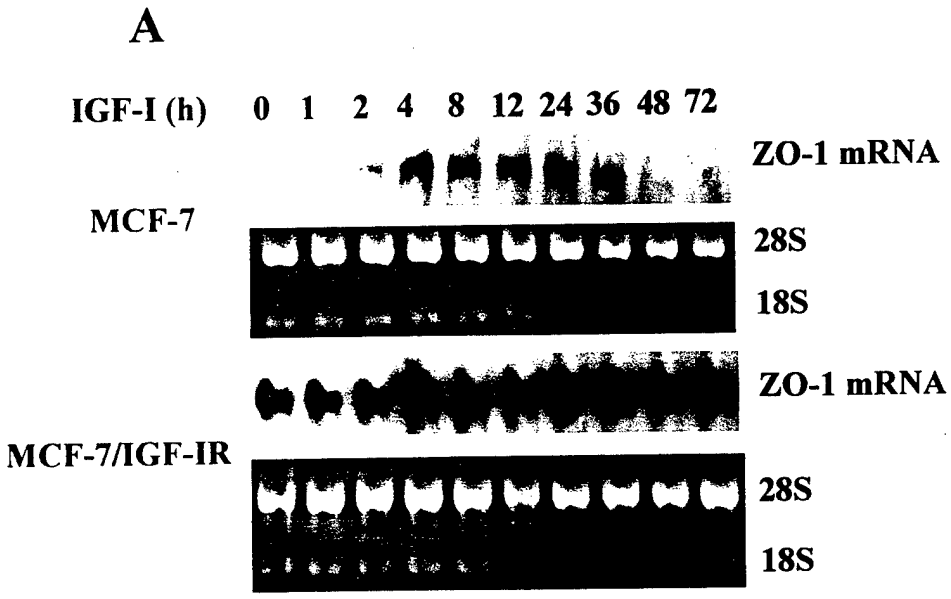
A
IGF-I (h) 0 1 2 4 8 12 24 36 48 72
ZO-1 mRNA
MCF-7
28S
18S
ZO-1 mRNA
MCF-7/IGF-IR
28S
18S

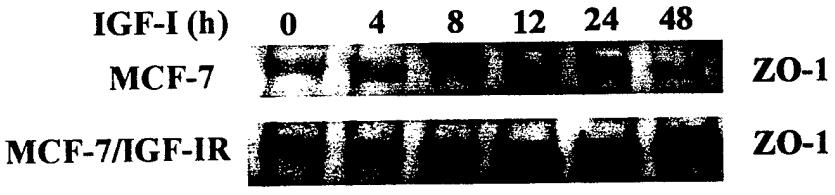
B
IGF-I (h) 0 4 8 12 24 48
MCF-7
ZO-1
MCF-7/IGF-IR
ZO-1

Fig. 5

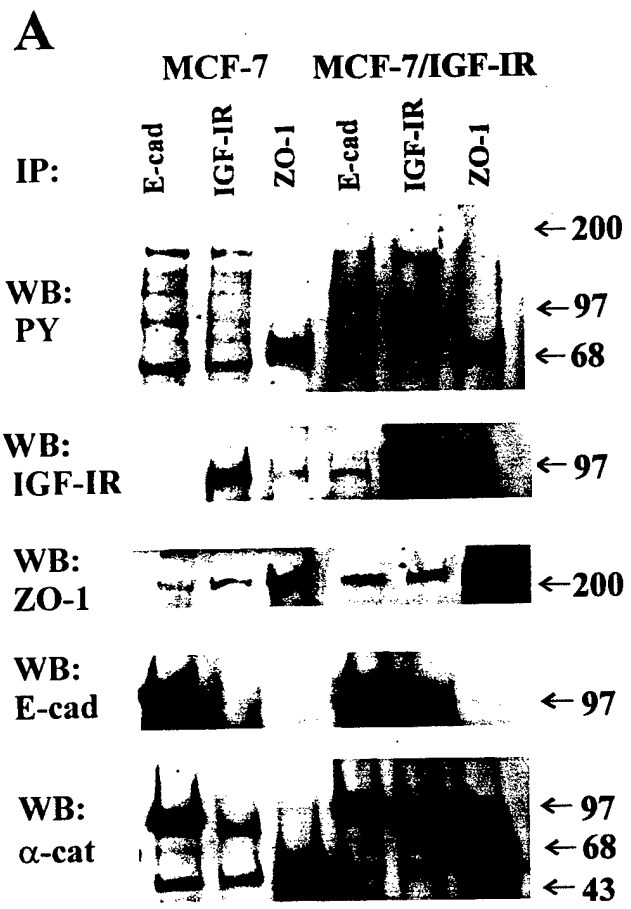
A
MCF-7
MCF-7/IGF-IR
IP:
E-cad
IGF-IR
ZO-1
E-cad
IGF-IR
ZO-1
WB:
PY
←200
←97
←68
WB:
IGF-IR
←97
WB:
ZO-1
←200
WB:
E-cad
←97
WB:
α-cat
←97
←68
←43

Fig. 5

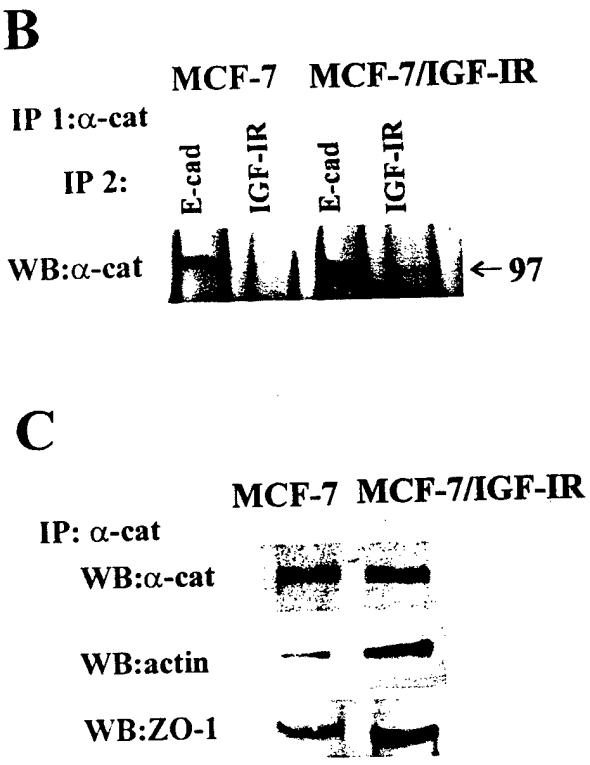
B
MCF-7
MCF-7/IGF-IR
IP 1:α-cat
IP 2:
E-cad
IGF-IR
E-cad
IGF-IR
WB:α-cat
←97
C
MCF-7
MCF-7/IGF-IR
IP: α-cat
WB:α-cat
WB:actin
WB:ZO-1

Fig. 6

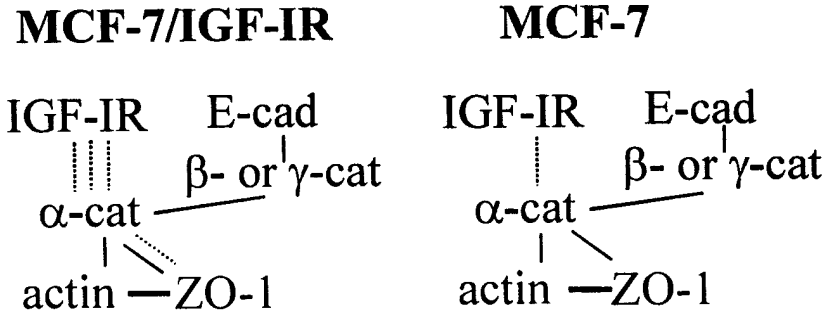
MCF-7/IGF-IR
IGF-IR
E-cad
β- or γ-cat
α-cat
actin
ZO-1
MCF-7
IGF-IR
E-cad
β- or γ-cat
α-cat
actin
ZO-1

Fig. 7

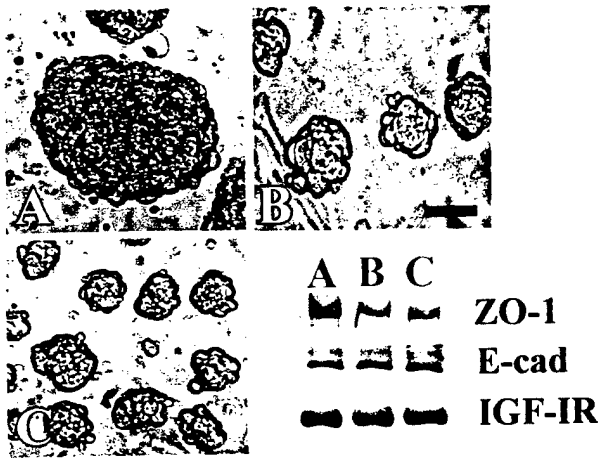

[CANCER RESEARCH 61, ●●–●●●, September 15, 2001]

Differential Insulin-like Growth Factor I Receptor Signaling and Function in Estrogen Receptor (ER)-positive MCF-7 and ER-negative MDA-MB-231 Breast Cancer Cells[1]

Monica Bartucci, Catia Morelli, Loredana Mauro, Sebastiano Ando', and Eva Surmacz[2]

Kimmel Cancer Center, Thomas Jefferson University, Philadelphia, Pennsylvania 19107 [M. B., C. M., L. M., E. S.], and Department of Cellular Biology, University of Calabria, Calabria, Italy [M. B., C. M., L. M., S. A.]

AQ: A

87036

ABSTRACT

Fn1 Fn2 **The insulin-like growth factor I receptor (IGF-IR) is a ubiquitous and multifunctional tyrosine kinase that has been implicated in breast cancer development. In estrogen receptor (ER)-positive breast tumors, the levels of the IGF-IR and its substrate, insulin-receptor substrate 1 (IRS-1), are often elevated, and these characteristics have been linked with increased radioresistance and cancer recurrence. *In vitro*, activation of the IGF-IR/IRS-1 pathway in ER-positive cells improves growth and counteracts apoptosis induced by anticancer treatments. The function of the IGF-IR in hormone-independent breast cancer is not clear. ER-negative breast cancer cells often express low levels of the IGF-IR and fail to respond to IGF-I with mitogenesis. On the other hand, anti-IGF-IR strategies effectively reduced metastatic potential of different ER-negative cell lines, suggesting a role of this receptor in late stages of the disease.**

Here we examined IGF-IR signaling and function in ER-negative MDA-MB-231 breast cancer cells and their IGF-IR-overexpressing derivatives. We demonstrated that IGF-I acts as a chemoattractant for these cells. The extent of IGF-I-induced migration reflected IGF-IR levels and required the activation of phosphatidylinositol 3-kinase (PI-3K) and p38 kinases. The same pathways promoted IGF-I-dependent motility in ER-positive MCF-7 cells. In contrast with the positive effects on cell migration, IGF-I was unable to stimulate growth or improve survival in MDA-MB-231 cells, whereas it induced mitogenic and antiapoptotic effects in MCF-7 cells. Moreover, IGF-I partially restored growth in ER-positive cells treated with PI-3K and ERK1/ERK2 inhibitors, whereas it had no protective effects in ER-negative cells. The impaired IGF-I growth response of ER-negative cells was not caused by a low IGF-IR expression, defective IGF-IR tyrosine phosphorylation, or improper tyrosine phosphorylation of IRS-1. Also, the acute (15-min) IGF-I activation of PI-3 and Akt kinases was similar in ER-negative and ER-positive cells. However, a chronic (2-day) IGF-I exposure induced the PI-3K/Akt pathway only in MCF-7 cells. The reactivation of this pathway in ER-negative cells by overexpression of constitutively active Akt mutants was not sufficient to significantly improve proliferation or survival (with or without IGF-I), which indicated that other pathways are also required to support these functions.

Our results suggest that in breast cancer cells, IGF-IR can control nonmitogenic processes regardless of the ER status, whereas IGF-IR growth-related functions may depend on ER expression.

INTRODUCTION

Fn3 The IGF-IR[3] is a ubiquitous, transmembrane tyrosine kinase that has been implicated in different growth-related and growth-unrelated processes critical for the development and progression of malignant tumors, such as proliferation, survival, and anchorage-independent growth, as well as cell adhesion, migration, and invasion (1, 2).

The IGF-IR is necessary for normal breast biology, but recent clinical and experimental data strongly suggest that the same receptor is involved in the development of breast cancer (1, 3). The IGF-IR is overexpressed (up to 14-fold) in ER-positive breast cancer cells compared with its levels in normal epithelial cells (1, 4, 5). The elevated expression and hyperactivation of the IGF-IR has been linked with increased radioresistance and cancer recurrence at the primary site (4). Similarly, high levels of IRS-1, a major signaling molecule of the IGF-IR, correlated with tumor size and shorter disease-free survival in ER-positive tumors (6, 7).

IGF-IR ligands, IGF-I and IGF-II, are strong mitogens for many hormone-dependent breast cancer cell lines and have been found in the epithelial and/or stromal component of breast tumors (1). Importantly, higher levels of circulating IGF-I predict increased breast cancer risk in premenopausal women (8). *In vitro*, activation of the IGF-IR, especially the IGF-IR/IRS-1/PI-3K pathway in ER-positive breast cancer cells, counteracts apoptosis induced by different anticancer treatments or low concentrations of hormones (1, 9–11). On the other hand, overexpression of either the IGF-IR or IRS-1 in ER-positive breast cancer cells improves responsiveness to IGF and, in consequence, results in estrogen-independent proliferation (1, 12, 13). In agreement with these observations, blockade of IGF-IR activity with various reagents targeting the IGF-IR or its signaling through IRS-1/PI-3K reduced the growth of breast cancer cells *in vitro* and/or *in vivo* (1, 12, 14–17).

The requirement for the IGF-IR/IRS-1 pathway for growth and survival appears to be a characteristic of ER-positive, more differentiated, breast cancer cells. By contrast, ER-negative tumors and cell lines, often exhibiting less differentiated, mesenchymal phenotypes, express low levels of the IGF-IR and often decreased levels of IRS-1 (1, 17, 18). Notably, these cells do not respond to IGF-I with growth (1, 19–22). Despite the lack of IGF-I mitogenic response, the metastatic potential of ER-negative breast cancer cells can be effectively inhibited by different compounds targeting the IGF-IR. For instance, blockade of the IGF-IR in MDA-MB-231 cells by an anti-IGF-IR antibody reduced migration *in vitro* and tumorigenesis *in vivo*, and expression of a soluble IGF-IR in MDA-MB-435 cells inhibited adhesion on the extracellular matrix and impaired metastasis in animals (14, 16, 23). These observations suggested that in ER-negative cells, some functions of the IGF-IR must be critical for metastatic cell spread. Here we addressed the possibility that in ER-negative cells, the IGF-IR selectively promotes growth-unrelated processes, such as migration and invasion, but is not engaged in the transmission of growth and survival signals. Using ER-negative MDA-MB-231 breast cancer cells, we studied IGF-I-dependent pathways involved in migration and the defects in IGF mitogenic signal. For comparison, relevant IGF-I responses were analyzed in ER-positive MCF-7 cells.

Received 8/18/00; accepted 7/17/01.

The costs of publication of this article were defrayed in part by the payment of page charges. This article must therefore be hereby marked *advertisement* in accordance with 18 U.S.C. Section 1734 solely to indicate this fact.

[1] This work was supported by Department of Defense Breast Cancer Research Program Grants DAMD17-96-1-6250, DAMD17-97-1-7211, and DAMD-17-99-1-9407 and by the American-Italian Cancer Foundation.

[2] To whom requests for reprints should addressed, at Kimmel Cancer Center, Thomas Jefferson University, 233 South Tenth Street, BLSB 631, Philadelphia, PA 19107. Phone: (215) 503-4512; Fax: (215) 923-0249; E-mail: surmacz1@jeflin.tju.edu.

[3] The abbreviations used are: IGF-IR, insulin-like growth factor I receptor; IRS-1, insulin-receptor substrate 1; ER, estrogen receptor; GFP, green fluorescent protein; mAb, monoclonal antibody; WB, Western blot; CS, calf serum; IP, immunoprecipitation; pAb, polyclonal antibody; MAPK, mitogen-activated protein kinase; PI-3K, phosphatidylinositol 3-kinase; ERK, extracellular signal-regulated kinase; GSK, glycogen synthase kinase; MEK, MAPK kinase; PRF-SFM, phenol red-free serum-free medium.

MATERIALS AND METHODS

Plasmids. The pcDNA3-IGF-IR expression plasmid encoding the wild-type IGF-IR under the cytomegalovirus promoter was described before (13). The expression plasmids encoding constitutively active forms of Akt kinase, *i.e.*, myristylated Akt and Akt with an activating point mutation (Akt/E40K), were obtained from Drs. P. Tsichlis and T. Chan (Kimmel Cancer Center) and were described before (24). The Akt plasmids contain the HA-tag, allowing for easy identification of Akt-transfected cells. The pCMS-EGFP expression vector encoding GFP was purchased from Clontech.

Cell Lines. MDA-MB-231 cells were obtained from American Type Culture Collection. MDA-MB-231/IGF-IR clones were generated by stable transfection of MDA-MB-231 cells with the plasmid pcDNA3-IGF-IR using a standard calcium phosphate precipitate procedure (13). Transfectants resistant to 1 mg/ml G418 were screened for IGF-IR expression by fluorescence-assisted cell sorting analysis using an anti-IGF-IR mouse mAb α-IR3 (10 μg/ml; Calbiochem) and a fluorescein-conjugated goat antimouse IgG2 (1 μg/ml; Calbiochem). Cells stained with the secondary antibody alone were used as a control. Additionally, the parental MDA-MB-231 cells and MCF-7/IGF-IR clones 12 and 15 (13), all expressing known levels of the IGF-IR, were analyzed in parallel. IGF-IR expression in MDA-MB-213-derived clones was then confirmed by WB with specific antibodies (listed below). In growth and migration experiments, we used control MCF-7/pc2 and MDA-MB-231/5 M cell lines, which have been developed by transfection of MCF-7 and MDA-MB-231 cells with the pcDNA3 vector. MCF-7, MCF-7/pc2, and MCF-7/IGF-IR cells were described in detail previously (13).

Transient Transfection. Seventy % confluent cultures of MDA-MB-231 and MCF-7 cells were transiently cotransfected with an Akt expression plasmid and a plasmid pCMS encoding GFP (Akt:GFP ratio, 20:1) using Fugene 6 (Roche). Transfection was carried out for 6 h in phenol red-free DMEM containing 0.5 mg/ml BSA, 1 μM $FeSO_4$, and 2 mM L-glutamine (referred to as PRF-SFM; Ref. 13); the optimal DNA:Fugene 6 ratio was 1 μg:3 μl. Upon transfection, the cells were shifted to fresh PRF-SFM, and the expression of total and active Akt kinase at 0 (media shift), 2, and 4 days was assessed by WB with specific antibodies (see below). In parallel, the efficiency of transfection was evaluated by scoring GFP-positive cells. In all experiments, at least 40% of transfected cells expressed GFP, which indicated a high transfection efficiency. In addition, the expression of Akt plasmids was monitored by measuring the cellular levels of HA-tag and Akt proteins by WB.

Cell Culture. MDA-MB-231 and MCF-7 cells were grown in DMEM:F12 (1:1) containing 5% CS. MDA-MB-231- and MCF-7-derived clones overexpressing the IGF-IR or expressing vector alone were maintained in DMEM:F12 plus 5% CS plus 200 μg/ml G418. In the experiments requiring 17β-estradiol- and serum-free conditions, the cells were cultured in PRF-SFM (13).

Growth Curves. To analyze the growth in serum-containing medium, the cells were plated in six-well plates in DMEM:F12 (1:1) containing 5% CS at a concentration of 1.5–2.0 $\times$ 10^5 cells/plate; the number of cells was then assessed by direct counting at 1, 2, and 4 days after plating. To study IGF-I-dependent proliferation, the cells were plated in six-well plates in the growth medium as above. The following day (day 0), the cells at ~50% confluence were shifted to PRF-SFM containing 20 ng/ml IGF-I. Cell number was determined at days 1, 2, and 4.

Apoptosis Assay. The cells grown on coverslips in normal growth medium were shifted to PRF-SFM at 70% confluence and then cultured in the presence or absence of 20 ng/ml IGF-I for 0, 12, 24, 48, and 96 h. Apoptosis in the cultures was determined with the *In Situ* Cell Death Detection kit, Fluorescein (Roche), following the manufacturer's instructions. The cells containing DNA strand breaks were stained with fluorescein-dUTP and detected by fluorescence microscopy. Cells that detached during the experiment were spun on glass slides using cytospin and processed as above. Apoptotic index (the percentage of apoptotic cells/total cell number in a sample field) was determined for adherent and floating cell populations, and the indices were combined.

Immunoprecipitation and Western Blotting. Seventy % cultures were shifted to PRF-SFM for 24 h and then stimulated with 20 ng/ml IGF-I for 15 min, 1 h, 1 day, or 2 days. Proteins were obtained by lysing the cells in a buffer composed of 50 mM HEPES (pH 7.5), 150 mM 1% Triton X-100, 1.5 mM $MgCl_2$, 1 mM $CaCl_2$, 5 mM EGTA, 10% glycerin, 0.2 mM Na_3VO_4, 1% phenylmethylsulfonyl fluoride, and 1% aprotinin. The IGF-IR was immunoprecipitated from 500 μg of protein lysate with anti-IGF-IR mAb (Calbiochem) and subsequently detected by WB with anti-IGF-IR pAb (Santa Cruz Biotechnology). IRS-1 was precipitated from 500 μg of lysate with anti-IRS-1 pAb (UBI) and detected by WB using the same antibody. Tyrosine phosphorylation (PY) of immunoprecipitated IRS-1 or IGF-IR was assessed by WB with anti-phosphotyrosine mAb PY20 (Transduction Laboratories). Akt, ERK1/ERK2, and p38 MAPKs (active and total), and active GSK-3 were measured by WB in 50 μg of whole cell lysates with appropriate antibodies from New England Biolabs. The expression of HA-tag was probed by WB in 50 μg of protein lysate with anti-HA mAb (Babco). The intensity of bands representing relevant proteins was measured by laser densitometry scanning.

IRS-1-associated PI-3K Activity. PI-3K activity was determined *in vitro*, as described by us before (25). Briefly, 70% cultures were synchronized in PRF-SFM for 24 h and then stimulated with 20 ng of IGF-I for 15 min or 2 days. Untreated cells were used as controls. IRS-1 was precipitated from 500 μg of cell lysates; IRS-1 IPs were then incubated in the presence of inositol and [^{32}P]ATP for 30 min at room temperature. The products of the kinase reaction were analyzed by TLC using TLC plates (Eastman Kodak). Radioactive spots representing PI-3P were visualized by autoradiography, quantified by laser densitometry (ULTRO Scan XL, Pharmacia), and then excised from the plates and counted in a beta counter.

Motility Assay. Chemotaxis and chemokinesis were tested in modified Boyden chambers containing porous (8-mm), polycarbonate membranes. The membranes were not coated with extracellular matrix. Briefly, 2 $\times$ 10^4 cells (synchronized in PRF-SFM for 24 h) were suspended in 200 μl of PRF-SFM and plated into upper wells. Lower wells contained 500 μl of PRF-SFM. To study chemotaxis, IGF-I (20 ng/ml) was added to lower wells only; to assess chemokinesis, IGF-I was placed in either upper wells only, or in both wells. After 24 h, the cells in the upper wells were removed, whereas the cells that migrated to the lower wells were fixed and stained in Coomassie Blue solution (0.25 g of Coomassie blue:45 ml water:45 ml methanol:10 ml glacial acetic acid) for 5 min. After that, the chambers were washed three times with H_2O. The cells that migrated to the lower wells were counted under the microscope (10, 26).

Inhibitors of PI-3K and MAPK. LY294002 (Biomol Research Labs) was used to specifically inhibit PI-3K (27). UO126 (Calbiochem), a specific inhibitor of MEK1/2, was used to block ERK1 and ERK2 kinases (28), and SB203580 (Calbiochem) was used to down-regulate p38 MAPK (29). To determine optimal concentrations of the compounds, different doses (1–100 μM) of the inhibitors were tested in cells treated for 1, 8, 12, and 24 h in PRF-SFM. Additionally, the efficacy of all inhibitors in blocking the phosphorylation of relevant downstream targets (Akt, ERK1/ERK2, and p38 kinases) was determined by WB. In this experiment, the cells were stimulated with IGF-I (20 ng/ml) for 15 min. LY294002 and UO126 were supplemented simultaneously with IGF-I, whereas SB203580 was added 30 min before IGF-I treatment. Ultimately, for both growth and migration experiments, LY294002 was used at the concentration 50 μM, UO126 at 5 μM, and SB203580 at 10 μM. At these doses, the inhibitors did not affect cell proliferation and survival at 24 h, with the exemption of LY294002, which inhibited (by 20%) the proliferation of MCF-7/IGF-IR clone 12 in PRF-SFM. A shorter treatment (12 h) with LY294002 had no impact on the growth and survival of the cells (evaluated by cell proliferation and *In Situ* Cell Death Detection assays, as described above). Thus, the effects of LY294002 on migration were assessed at 12 h, whereas the actions of UO126 and SB203580 were assessed at 24 h of treatment.

RESULTS

MDA-MB-231/IGF-IR Cells. To study growth-related and growth-unrelated effects of IGF-I in ER-negative cells breast cancer cells, we used the MDA-MB-231 cell line. These cells express low levels of the IGF-IR and do not respond to IGF-I with growth (19, 22). Because it has been established that mitogenic response to IGF-I requires a threshold level of the IGF-IR (*e.g.*, in NIH 3T3-like fibroblasts, ~1.5 $\times$ 10^4 IGF-IRs; Refs. 30, 31), our first goal was to test whether increasing IGF-IR expression would induce IGF-I-dependent growth in MDA-MB-231 cells. To this end, several MDA-MB-231 clones overexpressing the IGF-IR (MDA-MB-231/IGF-IR

AQ: B

AQ: C

cells) were generated by stable transfection, and the receptor content was analyzed by binding assay, fluorescence-assisted cell sorting analysis (data not shown), and WB (Fig. 1). We determined that MDA-MB-231 clones 2, 21, and 31 express approximately 3×10^4, 1.5×10^4, and 2.5×10^5 IGF-IRs/cell, respectively, whereas the parental MDA-MB-231 cells express approximately 7×10^3 IGF-IRs/cell (19). For comparison, $\sim 6 \times 10^4$ IGF-IRs were found in ER-positive MCF-7 cells (Fig. 1; Ref. 13).

IGF-IR Overexpression Does Not Enhance the Growth of MDA-MB-231/IGF-IR Cells in Serum-containing Medium. The analysis of growth profiles of different MDA-MB-231/IGF-IR clones indicated that overexpression of the IGF-IR never improved basal proliferation in normal growth medium, and in the case of clone 31, which expressed the highest IGF-IR content ($\sim 2.5 \times 10^5$ IGF-IRs/cell), an evident growth retardation at days 2 and 4 ($P < 0.05$) was observed (Fig. 2*A*). In contrast, similar overexpression of the IGF-IR in ER-positive MCF-7 cells significantly augmented proliferation (Fig. 2*B*). The growth of control clones MDA-MB-231/5 M and MCF-7/pc2 was comparable with that of the corresponding parental cell lines (Fig. 2).

IGF-IR Overexpression Does Not Promote IGF-I-dependent Growth or Survival of MDA-MB-321 Cells. Subsequent studies established that increasing the levels of the IGF-IR from 7×10^3 up

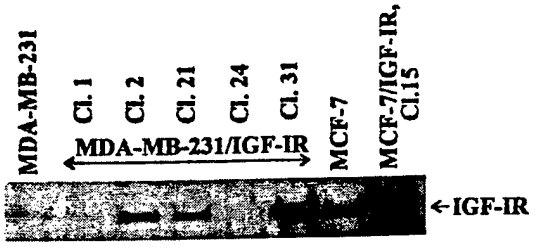

Fig. 1. MDA-MB-231/IGF-IR clones. MDA-MB-231/IGF-IR cells were generated by stable transfection with an IGF-IR expression vector, as described in "Materials and Methods." In several G418-resistant clones, the expression of the IGF-IR protein was tested in 50 μg of total protein lysate by WB with anti-β subunit IGF-IR pAb (Santa Cruz Biotechnology). For comparison, MCF-7 cells and MCF-7/IGF-IR clone 15 with known levels of IGF-IR (6×10^4 and 3×10^6, respectively; Ref. 13) are shown. Low levels of IGF-IR in MDA-MD-231 cells ($\sim 7 \times 10^3$ receptors/cell) are not well visible in this blot but were detectable in its phosphorylated form by IP and WB in 500 μg of protein lysates (see Fig. 4*A*). The estimated expression of the IGF-IR in clones 2, 21, and 31 is 1.5×10^4, 3×10^4, and 2.5×10^5 receptors/cell, respectively.

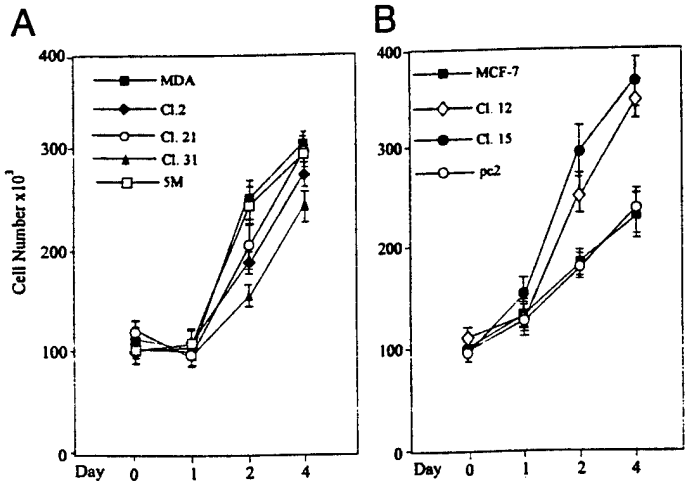

Fig. 2. Effect of IGF-IR overexpression on the growth of ER-negative and ER-positive cells in serum-containing medium. MDA-MB-231 cells, MDA-MB-231/IGF-IR clones 2, 21, and 31 (*A*), and their ER-positive counterparts, MCF-7 cells and MCF-7/IGF-IR, clones ER 12 and 15 (*B*), were plated in DMEM:F12 plus 5% CS. The cells were counted at 50% confluence (day 0) and at subsequent days 1, 2, and 4. Control clones MDA-MB-231/5 M and MCF-7/pc2 expressing the pcDNA3 vector alone were used as controls (*A* and *B*). The results are averages from three experiments. *Bars*, SD.

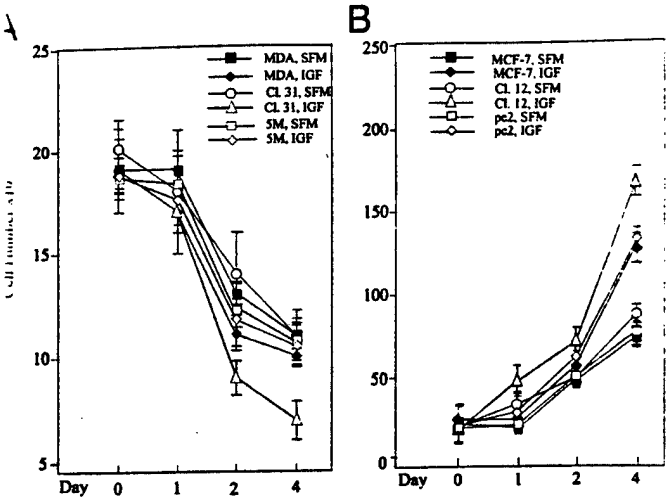

Fig. 3. IGF-I-dependent growth and survival of ER-negative and ER-positive breast ncer cells. ER-negative (*A*) and ER-positive (*B*) cells were synchronized in PRF-SFM id treated with IGF-I, as described in "Materials and Methods." The cells were counted : days 0, 1, 2, and 4 of treatment. The results are averages from at least three experiments. *ars*, SD.

Table 1 *Effects of IGF-I on apoptosis in ER-negative and ER-positive cells*

Apoptosis was studied in MDA-MB-231 cells, MDA-MB-231/IGF-IR clone 31, ICF-7 cells, and MCF-7/IGF-IR clone 12. The cells were cultured for 48 h in PRF-SFM, id the apoptotic index (% apoptotic cells/total cell number in the field) was determined v terminal deoxynucleotidyl transferase-mediated nick end labeling, as described in 'Aaterials and Methods." The results are averages from at least three experiments; SDs :e given.

Cell line	Apoptosis (%)	
	SFM	SFM + IGF-I
MDA-MB-231	41.4 ± 3.0	46.0 ± 1.9
MDA-MB-231/IGF-IR	50.1 ± 4.1	53.3 ± 4.2
MCF-7	14.5 ± 0.2	4.2 ± 0.1
MCF-7/IGF-IR	10.1 ± 1.3	2.8 ± 0.1

) 2.5×10^5 was not sufficient to induce IGF-I-dependent growth :sponse in MDA-MB-231 cells. In fact, similar to the parental and IDA-MB-231/5 M cells, all MDA-MB-231/IGF-IR clones were pro-ressively dying in PRF-SFM with or without 20 ng/ml IGF-I (Fig. A). In all ER-negative cell lines, the rate of cell death was signifi- F3 antly increased at days 2 and 4 of the experiment. Notably, at these ıer time points, MDA-MB-231/IGF-IR clone 31 was dying faster in ıe presence of IGF-I than in PRF-SFM and more rapidly than the arental cells (Fig. 3*A* and data not shown). Conversely, in ER-ositive cells, the stimulation of the IGF-IR always induced prolifer-ion. In addition, at later time points, especially at day 4, the growth ıe in IGF-I was significantly ($P < 0.05$) increased in MCF-7/IGF-IR AQ: D ells relative to that in MCF-7 or MCF-7/pc2 cells (Fig. 3*B*).

The analysis of the antiapoptotic effects of IGF-I in the above cell nes cultured for 48 h under PRF-SFM indicated that IGF-I reduced optosis, by ~3-fold, in ER-positive cells, but it was totally ineffec-ve in MDA-MB-231 and MDA-MB-231/IGF-IR cells (Table 1). T1

IGF-IR Signaling in MDA-MB-231 and MDA-MB-231/IGF-IR Cells. Next, we investigated molecular basis underlying the lack of GF-I growth response in ER-negative cells. IGF-I signaling was udied in MDA-MB-231 cells, MDA-MB-231, clone 31, and in arallel, in ER-positive MCF-7 and MCF-7/IGF-IR cells. The exper-nents focused on IGF-IR tyrosine kinase activity and several pos-eceptor signaling pathways that are known to control the growth and rvival of ER-positive breast cancer cells (and many other cell pes), *i.e.*, the IRS-1/PI-3K, Akt, and ERK1/ERK2 pathways (1, 17, 3. 32–34). We also analyzed other IGF-I effectors that have been

shown to contribute to nonmitogenic responses in ER-positive breast cancer cells, such as p38 kinase and SHC (10, 26, 35).

Because both acute and chronic effects of growth factors are important for biological response (36), we studied IGF-IR signaling at different times after stimulation: 15 min, 1 h, 2 days, and 4 days. In both ER-positive and ER-negative cell types, IGF-I signaling seen at 15 min was identical to that at 1 h, whereas IGF-I response at 2 days was similar to that at 4 days. Thus, Fig. 4 demonstrates the representative results obtained with cells stimulated for 15 min and 2 days. F4

In MDA-MB-231 and MDA-MB-231/IGF-IR cells, IGF-IR and its major substrate, IRS-1, were tyrosine phosphorylated at both time points in a manner roughly reflecting the receptor levels. The activation of both molecules was stronger just after stimulation and weaker at 2 days of the treatment (Fig. 4*A*). Analogous IGF-I effects were seen in MCF-7 cells and their IGF-IR-overexpressing derivatives (Fig. 4*B*). A basal level of IGF-IR and IRS-1 tyrosine phosphorylation was observed in cells expressing high receptor levels. This effect most likely can be attributed to the autocrine stimulation of the IGF-IR by IGF-I-like factors (12).

One of the major growth/survival pathways initiated at IRS-1 is the PI-3K pathway (32, 37). The repeated measurements of IRS-1-associated PI-3K activity *in vitro* demonstrated that at 15 min after IGF-I addition, PI-3K activity was similar in both cell types, but at 2 days, in MDA-MB-231 and MDA-MB-231/IGF-IR cells, IGF-I did not stimulate PI-3K through IRS-1, or induced it very weakly, whereas in MCF-7 and MCF-7/IGF-IR cells, a significant level of PI-3K activation was observed (Fig. 5). F5

The *in vitro* activity of PI-3K was reflected by the stimulation of its downstream effector, Akt kinase. At 15 min, Akt was up-regulated in response to IGF-I an all cell lines, but at 2 days, no effects of IGF-I were seen in MDA-MB-231 and MDA-MB-231/IGF-IR cells, whereas up-regulation of Akt was still evident in MCF-7 and MCF-7/IGF-IR cells (Fig. 4, *C* and *D*). Akt is known to phosphorylate (on Ser-9) and down-regulate GSK-3β (23, 32, 34). We found that in both cell types, the phosphorylation of GSK-3β reflected the dynamics of Akt activity, with no induction of phosphorylation observed at 2 days in ER-negative cells (Fig. 4*C*) and IGF-I-stimulated phosphorylation in MCF-7 and MCF-7/IGF-IR cells (by 40 and 120%, respectively; Fig. 4*D*).

Another IGF-IR growth/survival pathway involves ERK1 and ERK2 kinases (1, 36, 38). This pathway was strongly up-regulated at 15 min and weakly induced at 2 days in MCF-7 and MCF-7/IGF-IR cells. In MDA-MB-231 and MDA-MB-231/IGF-IR cells, the basal activation of ERK1/2 kinases was always high, and the addition of IGF-I only minimally (10–20%) induced the enzymes at 15 min with no effects seen at 2 days (Fig. 4, *E* and *F*).

p38, a stress-induced MAPK and a known mediator of nongrowth responses in breast cancer cells (35), was strongly stimulated by IGF-I in ER-negative cells at 15 min (Fig. 4*E*). By contrast, in ER-positive cells, the enzyme was much stronger when induced at 2 days than at 15 min (Fig. 4*F*). The stimulation of SHC, a substrate of the IGF-IR involved in migration and growth in ER-positive cells (10, 26), was weak in all cell types, and no differences in the activation patterns were observed (data not shown).

Reactivation of Akt Kinase in MDA-MB-231 Cells. Previous results indicated that MDA-MB-231 and MDA-MB-231/IGF-IR cells are unable to sustain IGF-I-dependent activation of the PI-3K/Akt survival pathway when cultured in the absence of serum for 2–4 days. Consequently, we tested whether cell death under PRF-SFM conditions can be reversed by a forced overexpression of the Akt kinase. Two different expression plasmids encoding constitutively active forms of Akt, Myr-Akt, and Akt/E40K (24) were transiently transfected into MDA-MB-231 cells. The efficiency of transfection was at least 40% (by scoring GFP-positive cells); correspondingly, the transfected cells expressed elevated (by ~40%) levels of the Akt protein and exhibited enhanced Akt phosphorylation (Fig. 6*A*). The improved biological activity of Akt in the transfected cells was indicated by down-regulation of the prolonged ERK1/2 stimulation (39, 40), which was noticeable at day 2 (data not shown) and most pronounced at day 4 (~50 and 40% for Myr-Akt and Akt/E40K, respectively; Fig. 6*B*) The expression of constitutively active Akt mutants was reflected by a tendency of MDA-MB-231 cells to survive better at 2 days after transfection (at the time of the greatest Akt activity), but the differ- F6

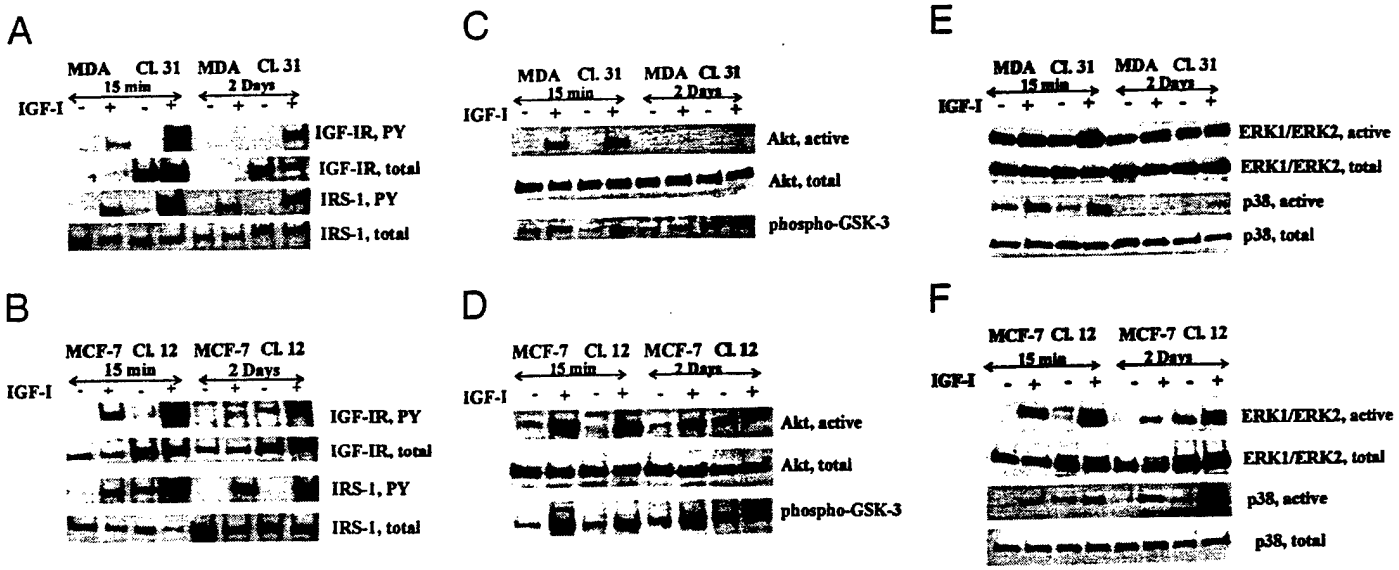

Fig. 4. IGF-I signaling in ER-negative and ER-positive breast cancer cells. The activation of IGF-IR/IRS-1 signaling (*A* and *B*), Akt/GSK-3 signaling (*C* and *D*), and ERK1/ERK2 and p38 kinase signaling (*E* and *F*) was tested in MDA-MB-231 cells, MDA-MB-231/IGF-IR clone 31, MCF-7 cells, and MCF-7/IGF-IR clone 12. The cells were synchronized in PRF-SFM and treated with IGF-I for 15 min or 2 days. The cellular levels of the IGF-IR and IRS-1 were detected by IP and WB in 500 μg of total protein lysate using specific antibodies (see "Materials and Methods"). IGF-IR and IRS-1 tyrosine phosphorylation (PY) was assessed upon stripping and reprobing the same filters with the anti-PY20 antibody. The levels and activity of Akt, GSK-3, ERK1/ERK2, and p38 kinases were probed by WB in 50 μg of total cellular lysates using specific antibodies. The antibodies used are listed in "Materials and Methods." Representative results of at least three repeats are shown. Note decreased IRS-1 expression in *15 min IGF-I* treatment in ER-positive cells, as described before (47).

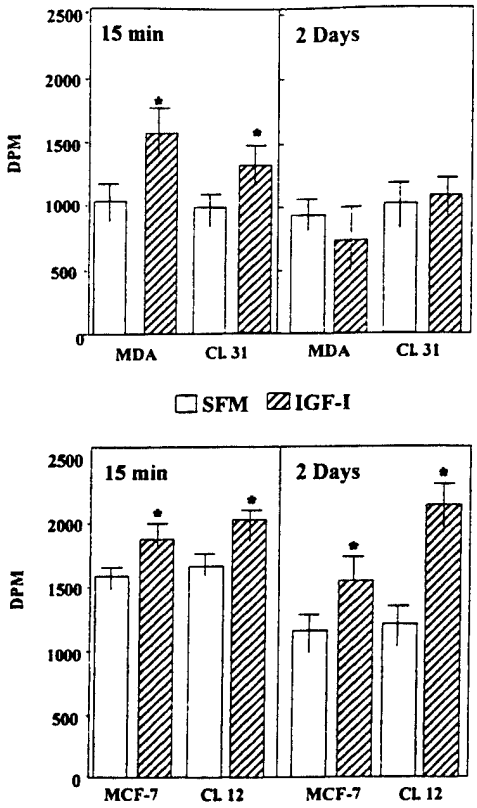

Fig. 5. IGF-I-induced PI-3K activity in ER-negative and ER-positive cells. MDA-MB-231 cells, MDA-MB-231/IGF-IR clone 31, MCF-7 cells, and MCF-7/IGF-IR clone 12 were synchronized in PRF-SFM and treated with IGF-I for 15 min or 2 days. IRS-1-bound PI-3K activity was measured *in vitro* in IRS-1 IPs as described in "Materials and Methods." The experiments were repeated three times for ER-positive cells and five times for ER-negative cells. *Bars*, SD. *, statistically significant differences between untreated and IGF-I-treated cells.

ences did not reach statistical significance ($P > 0.05$; Fig. 6*C* and data not shown).

Inhibition of IGF-IR Signaling Pathways. To complement the above studies, we examined the importance of the PI-3K, ERK1/ERK2, and p38 kinase pathways in IGF-I-dependent growth and survival of ER-positive and ER-negative breast cancer cells using specific inhibitors (27–29). The efficacy of PI-3K and ERK1/ERK2 inhibitors was first tested by establishing their effects on the activity of target proteins (Fig. 7). Table 2 demonstrates the impact of the compounds on cell growth/survival at 2 days of treatment. The inhibition of PI-3K with LY294002 reduced the growth of MCF-7 and MCF-7/IGF-IR cells, but it did not influence or had only minimal effects on MDA-MB-231 and MDA-MB-231/IGF-IR cells. Furthermore, the action of LY294002 was counteracted by IGF-I in ER-positive, but not in ER-negative, cells. The inhibition of MEK1/2 and ERK1/ERK2 with UO126 reduced the growth and/or survival in both cell types, but only in MCF-7 and MCF-7/IGF-IR cells was IGF-I able to oppose this effect. Down-regulation of p38 kinase with SB203580 reduced the survival of MDA-MB-231 and MDA-MB-231/IGF-IR cells and to a lesser extent the growth and survival of MCF-7 and MCF-7/IGF-IR cells. IGF-I did not reverse the antimitogenic action of the p38 kinase inhibitor in either of the cell lines studied (Table 2). Cumulatively, these results suggested that in ER-positive cells, IGF-I transmits mitogenic signals through PI-3K and ERK1/ERK2 pathways. By contrast, IGF-I does not induce growth or survival signal through these pathways in ER-negative cells.

IGF-I Stimulates Migration of MDA-MB-231 Cells. We investigated the nonmitogenic effects of IGF-I in ER-negative and ER-positive breast cancer cells. Unlike with the growth and survival responses, we found that the IGF-IR transmitted nonmitogenic signals in MDA-MB-231 and MDA-MB-231/IGF-IR cells. Specifically, in the chemotaxis experiments, IGF-I placed in lower wells stimulated migration of ER-negative cells in a manner reflecting IGF-IR content. Similarly, the same IGF-I doses induced migration in ER-positive cells (Table 3). The addition of IGF-I to the upper well or both upper and lower wells always suppressed chemotaxis of all cell lines (Table 3).

IGF-I Pathways Regulating Migration of MDA-MB-231 Cells. Using the inhibitors of PI-3K, ERK1/ERK2, and p38 kinases, we determined which pathways of the IGF-IR are involved in migration of ER-negative and ER-positive cells. The treatment was carried out for 24 h (UO126 and SB203580) or 12 h (LY294002) and did not affect cell growth and/or survival with or without IGF-I (see "Materials and Methods"). As demonstrated in Table 4, down-regulation of PI-3K with LY294002 inhibited basal migration of both cell types, with a more pronounced effect in ER-negative cells. Similarly, blockade of p38 kinase inhibited motility of all cell lines studied. The inhibition of MEK1/2 and ERK1/2 with UO126 never suppressed the

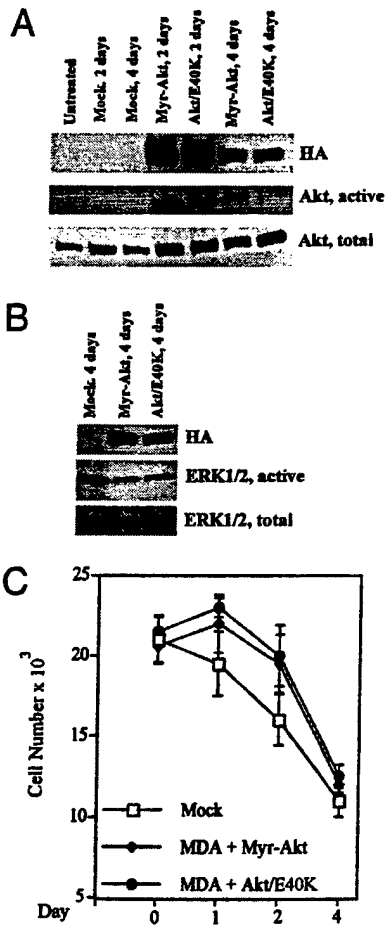

Fig. 6. Effect of increased Akt activity on the survival of MDA-MB-231 cells. MDA-MB-231 cells were transiently transfected with expression plasmids encoding two different constitutively active Akt kinase mutants (Myr-Akt and Akt/E40K; Ref. 24). The Akt vectors contained HA-tag for easy detection. The cells treated with the transfection mixture lacking plasmid DNA (*Mock*) served as control. The expression of the plasmids, as well as the activity and the levels of Akt kinase in the transfected cells, was monitored at 2 and 4 days after transfection. Fifty μg of total protein lysates were sequentially probed by WB with anti-HA, anti-active Akt and then anti-total Akt-specific antibodies (described in "Materials and Methods"). Representative results of four repeats are shown (*A*). To assess biological activity of Akt, the levels of total and active ERK1/2 in cells transfected with the Myr-Akt expression vector were probed in 50 μg of total cell lysate using specific antibodies; the inhibition of ERK1/2 at 4 days after transfection is shown (*B*). *C*, in parallel, the number of cells was determined at days 0 (posttransfection medium change), 1, 2, and 4 after transfection. The results are averages from four experiments. *Bars*, SD.

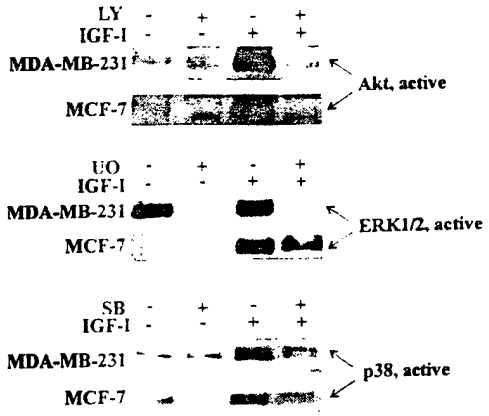

Fig. 7. PI-3K and MAPK inhibitors. Synchronized cultures of MDA-MB-231 and MCF-7 cells were treated with LY294002, UO126, or SB203580 in the presence or absence of IGF-I, as described in "Materials and Methods." The activities of Akt, ERK1/ERK2, and p38 kinases were determined by WB in 50 μg of protein lysates using specific antibodies. Representative results are shown.

migration of ER-positive and ER-negative cells; in fact, the compound stimulated cell motility. The addition of IGF-I as a chemoattractant significantly counteracted the effects of all three inhibitors; however, no clear association between the cellular levels of the IGF-IR and this competing action of IGF-I was noted (Table 4). These results suggested that IGF-I-dependent motility in both types of cells requires the PI-3K and p38 pathways but does not rely on the activity of ERK1/ERK2.

DISCUSSION

The experimental and clinical evidence supports the notion that hyperactivation of the IGF-IR may be critical in early steps of breast cancer development, promoting cell growth, survival, and resistance to therapeutic treatments. However, the function of the IGF-IR in the later stages of the disease, including metastasis, is still obscure (1). For instance, whereas the IGF-IR has been found overexpressed in primary breast tumors, its levels, similar to ER levels, appear to undergo reduction during the course of the disease (1, 18). According to Pezzino *et al.* (41), who studied the IGF-IR status in two patient subgroups representing either a low risk (ER- and progesterone receptor-positive, low mitotic index, diploid) or a high risk (ER- and progesterone receptor-negative, high mitotic index, aneuploid) population, there is a highly significant correlation between IGF-IR expression and better prognosis. Similar conclusions were reached by Peyrat and Bonneterre (42) and recently by Schnarr *et al.* (18). Therefore, it has been proposed that similar to the ER, the IGF-IR marks more differentiated tumors with better clinical outcome. However, it has also been argued that the IGF-IR may play a role in early steps of tumor spread because node-positive/IGF-IR-positive tumors appeared to have a worse prognosis than node-negative/IGF-IR-positive tumors (1, 42). In addition, quite rare cases of ER-negative but IGF-IR-positive tumors are associated with shorter disease-free survival (43).

In breast cancer cell lines, a hormone-dependent and less aggressive phenotype correlates with a good IGF-IR expression (1, 19, 42). By contrast, different ER-negative, breast cancer cell lines express low levels of the IGF-IR and generally do not respond to IGF-I with growth (1, 18–22). However, many ER-negative cell lines appear to depend on the IGF-IR for tumorigenesis and metastasis. For instance, blockade of the IGF-IR in MDA-MB-231 cells by anti-IGF-IR antibody reduced migration *in vitro* and tumorigenesis *in vivo*, and expression of a soluble IGF-IR in MDA-MB-435 cells impaired growth, tumorigenesis, and metastasis in animal models (1, 14, 16, 23). These observations suggest that some growth-unrelated pathways of the IGF-IR may be operative in the context of ER-negative cells.

Here we studied whether this particular IGF-I dependence of ER-negative breast cancer cells relates to the nonmitogenic function of the IGF-IR, such as cell migration. Our experiments indicated that the IGF-IR is an effective mediator of cell motility. Furthermore, IGF-I-induced migration was proportional to IGF-IR content. We demonstrated, for the first time, that in MDA-MB-231 ER-negative cells, IGF-IR signaling pathways responsible for cell movement include PI-3K and p38 kinases. Indeed, an acute IGF-I stimulation of MDA-MB-231 and MDA-MB-231/IGF-IR cells appears to induce both PI-3K and p38 kinases, suggesting that this short-time activation may be involved in migration. Both of these pathways have been shown previously to regulate cell motility in breast cancer cells and other cell types (35, 44). Interestingly, the migration of both ER-negative and ER-positive cells was enhanced by a specific MEK1/MEK2 inhibitor UO126. We observed this effect over a broad range of UO126 doses (1–10 μM) and in several MDA-MB-231- and MCF-7-derived clones; the same doses always suppressed cell proliferation in serum-containing medium and PRF-SFM (data not shown and Table 2). These

Table 3 *IGF-I-induced migration in ER-negative and ER-positive breast cancer cells*

The IGF-I-induced migration of MDA-MB-231 and MCF-7 cells, their IGF-IR-overexpressing derivatives, as well as control clones MDA-MB-231/5M and MCF-7/pc2, was determined after 24 hr, as described in "Materials and Methods." At this time point, IGF-I did not produce statistically significant differences in the growth and survival of the cells studied (Fig. 3). Migration (%) represents the difference (in %) between basal migration in PRF-SFM and migration in the presence of IGF-I. The chemotaxis results are averages (±SE) from at least nine experiments. The chemokinesis results are averages (±SE) from three experiments.

	Migration (%)[a]		
Cell line	Lower well	Upper well	Both wells
MDA-MB-231	+24 ± 3.9	+2 ± 0.1	+7 ± 0.4
MDA-MB-231/IGF-IR	+79 ± 4.1	+10 ± 0.1	+12 ± 0.5
MDA-MB-231/5M	+20 ± 2.0	+1 ± 0.0	+5 ± 0.1
MCF-7	+23 ± 4.7	−1 ± 0.0	−2 ± 0.0
MCF-7/IGF-IR	+47 ± 5.6	−10 ± 0.5	−8 ± 0.2
MCF-7/pc2	+17 ± 3.1	0 ± 0.0	−1 ± 0.0

[a] IGF-I.

Table 2 *Effects of PI-3K and MAPK inhibitors on growth and survival of ER-negative and ER-positive breast cancer cells*

MDA-MB-231 cells, MDA-MB-231/IGF-IR clone 31, MCF-7 cells, and MCF-7/IGF-IR clone 12 were cultured in PRF-SFM with or without IGF-I in the presence or absence of the inhibitors for 48 h, as described in "Materials and Methods." The difference (in percentages) between the number of live cells under treatment and the number of cells cultured under control conditions (without inhibitors) was defined as inhibition (%). The results are averages from three experiments; SDs are given.

	Inhibition (%)					
	LY294002 (PI-3K)		UO126 (MEK)		SB203580 (p38)	
Cell line	SFM	+IGF	SFM	+IGF	SFM	+IGF
MDA-MB-231	9.4 ± 1.0	7.8 ± 0.8	35.0 ± 2.5	39.0 ± 2.7	47.8 ± 2.2	42.5 ± 4.4
MDA-MB-231/IGF-IR	11.1 ± 1.2	12.3 ± 0.9	18.3 ± 0.9	22.9 ± 1.3	29.5 ± 2.0	35.6 ± 3.6
MCF-7	68.8 ± 3.3	35.0 ± 1.2	42.6 ± 3.8	26.3 ± 2.5	11.7 ± 1.2	10.0 ± 0.4
MCF-7/IGF-IR	73.2 ± 6.7	34.6 ± 2.7	49.4 ± 3.9	20.2 ± 1.5	24.7 ± 0.2	25.9 ± 0.9

Table 4 *Effects of PI-3K and MAPK inhibitors on migration of ER-negative and ER-positive breast cancer cells*

The migration of MDA-MB-231 cells, MDA-MB-231/IGF-IR clone 31, MCF-7 cells, and MCF-7/IGF-IR clone 12 was tested in modified Boyden chambers as described in "Materials and Methods." The inhibitors were added to the upper wells at the time of cell plating, and their effect on basal (SFM) or IGF-I-induced (+IGF) migration was assessed after 24 h (for UO126 and SB203580) or 12 h (for LY94002). At these time points, the compounds did not affect cell growth and survival. The values represent the percentage of change relative to the migration at basal conditions in PRF-SFM (SFM) without inhibitors or chemoattractants. The experiments were repeated at least three times; the average results (±SD) are given.

	Change (%)					
	LY294002 (PI-3K)		UO126 (MEK)		SB203580 (p38)	
Cell line	SFM	+IGF	SFM	+IGF	SFM	+IGF
MDA-MB-231	−45.1 ± 1.1	−18.9 ± 0.9	+53.4 ± 3.5	+36.4 ± 2.2	−30.2 ± 2.9	−8.5 ± 0.7
MDA-MB-231/IGF-IR	−38.3 ± 3.5	−12.2 ± 0.4	+29.0 ± 2.0	+12.6 ± 0.7	−40.1 ± 0.4	−2.5 ± 0.0
MCF-7	−24.7 ± 1.2	−9.6 ± 0.9	+94.9 ± 3.9	+56.4 ± 1.7	−18.9 ± 1.1	−5.6 ± 0.2
MCF-7/IGF-IR	−20.4 ± 1.0	−8.0 ± 0.7	+65.6 ± 5.4	+23.8 ± 1.9	−24.8 ± 0.8	−1.7 ± 0.1

peculiar effects suggest that MEK1/2 may represent a regulatory point balancing mitogenic and nonmitogenic cell responses.

In contrast with the positive effects of IGF-I on cell motility in ER-negative and ER-positive breast cancer cells, this growth factor never stimulated the proliferation of MDA-MB-231 cells, whereas it induced the growth of MCF-7 cells and MCF-7-derived clones overexpressing the IGF-IR. It is has been established by Rubini *et al.* (30) and Reiss *et al.* (31) that mitogenic response to IGF-I requires a threshold level of IGF-IR expression (in fibroblasts, $\sim 1.5 \times 10^4$). Here, we demonstrated that increasing the levels of the IGF-IR from $\sim 7 \times 10^3$ up to $\sim 2.5 \times 10^5$ and subsequent up-regulation of IGF-IR tyrosine phosphorylation was not sufficient to induce IGF-I-dependent growth of MDA-MB-213 cells. Similar results were obtained by Jackson and Yee (21), who showed that overexpression of IRS-1 in ER-negative MDA-MB-435A and MDA-MB-468 breast cancer cells did not stimulate IGF-I-dependent mitogenicity. These authors suggested that the lack of IGF-I response, even in IRS-1-overexpressing ER-negative cells, was related to insufficient stimulation of ERK1/ERK2 and PI-3K pathways (21). Defective insulin response in ER-negative cell lines has also been described by Costantino *et al.* (45) and linked with an increased tyrosine phosphatase activity.

Our experiments suggested that the lack of IGF-I mitogenicity in MDA-MB-231 and MDA-MB-231/IGF-IR cells was not related to the impaired IGF-IR or IRS-1 tyrosine phosphorylation. The cells were also able to respond to an acute IGF-I stimulation with a marked activation of the PI-3K/Akt and ERK-1/ERK2 pathways. We hypothesize that this transient stimulation could be sufficient to induce some IGF-I response, such as cell motility. Mitogenic response, on the other hand, may rely on a more sustained activation of critical IGF-IR signals, as demonstrated before with mouse embryo fibroblasts (36). Indeed, the most significant difference in IGF-I signal between ER-negative and ER-positive cells rested in the impaired long-term stimulation of the PI-3K/Akt pathway; MDA-MB-231 and MDA-MB-231/IGF-IR cells were unable to sustain this IGF-I-induced signal for 1 or 2 days, whereas in MCF-7 and MCF-7/IGF-IR cells, the PI-3K/Akt pathway was still active at this time. The subsequent experiments with MDA-MB-231 cells transfected with constitutively active Akt mutants demonstrated that the increased biological activity of Akt was not sufficient to completely reverse cell death in PRF-SFM (Fig. 6*C* and data not shown). This suggested that although a sustained Akt activity could be important in the survival of breast cancer cells, other pathways, or a proper equilibrium between Akt and other pathways (such as ERK1/2), are also critical. The latter possibility could be supported by our finding that hyperactivation of Akt down-regulates the ERK1/2 pathway. Normally, this pathway appears to play a role in the survival of ER-negative cells (Table 2).

In summary, our data suggest that IGF-IR signaling and function may be different in hormone-dependent and -independent breast cancer cells. In ER-positive MCF-7 cells, IGF-IR transmits various signals, such as growth, survival, migration, and adhesion. In ER-negative MDA-MB-231 cells, the growth-related functions of the IGF-IR become attenuated, but the receptor is still able to control nonmitogenic processes, such as migration. It is likely that this kind of evolution is also involved with the response to other growth factors. Epidermal growth factor, for instance, is an effective mitogen for ER-positive breast cancer cells but does not stimulate the proliferation or survival in MDA-MB-231 cells, despite high EGF-R expression (46). However, as demonstrated recently by Price *et al.* (46), EGF is a potent chemoattractant for MDA-MB-231 cells. EGF-induced migration in MDA-MB-231 cells requires PI-3K and phospholipase Cγ and is not inhibited by antagonists of ERK1/ERK2.

In conclusion, mitogenic and nonmitogenic pathways induced by growth factors in breast cancer cells may be dissociated, and attenuation of one is not necessarily linked with the cessation of the other. Delineating the nonmitogenic responses will be critical for the development of drugs specifically targeting metastatic cells.

REFERENCES

1. Surmacz, E. Function of the IGF-IR in breast cancer. J. Mammary Gland Biol. Neopl., *5:* 95–105, 2000.
2. Baserga, R. The IGF-I receptor in cancer research. Exp. Cell Res., *253:* 1–6, 1999.
3. Kleinberg, D. L., Feldman, M., and Ruan, W. J. IGF-I: an essential factor in terminal end bud formation and ductal morphogenesis. Mammary Gland Biol. Neopl., *5:* 7–17, 2000.
4. Turner, B. C., Haffty, B. G., Narayanann, L., Yuan, J., Havre, P. A., Gumbs, A., Kaplan, L., Burgaud, J-L., Carter, D., Baserga, R., and Glazer, P. M. IGF-I receptor and cyclin D1 expression influence cellular radiosensitivity and local breast cancer recurrence after lumpectomy and radiation. Cancer Res., *57:* 3079–3083, 1997.
5. Resnik, J. L., Reichart, D. B., Huey, K., Webster, N. J. G., and Seely, B. L. Elevated insulin-like growth factor I receptor autophosphorylation and kinase activity in human breast cancer. Cancer Res., *58:* 1159–1164, 1998.
6. Rocha, R. L., Hilsenbeck, S. G., Jackson, J. G., Van Der Berg, C. L., Weng, C-W., Lee, A. V., and Yee, D. Insulin-like growth factor binding protein 3 and insulin receptor substrate 1 in breast cancer: correlation with clinical parameters and disease-free survival. Clin. Cancer Res., *3:* 103–109, 1997.
7. Lee, A. V., Jackson, J. G., Gooch, J. L., Hilsenbeck, S. G., Coronado-Heinsohn, E., Osborne, C. K., and Yee, D. Enhancement of insulin-like growth factor signaling in human breast cancer: estrogen regulation of insulin receptor substrate-1 expression *in vitro* and *in vivo*. Mol. Endocrinol., *10:* 787–796, 1999.
8. Hankinson, S. E., Willet, W. C., Colditz, G. A., Hunter, D. J., Michaud, D. S., Deroo, B., Rosner, B., Speitzer, F. E., and Pollak, M. Circulating concentrations of insulin-like growth factor and risk of breast cancer. Lancet, *35:* 1393–1396, 1998.
9. Dunn, S. E., Hardman, R. A., Kari, F. W., and Barrett, J. C. Insulin-like growth factor I (IGF-I) alters drug sensitivity of HBL100 human breast cancer cells by inhibition of apoptosis induced by diverse anticancer drugs. Cancer Res., *57:* 2687–2693, 1997.
10. Nolan, M., Jankowska, L., Prisco, M., Xu, S., Guvakova, M., and Surmacz, E. Differential roles of IRS-1 and SHC signaling pathways in breast cancer cells. Int. J. Cancer, *72:* 828–834, 1997.
11. Gooch, J. L., Van Den Berg, C. L., and Yee, D. Insulin-like growth factor (IGF)-I rescues breast cancer cells from chemotherapy-induced cell death—proliferative and anti-apoptotic effects. Breast Cancer Res. Treat., *56:* 1–10, 1999.
12. Surmacz, E., and Burgaud, J-L. Overexpression of IRS-1 in the human breast cancer cell line MCF-7 induces loss of estrogen requirements for growth and transformation. Clin. Cancer Res., *1:* 1429–1436, 1995.
13. Guvakova, M. A., and Surmacz, E. Overexpressed IGF-I receptors reduce estrogen growth requirements, enhance survival and promote cell-cell adhesion in human breast cancer cells. Exp. Cell Res., *231:* 149–162, 1997.

14. Dunn, S. E., Ehrlich, M., Sharp, N. J. H., Reiss, K., Solomon, G., Hawkins, R., Baserga, R., and Barrett, J. C. A dominant negative mutant of the insulin-like growth factor I receptor inhibits the adhesion, invasion and metastasis of breast cancer. Cancer Res., *58*: 3353–3361, 1998.
15. Neuenschwander, S., Roberts, C. T., Jr., and LeRoith, D. Growth inhibition of MCF-7 breast cancer cells by stable expression of an insulin-like growth factor I receptor antisense ribonucleic acid. Endocrinology, *136:* 4298–4303, 1995.
16. Arteaga, C. L., Kitten, L. J., Coronado, E. B., Jacobs, S., Kull, F. C., Jr., Allred, D. C., and Osborne, C. K. Blockade of the type I somatomedin receptor inhibits growth of human breast cancer cells in athymic mice. J. Clin. Investig., *84*: 1418–1423, 1989.
17. Jackson, J. G., White, M. F., and Yee, D. Insulin receptor substrate-1 is the predominant signaling molecule activated by insulin-like growth factor I, insulin, and interleukin-4 in estrogen receptor-positive human breast cancer cells. J. Biol. Chem., *273*: 9994–10003, 1998.
18. Schnarr, B., Strunz, K., Ohsam, J., Benner, A., Wacker, J., and Mayer, D. Down-regulation of insulin-like growth factor-I receptor and insulin receptor substrate-1 expression in advanced human breast cancer. Int. J. Cancer, *89*: 506–513, 2000.
19. Peyrat, J. P., Bonneterre, J., Dusanter-Fourt, I., Leroy-Martin, B., Dijane, J., and Demaille, A. Characterization of insulin-like growth factor 1 receptors (IGF-IR) in human breast cancer cell lines. Bull. Cancer, *76*: 311–309, 1989.
20. Sepp-Lorenzino, L., Rosen, N., and Lebwohl, D. Insulin and insulin-like growth factor signaling are defective in MDA-MB-468 human breast cancer cell line. Cell Growth Differ., *5*: 1077–1083, 1994.
21. Jackson, J., and Yee, D. IRS-1 expression and activation are not sufficient to activate downstream pathways and enable IGF-I growth response in estrogen receptor negative breast cancer cells. Growth Horm. IGF Res., *9:* 280–289, 1999.
22. Godden, J., Leake, R., and Kerr, D. J. The response of breast cancer cells to steroid and peptide growth factors. Anticancer Res., *12:* 1683–1688, 1992.
23. Doerr, M., and Jones, J. The roles of integrins and extracellular matrix proteins in the IGF-IR-stimulated chemotaxis of human breast cancer cells. J. Biol. Chem., *271*: 2443–2447, 1996.
24. Chan, T. O., Rittenhouse, S. E., and Tsichlis, P. N. AKT/PKB and other D3 phosphoinositide-regulated kinases: kinase activation by phosphoinositide-dependent phosphorylation. Annu. Rev. Biochem., *68:* 965–1014, 1999.
25. Guvakova, M. A., and Surmacz, E. Tamoxifen interferes with the insulin-like growth factor I receptor (IGF-IR) signaling pathway in breast cancer cells. Cancer Res., *57*: 2606–2610, 1997.
26. Mauro, L., Sisci, D., Bartucci, M., Salerno, M., Kim, J., Tam, T., Guvakova, M., Ando, S., and Surmacz, E. SHC-$\alpha_5\beta_1$ integrin interactions regulate breast cancer cell adhesion and motility. Exp. Cell Res., *252*: 439–448, 1999.
27. Vlahos, C. J., Matter, W. F., Hui, K. Y., and Brown, R. F. A specific inhibitor of phosphatidylinositol 3-kinase, 2-(4-morpholinyl)-8-phenyl-4*H*-1-benzopyran-4-one (LY294002). J. Biol. Chem., *269:* 5241–5248, 1994.
28. Favata, M., Horiuchi, K. Y., Manos, E., Daulerio, A. J., Stradley, D. A., Feeser, W. S., van Dyk, D. E., Pitts, W. J., Earl, R. A., Hobbs, F., Copeland, R. A., and Magolda, R. L. Identification of a novel inhibitor of mitogen-activated protein kinase kinase. J. Biol. Chem., *273*: 18623–18632, 1998.
29. Lee, J. C., Kassis, S., Kumar, S., Badger, A., and Adams, J. p38 mitogen-activated protein kinase inhibitors—mechanisms and therapeutic potentials. Pharmacol. Ther., *82*: 389–397, 1999.
30. Rubini, M., Hongo, A., D'Ambrosio, C., and Baserga, R. The IGF-IR in mitogenesis and transformation of mouse embryo fibroblasts: role of receptor number. Exp. Cell Res., *230:* 284–292, 1997.
31. Reiss, K., Valentinis, B., Tu, X., Xu, S-Q., and Baserga, R. Molecular markers of IGF-I-mediated mitogenesis. Exp. Cell Res., *242*: 361–372, 1998.
32. Shepherd, P. R., Withers, D., and Siddle, K. Phosphoinositide3-kinase: the key switch mechanism in insulin signalling. Biochem. J., *333*: 471–490, 1998.
33. Dufourny, B., Alblas, J., van Teeffelen, H. A., van Schaik, F. M., van der Burg, B., Steenbergh, P. H., and Sussenbach, J. S. Mitogenic signaling of insulin-like growth factor I in MCF-7 human breast cancer cells requires phosphatidylinositol 3-kinase and is independent of mitogen-activated protein kinase. J. Biol. Chem., *272:* 31163–31171, 1997.
34. Vanhaesebroeck, B., and Alessi, D. R. The PI3K-PDK1 connection: more than just a road to PKB. Biochem. J., *15:* 561–576, 2000.
35. Huang, S., New, L., Pan, Z., Han, J., and Nemerow, G. L. Urokinase plasminogen activator/urokinase-specific surface receptor expression and matrix invasion by breast cancer cells requires constitutive p38α mitogen-activated protein kinase activity. J. Biol. Chem., *275:* 12266–12272, 2000.
36. Swantek, J. L., and Baserga, R. Prolonged activation of ERK2 by epidermal growth factor and other growth factors requires a functional insulin-like growth factor 1 receptor. Endocrinology, *140:* 3163–3169, 1999.
37. White, M. F. The IRS-signalling system: a network of docking proteins that mediate insulin action. Mol. Cell. Biochem., *182*: 3–11, 1998.
38. Peruzzi, F., Prisco, M., Dews, M., Salomoni, P., Grassilli, E., Romano, G., Calabretta, B., and Baserga, R. Multiple signaling pathways of the insulin-like growth factor 1 receptor in protection from apoptosis. Mol. Cell. Biol., *19*: 7203–7215, 1999.
39. Zimmermann, S., and Moelling, K. Phosphorylation and regulation of Raf by Akt (protein kinase B). Science (Wash. DC), *286:* 1741–1744, 1999.
40. Rommel, C., Clarke, B. A., Zimmermann, S., Nunez, L., Rossman, R., Reid, K., Moelling, K., Yancopoulos, G. D., and Glass, D. J. Differentiation stage-specific inhibition of the Raf-MEK-ERK pathway by Akt. Science (Wash. DC), *286:* 1738–1740, 1999.
41. Pezzino, V., Papa, V., Milazzo, G., Gliozzo, B., Russo, P., and Scalia, P. L. Insulin-like growth factor-I (IGF-I) receptors in breast cancer. Ann. NY Acad. Sci., *784:* 189–201, 1996.
42. Peyrat, J. P., and Bonneterre, J. Type 1 IGF receptor in human breast diseases. Breast Cancer Res. Treat., *22:* 59–67, 1992.
43. Railo, M. J., Smitten, K., and Pekonen, F. The prognostic value of insulin-like growth factor I in breast cancer. Results of a follow-up study on 126 patients. Eur. J. Cancer, *30A:* 307–311, 1994.
44. Guvakova, M., and Surmacz, E. The activated insulin-like growth factor I receptor induces depolarization in breast cancer cells characterized by actin filament disassembly and tyrosine dephosphorylation of FAK, Cas, and paxillin. Exp. Cell Res., *251:* 244–255, 1999.
45. Costantino, A., Milazzo, G., Giorgino, F., Russo, P., Goldfine, I. D., Vigneri, R., and Belfiore, A. Insulin-resistant MDA-MB231 human breast cancer cells contain a tyrosine kinase inhibiting activity. Mol. Endocrinol., *7:* 1667–1679, 1993.
46. Price, J. T., Tiganis, T., Agarwal, A., Djakiew, D., and Thompson, E. W. Epidermal growth factor promotes MDA-MB-231 breast cancer cell migration through a phosphatidylinositol 3′-kinase and phospholipase C-dependent mechanism. Cancer Res., *59:* 5475–5478, 1999.
47. Lee, A. V., Gooch, J. L., Oesterreich, S., Guler, R. L., and Yee, D. Insulin-like growth factor I-induced degradation of insulin receptor substrate 1 is mediated by the 26S proteasome and blocked by phosphatidylinositol 3′-kinase inhibition. Mol. Cell. Biol., *20:* 1489–1496, 2000.

Experimental Cell Research 252, 439–448 (1999)
Article ID excr.1999.4639, available online at http://www.idealibrary.com on IDEAL®

SHC–α5β1 Integrin Interactions Regulate Breast Cancer Cell Adhesion and Motility

Loredana Mauro,*,†,[1] Diego Sisci,*,†,[1] Monica Bartucci,*,† Michele Salerno,*,† Jerry Kim,* Timothy Tam,* Marina A. Guvakova,* Sebastiano Ando,† and Eva Surmacz*,[2]

*Kimmel Cancer Institute, Thomas Jefferson University, Philadelphia, Pennsylvania 19107; and †Department of Cellular Biology, Faculty of Pharmacy, University of Calabria, Cosenza, Italy

The oncogenic SHC proteins are signaling substrates for most receptor and cytoplasmic tyrosine kinases (TKs) and have been implicated in cellular growth, transformation, and differentiation. In tumor cells overexpressing TKs, the levels of tyrosine phosphorylated SHC are chronically elevated. The significance of amplified SHC signaling in breast tumorigenesis and metastasis remains unknown. Here we demonstrate that seven- to ninefold overexpression of SHC significantly altered interactions of cells with fibronectin (FN). Specifically, in human breast cancer cells overexpressing SHC (MCF-7/SHC) the association of SHC with α5β1 integrin (FN receptor) was increased, spreading on FN was accelerated, and basal growth on FN was reduced. These effects coincided with an early decline of adhesion-dependent MAP kinase activity. Basal motility of MCF-7/SHC cells on FN was inhibited relative to that in several cell lines with normal SHC levels. However, when EGF or IGF-I was used as the chemoattractant, the locomotion of MCF-7/SHC cells was greatly (approx fivefold) stimulated, while it was only minimally altered in the control cells. These data suggest that SHC is a mediator of the dynamic regulation of cell adhesion and motility on FN in breast cancer cells. © 1999 Academic Press

Key Words: **SHC; α5β1 integrin; fibronectin; motility; breast cancer.**

INTRODUCTION

The ubiquitous SH2 homology/collagen homology (SHC) proteins (p46, p52, and p66) are overlapping SH2-PTB adapter proteins that are targets and downstream effectors of most transmembrane and cytoplasmic tyrosine kinases (TKs) [1, 2]. Consequently, overexpression of $p52^{SHC}$ and $p46^{SHC}$ (referred to as SHC hereinafter) amplifies various cellular responses; for instance, it induces mitogenic effects of growth factors in NIH 3T3 mouse fibroblasts and myeloid cells [1, 3], stimulates differentiation in PC12 rat pheochromocytoma [4], and augments hepatocyte growth factor (HGF)-induced proliferation and migration in A549 human lung adenocarcinoma [5]. Overexpressed SHC is oncogenic in NIH 3T3 mouse fibroblasts, but amplification of $p66^{SHC}$ isoform does not induce transformation [1, 6, 7] and may even inhibit growth pathways [8]. Importantly, increased tyrosine phosphorylation of SHC, which has been noticed in different tumor cell lines, is a marker of receptor or cytoplasmic TKs overexpression [2]. In breast cancer, for instance, SHC is hyperphosphorylated in cells overexpressing ERB-2 and c-Src [9, 10]. Whether such amplification of SHC signaling contributes to the development of a more aggressive phenotype of breast tumor cells remains unknown.

The effector pathways downstream of SHC are partially known. Upon tyrosine phosphorylation by TKs, SHC associates with the GRB2/SOS complex and subsequently stimulates the canonical Ras–MAPK (p42 and p44 mitogen-activated protein kinases) signal transduction cascade [1, 6, 7]. SHC/GRB2 binding and the activation of Ras are prerequisites for SHC-induced mitogenesis and transformation in NIH mouse fibroblasts [6]. In addition, SHC has been described as associating with adapters Crk II [11] and GRB7 [12] as well as with a signaling protein p145 [13, 14] and PEST tyrosine phosphatase [15] in various experimental systems. However, SHC pathways incorporating these signaling intermediates and their biological significance are not well understood.

There is substantial evidence suggesting that in addition to its role in mitogenesis and transformation, SHC regulates nongrowth processes, such as cell adhesion and motility. For instance, overexpressed SHC improved motility in HGF-stimulated melanoma cells [5], and downregulation of SHC reduced epidermal growth factor (EGF)-dependent migration in MCF-7 breast cancer cells [16]. SHC was also essential for

[1] L.M. and D.S. contributed equally to this work.

[2] To whom correspondence and reprint requests should be addressed at Kimmel Cancer Institute, Thomas Jefferson University, 233 S. 10th Street, BLSB 606, Philadelphia, PA 19107. Fax: 215-923-0249. E-mail: surmacz1@jeflin.tju.edu.

0014-4827/99 $30.00

kidney epithelial cell scattering mediated by the receptors c-met, c-ros, and c-neu [17]. The mechanisms by which SHC regulates cell adhesion and motility are still obscure.

In several cell types (Jurkat, HUVEC, MG-63, and A431 cells), SHC couples with certain ECM receptors, specifically with the integrins $\alpha1\beta1$, $\alpha5\beta1$, $\alpha v\beta3$, and $\alpha6\beta4$, but not with $\alpha2\beta1$, $\alpha3\beta1$, and $\alpha6\beta1$ [18]. Association of SHC with integrins may result in phosphorylation of SHC by integrin-associated TKs (Fyn, other Src-like kinases, FAK, or FAK-associated kinases) and subsequent activation of MAPK [18–21]. The biological significance of integrin-stimulated MAPK activity is not well understood. However, recent data indicated that it positively regulates cell growth and survival [18, 22], but is not essential for cell migration [23].

This work addresses the consequences of amplified SHC signaling on proliferation, transformation, adhesion, and motility in breast cancer MCF-7 cells. In these cells, SHC is an important intermediate of different signaling pathways. Growth factors present in serum, such as IGF-I and EGF, can induce SHC through their cognate receptors [1, 16, 24]. Estrogens (also contained in serum) may elevate tyrosine phosphorylation of SHC via cytoplasmic TKs of the Src family [25]. In addition, SHC can be stimulated by cytoplasmic TKs as a result of cell spreading on ECM [18]. MCF-7 cells express several integrin receptors: $\alpha2\beta1$, $\alpha3\beta1$, $\alpha5\beta1$, and $\alpha v\beta5$ [26]. Of those, $\alpha5\beta1$, a FN receptor, is known to associate with SHC, while $\alpha2\beta1$ and $\alpha3\beta1$ are not SHC binding proteins [18].

The interactions of cells with FN have been reported to influence or control different processes regulating the behavior of cancer cells, namely cell migration, invasion, and metastasis as well as survival and proliferation [27]. The exact role of $\alpha5\beta1$ FN receptors in tumor progression is not clear. It has been shown that extracellular matrix recognition by $\alpha5\beta1$ integrin is a negative regulator of cell growth and may be lost in some tumor cells [28]. In agreement with this, overexpression of $\alpha5\beta1$ integrin and improved cell spreading on FN can reduce cell growth and transformation *in vivo* and reverse tumorigenicity *in vitro* [29, 30]. On the other hand, FN receptors may play a role in later stages of tumor progression since blocking $\alpha5\beta1$ integrin abrogated cell spread in experimental breast metastasis [31]. The importance of SHC signaling in the interactions of breast cancer cells with FN has not been studied and is a subject of this work.

MATERIALS AND METHODS

Cell lines and cell culture conditions. MCF-7 cells are estrogen receptor positive cells of a low tumorigenic and metastatic potential. The growth of MCF-7 cells is controlled by estrogens, such as estradiol (E2), and growth factors, such as IGF-I and EGF [32, 33]. MCF-7 cells express several integrins, including $\alpha5\beta1$ (FN receptor), $\alpha2\beta1$ (collagen, COL receptor), $\alpha3\beta1$ (COL/FN/laminin 5 receptor), and $\alpha v\beta5$ (vitronectin receptor) [26].

MCF-7/SHC clones 1 and 9 are MCF-derived cells stably transfected with the expression plasmid pcDNA3/SHC containing a human SHC cDNA encoding $p55^{SHC}$ and $p47^{SHC}$. The clones expressing the transgene were selected in 2 mg/ml G418, and the levels of SHC expression in 20 G418-resistant clones were determined by Western blotting (WB) in whole cell protein lysates, as described below.

As control cells, we used several MCF-7-derived clones with modified growth factor signaling pathways: specifically, MCF-7/IRS-1, clones 3 and 18, which are MCF-7 cells overexpressing insulin receptor substrate 1 (IRS-1) [32]; MCF-7/IGF-IR, clone 17, which is an MCF-7-derived clone overexpressing the insulin-like growth factor 1 receptor (IGF-IR) [33]; and MCF-7/anti-SHC, clone 2, with SHC levels decreased by 50% due to the stable expression of an anti-SHC RNA [16].

MCF-7 cells were grown in DMEM:F12 (1:1) containing 5% calf serum (CS). MCF-7-derived clones were maintained in DMEM:F12 plus 5% CS plus 200 μg/ml G418. In the experiments requiring E2- and serum-free conditions, the cells were cultured in phenol red-free DMEM containing 0.5 mg/ml BSA, 1 μM FeSO4, and 2 mM L-glutamine (referred to as PRF–SFM).

Monolayer growth. Cells were plated at a concentration 1.5–2.0 $\times$ 10^5 in six-well plates in the growth medium; the following day (day 0), the cells at approximately 50% confluence were shifted to PRF–SFM containing 1 or 20 ng/ml IGF-I or 1 or 10 ng/ml EGF. After 4 days, the number of cells was determined by direct counting.

Anchorage-independent growth. Transforming potential of the cells (anchorage independence) was measured by their ability to form colonies in soft agar, as previously described [32]. The cells, 1 $\times$ 10^3/35-mm plate, were grown in a medium solidified with 0.2% agarose. The solidified medium contained either (i) DMEM:F12 supplemented with 10% FBS or 5% CS or (ii) PRF–SFM with 200 ng/ml IGF-I, 50 ng/ml EGF, or 200 ng/ml IGF-I plus 50 ng/ml EGF. After 21 days of culture, the colonies greater then 100 μm in diameter were counted using an inverted phase–contrast microscope.

Adhesion on FN or COL. Cells synchronized for 24 h in PRF–SFM were seeded in 60-mm plates coated with FN (50 μg/ml) or COL (20 μg/ml). Before the experiment, the plates were blocked with 3% BSA for 3 h at 37°C and then washed once with PBS. To inactivate $\alpha5\beta1$ integrin, the cells were incubated with a blocking $\alpha5\beta1$ Ab 10 μg/ml (Chemicon) for 30 min before plating. Cell morphology was recorded using an inverted phase–contrast microscope with a camera. Percentage of nonadherent cells was determined by counting the number of floating cells vs. the number of cells originally inoculated in the plate.

Growth on FN. Cells (0.5 $\times$ 10^5/ml) were seeded in 12-well plates coated with FN (50 μg/ml) in normal growth medium with or without EGF (10, 50, or 100 ng/ml) or IGF-I (20 or 100 ng/ml). The cells were counted after 4 days of culture.

Motility assay. Motility was tested in modified Boyden chambers containing porous (8-mm) polycarbonate membranes. The undersides of membranes were coated with either 20 μg/ml COL IV or 50 μg/ml FN, as described by Mainiero *et al.* [34]. According to this protocol, collagen (COL) or FN covered not only the underside of the membrane, but also diffused into the pores where cell contact with ECM was initiated. Synchronized cells (2 $\times$ 10^4) suspended in 200 μl of PRF–SFM were plated into upper chambers. Lower chambers contained 500 μl of PRF–SFM with EGF (1 and 10 ng/ml) or IGF-I (20 ng/ml). After 12 h, the cells in the upper chamber were removed, while the cells that migrated to the lower chamber were fixed and stained in Coomassie blue solution (0.25 g Coomassie blue/45 ml water/45 ml methanol/10 ml glacial acetic acid) for 5 min. After that, the chambers were washed three times with H_2O. The cells that migrated to the lower chamber were counted under the microscope as described before [16].

Immunoprecipitation and Western blotting. Proteins were obtained by lysis of cells with a buffer containing 50 mM Hepes, pH 7.5, 150 mM NaCl, 1% Triton X-100, 1.5 mM $MgCl_2$, 1 mM $CaCl_2$, 100 mM NaF, 0.2 mM Na_3VO_4, 1% PMSF, 1% aprotinin. The expression of SHC in transfectants and the parental cells was assessed in 50 μg of total cell lysate using an anti-SHC monoclonal antibody (mAb) (Transduction Laboratories). Alternatively, SHC was detected by immunoprecipitation (IP) from 250–1000 μg (specific amounts are given under the figures) of protein lysate with an anti-SHC polyclonal antibody (pAb) (Transduction Laboratories), followed by WB with an anti-SHC mAb (Transduction Laboratories). Tyrosine phosphorylation of SHC was measured by WB using an anti-phosphotyrosine mAb PY20 (Transduction Laboratories). The levels of $\alpha5\beta1$ integrin were assessed in 1 mg of protein lysate by IP with an anti-$\alpha5\beta1$ pAb (Chemicon) and WB using an anti-$\beta1$ mAb (Chemicon). The amounts of integrin-associated SHC were measured in $\alpha5\beta1$ integrin immunoprecipitates with an anti-SHC pAb (Chemicon). The intensity of bands representing relevant proteins was measured by laser densitometry scanning.

MAPK activity. The phosphorylated forms of p42 and p44 MAPK were identified by WB in 50 μg of whole cell lysates with an anti-phospho-MAPK (Thr202/Tyr204) mAb (New England Biolabs). The total levels of MAPK were determined with an anti-MAPK pAb (New England Biolabs). Adhesion-induced MAPK activity was assessed in cells plated either on COL IV or FN and then lysed at different times after plating (0–24 h). To determine EGF-induced MAPK activity, the cells were plated on different substrates, allowed to attach for 1 h, and then treated with 10 ng/ml EGF. The cells were lysed at different times (0–24 h) of the treatment and MAPK activity was measured as described above.

Statistical analysis. The results of cell growth experiments were analyzed by Student t test.

RESULTS

Basal and growth factor-induced SHC tyrosine phosphorylation is increased in MCF-7/SHC cells. To investigate the implications of increased SHC signaling in breast cancer cells, we developed several MCF-7-derived clones stably overexpressing $p46^{SHC}$ and $p52^{SHC}$. Of 20 G418 resistant clones, 7 exhibited SHC overexpression, as determined by WB (data not shown). Two representative clones, MCF-7/SHC, 1 and MCF-7/SHC, 9, with a seven- and ninefold SHC amplification, respectively, were selected for subsequent experiments (Fig. 1). The greater amount of SHC in these clones was reflected by increased levels of SHC tyrosine phosphorylation, which was evident in both continuously proliferating (Fig. 1A) and EGF-stimulated cultures (Fig. 1B). The extent of SHC tyrosine phosphorylation roughly corresponded to the cellular levels of the protein (Fig. 1A and B).

Overexpression of SHC has minimal effects on cell growth on plastic and does not enhance transformation in soft agar. The significant hyperactivation of SHC in MCF-7/SHC cells suggested that growth properties of these cells might have been altered. First we determined that in serum-containing medium or PRF–SFM, the growth rate of MCF-7/SHC clones was comparable to that of the parental cells or other cell lines with normal SHC levels (data not shown). Next, we studied mitogenic response to EGF and IGF-I, growth factors which stimulate tyrosine phosphorylation of SHC [1, 24] and require SHC for their growth action [16]. We found that relative to MCF-7 cells, MCF-7/SHC clones exhibited only moderately (20–40%) enhanced growth response to IGF-I or EGF (Fig. 1C). Under the same conditions, the proliferation of a control clone MCF-7/anti-SHC, 2 was substantially (at least by 50%) reduced (Fig. 1C), as we demonstrated previously [16].

Since SHC is oncogenic when overexpressed in NIH mouse fibroblasts [1], we assessed transforming potential of MCF-7/SHC clones in soft agar assay. Despite significant SHC overexpression in these cells, in several repeat experiments and under different growth conditions used, anchorage-independent growth of MCF-7/SHC cells was never enhanced relative to that seen in MCF-7 cells (Table 1). In the same assay, MCF-7 cells overexpressing IRS-1, i.e., MCF-7/IRS-1, clone 3, exhibited increased transformation in the presence of serum or IGF-I [32], typical for these cells.

SHC associates with $\alpha5\beta1$ integrin (FN receptor) in MCF-7 cells, and the abundance of SHC/$\alpha5\beta1$ integrin complexes is increased in MCF-7/SHC cells. The limited or absent effects of SHC overexpression on mitogenic and transforming potential of MCF-7 cells prompted us to assess the role of SHC in nongrowth processes, specifically, adhesion and motility. Because interactions of cells with FN have been implicated in the growth and metastatic behavior of breast cancer cells [30, 31] and since SHC is a potential mediator of FN receptor signaling [18, 21], we investigated how overexpressed SHC affects the function of $\alpha5\beta1$ integrin in MCF-7 cells. The first observation was that the levels of SHC, especially $p46^{SHC}$, associated with $\alpha5\beta1$ were markedly increased (~sevenfold) in MCF-7/SHC clones compared with that in MCF-7 cells or in several cell lines with normal levels of SHC but overexpressing other signaling proteins (IRS-1 or the IGF-IR) (Fig. 2). Interestingly, the amount of $p46^{SHC}$ associated with $\alpha5\beta1$ integrin was similar in both MCF-7/SHC clones, regardless of the level of SHC overexpression (Fig. 2). This suggests that the extent of SHC/$\alpha5\beta1$ binding is not directly proportional to total cellular SHC levels and that $\alpha5\beta1$/SHC complex formation is a saturable process, possibly determined by the limited expression of $\alpha5\beta1$ integrin in MCF-7 cells [30].

MCF-7/SHC cells exhibit increased adhesion to FN. Because of the enhanced association of SHC with $\alpha5\beta1$ integrin in MCF-7/SHC cells, we examined the role of SHC in cellular interactions with FN using cell lines with normal, amplified, or reduced SHC levels. We found that the overexpression of SHC was associated with an accelerated cell adhesion to FN, while the reduction of SHC levels blocked cell spreading on the substrate (Fig. 3 and Table 2). The differences in the

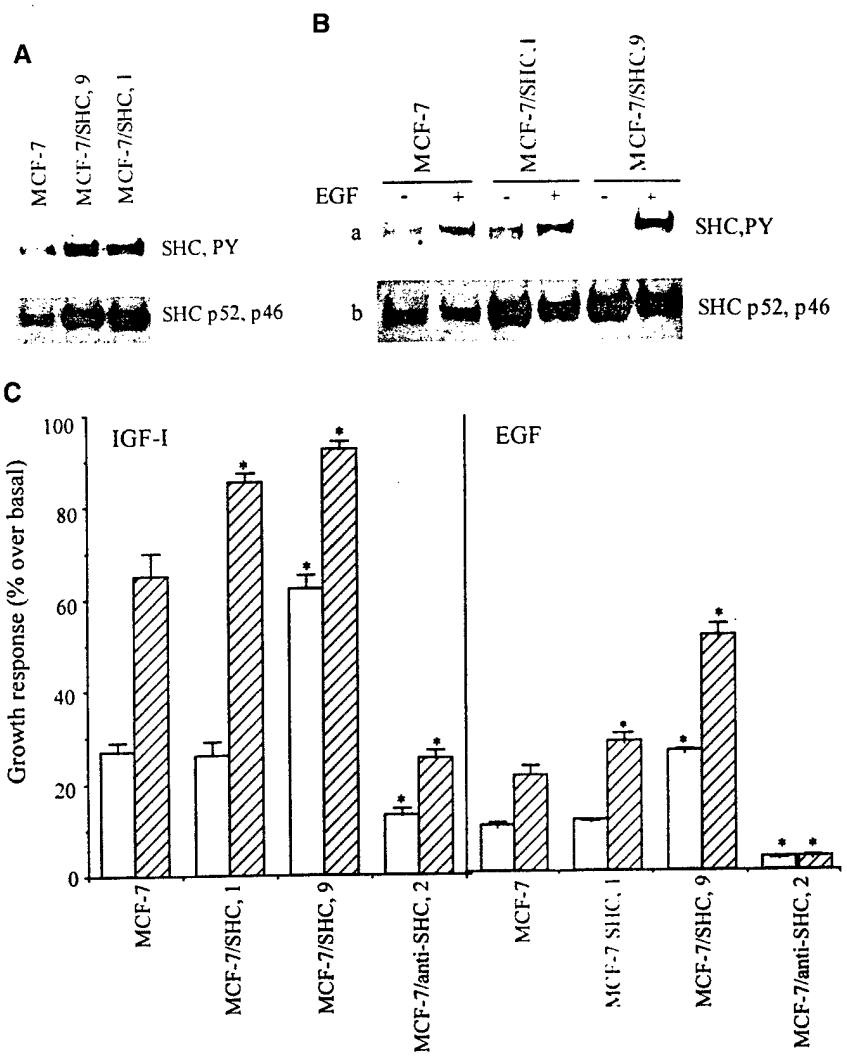

FIG. 1. MCF-7/SHC cells. (A) SHC expression and tyrosine phosphorylation in proliferating cells. The protein levels and tyrosine phosphorylation (PY) of $p52^{SHC}$ and $p46^{SHC}$ in two selected MCF-7/SHC clones 1 and 9 were determined in 750 μg of protein lysate by IP and WB with specific antibodies, as detailed under Materials and Methods. Cell lysates were isolated from logarithmic cultures maintained in normal growth medium. (B) SHC expression and tyrosine phosphorylation in growth-factor-stimulated cells. 70% confluent cultures were synchronized in PRF-SFM for 24 h and then stimulated with 10 ng EGF for 15 min. SHC levels and tyrosine phosphorylation (PY) were studied by IP and WB in 250 μg of protein lysates. Note that lane MCF-7/SHC, 1, EGF (+) is overloaded. (C) Growth response of MCF-7/SHC cells to IGF-I and EGF. The cells at 50% confluence were synchronized in PRF–SFM and stimulated with mitogens for 4 days as described under Materials and Methods. Abscissa, cell lines; ordinate, the percentage of growth increase over that in PRF-SFM. Solid bars, low doses: IGF-I 1 ng/ml or EGF 1 ng/ml; striped bars, high doses, IGF-I 20 ng/ml or EGF 10 ng/ml. High doses of IGF-I or EGF are the EC_{50} concentrations in these cells. SD is marked by solid bars; asterisks indicate statistically significant differences ($P \leq 0.05$) between the growth responses of MCF-7/SHC or MCF-7/anti-SHC cells and identically treated MCF-7 cells. The results are average of four experiments.

dynamics of cell interactions with FN were most evident at 1 h after plating (Fig. 3B and Table 2). Specifically, while at this time both MCF-7/SHC clones were well spread on FN, and almost no floating cells were observed, only ~50% of MCF-7 cells exhibited initial attachment to the substrate (cells were still rounded but with distinct membrane protrusions), and MCF-7/anti-SHC cells remained completely suspended. At 2 and 6 h after plating, MCF-7 and MCF-7/SHC clones were attached to FN and the differences in adhesion among these cell lines were unremarkable. At the same time, MCF-7/anti-SHC cells were in minimal contact with FN (Table 2). After 24 h, MCF-7/anti-SHC cells formed small aggregates demonstrating limited contact with the substrate, but all other tested cell lines (represented here by MCF-7 cells) were fully attached (Fig. 3D and Table 2). At 48 h, MCF-7/anti-SHC cells were completely detached, while MCF-7 and MCF-7/SHC cells begun proliferation on FN (data not shown).

Our experiments also indicated that the adhesion of MCF-7/SHC cells to FN was mediated by $\alpha 5\beta 1$ integrin, since this process was totally blocked with a spe-

TABLE 1

Anchorage-Independent Growth of MCF-7/SHC Cells

Cell line	Number of colonies				
	10% FBS	5% CS	SFM + IGF-I	SFM + EGF	SFM + IGF-I + EGF
MCF-7	172	105	2	1	12
MCF-7/SHC, 1	164	90	0	0	9
MCF-7/SHC, 9	155	88	0	0	10
MCF-7/IRS-1, 3	213	131	25	10	22

Note. The cells were tested in soft agar as described under Materials and Methods. The agar-solidified medium was either DMEM:F12 with 10% FBS or 5% CS or PRF–SFM with EGF (200 ng/ml), IGF-I (50 ng/ml), or EGF plus IGF-I (50 plus 200 ng/ml, respectively). MCF-7/IRS-1, clone 3, characterized by an increased transforming potential [30], was used as a positive control. The experiment was repeated seven times. Average number of colonies of the size at least 100 μm in diameter is given.

cific anti-$\alpha5\beta1$ blocking antibody (Fig. 3C), but not with a control goat IgG (not shown).

In contrast with the results obtained on FN, the dynamics of cell adhesion on COL, which is mediated by an integrin not associating with SHC ($\alpha5\beta1$) [18], were similar in all tested cell lines, regardless of the levels of SHC expression. Specifically, all cells tested initiated contacts with COL at 15 min and completed attachment at 1 h after plating (data not shown).

Overexpression of SHC modulates adhesion-dependent, but not growth factor-induced, MAP kinase activity on FN. Cell adhesion to ECM and the activation of different integrin-associated cytoplasmic TKs result in the stimulation of MAPK activity [35]. This process can be mediated through SHC, which, as a substrate of TKs (e.g., Fyn, other c-Src-like kinases, or FAK), is tyrosine phosphorylated, binds the GRB2/SOS complex, and stimulates Ras [18, 19, 21]. The integrin–MAPK pathway can also be induced in a SHC-independent way, through FAK–GRB2-SOS–Ras signaling [20, 21]. Here we studied the effect of SHC amplification on adhesion-dependent MAPK response in MCF-7 and MCF-7/SHC cells. Figure 4 demonstrates representative results obtained with MCF-7/SHC, 1 cells; the results with the clone MCF-7/SHC, 9 were similar.

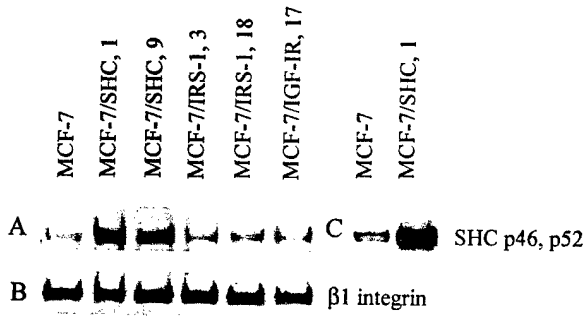

FIG. 2. SHC associates with $\alpha5\beta1$ integrin. The amounts of SHC associated with $\alpha5\beta1$ integrin in MCF-7/SHC cells, MCF-7 cells, and several control clones with normal SHC levels but increased levels of IRS-1 (MCF-7/IRS-1, clones 3 and 18) or the IGF-IR (MCF-7/IGF-IR, clone 17) were determined in 750 μg of protein lysate by IP with an anti-$\alpha5\beta1$ pAb and WB with an anti-SHC pAb (A). The expression of $\alpha5\beta1$ integrin in the cells was determined after stripping the above blot and reprobing with the anti-$\beta1$ pAb (only the β subunit is shown) (B). To locate the position of SHC isoforms on the gel, SHC proteins were precipitated from 250 μg of MCF-7 and MCF-7/SHC, 1 cell lysates with an anti-SHC pAb, run in parallel with $\alpha5\beta1$ integrin IP samples and probed with an anti-SHC mAb (C). Note: The $\alpha5\beta1$ integrin IP samples could not be reprobed with the SHC mAb because of strong antibody cross-reaction.

First, we found that overexpression of SHC significantly modulated MAPK activation in cells spread on FN, but on COL (Fig. 4A). Specifically, on COL, MCF-7 and MCF-7/SHC cells responded similarly—the activation of MAPK was biphasic, with a peak between 30 min and 4 h after plating, followed by a decline of activity at 8 h, and then an increased activity between 12 and 24 h. In contrast, on FN, the dynamics of MAPK response was different—in MCF-7 cells, the stimulation of MAPK was the highest at 1 h after plating and the kinases remained highly stimulated for up to 8 h. In MCF-7/SHC cells, MAPK was activated at 30 min after plating, reached the maximum at 1 h, and rapidly declined at 4 h to reach basal levels at 24 h (Fig. 4A). The activation of MAPK in suspended cells was undetectable (not shown).

Next, we investigated whether SHC overexpression affects growth-factor-induced MAPK response in cells plated on FN. We used EGF in this experiment since this mitogen induces SHC phosphorylation more strongly than IGF-I in MCF-7 cells (Surmacz *et al.*, unpublished observations). The patterns of EGF-stimulated MAPK activity were remarkably similar on COL and FN (a peak between 15 min and 1 h after treatment followed by a decline to basal levels) in both MCF-7 and MCF-7/SHC cells (Fig. 4B).

Since MAPK pathway contributes to cell growth, we studied whether the reduced duration of adhesion-dependent MAP activity reflects mitogenicity of MCF-7/

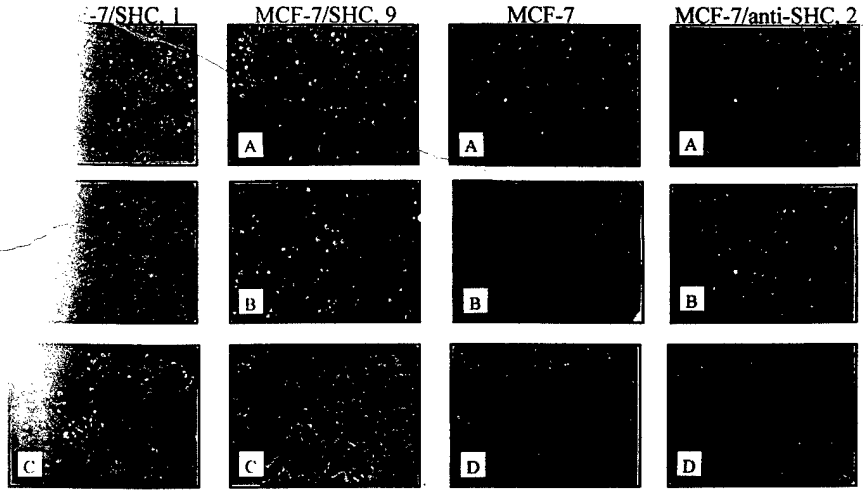

FIG. 3. Adhesion of MCF-7/SHC clones on FN. MCF-7/SHC clones 1 and 9 (amplified SHC), MCF-7 cells (normal SHC levels) and MCF-7/anti-SHC, clone 2 (reduced SHC levels) were synchronized for 24 h in PRF–SFM and plated on FN (50 μg/ml) in PRF–SFM. The cells were photographed at times 0 (A) and 1 h (B). The role of α5β1 integrin in the adhesion of MCF-7/SHC clones 1 and 9 was assessed by blocking the FN receptor with a specific antibody 30 min before cell plating (C), as described under Materials and Methods. The long-term (24 h) adhesion of MCF-7 and MCF-7/anti-SHC, clone 2, is shown in panels D.

SHC cells cultured on FN (Table 3). Indeed, we found that overexpression of SHC coincided with a significant (~twofold) growth inhibition. Interestingly, the addition of EGF (different doses, up to 100 ng/ml) to growth medium did not improve proliferation of MCF-7/SHC or MCF-7 cells on FN. The addition of IGF-I (doses up to 100 ng/ml) only minimally (9–22%) stimulated growth under the same conditions (Table 3).

Overexpression of SHC inhibits basal motility on FN, and IGF-I or EGF mobilizes MCF-7/SHC cells. We investigated whether increased binding of SHC to α5β1 integrin affects cell motility in FN-coated inserts. We found that basal migration of MCF-7/SHC cells was significantly (~fourfold) reduced compared with that of MCF-7 cells and several MCF-7-derived cell lines containing normal amounts of SHC (Fig. 5). In contrast, the motilities of MCF-7/SHC clones in COL-coated inserts were similar ($P \geq 0.05$) to those seen with other tested cell lines (Fig. 5).

The use of EGF or IGF-I as chemoattractants significantly (~five- to sevenfold, $P \leq 0.01$) improved the migration of MCF-7/SHC cells toward FN, but not to COL. The mitogens did not affect motility of other cells to COL, except some inhibition of MCF-7/IRS-1, clone 18 with 10 ng/ml EGF. Interestingly, in FN-coated inserts, 10 ng/ml EGF stimulated the migration of MCF-7/IRS-1 cells; however, the extent of this stimulation was much lower than that of SHC overexpressing clones (Fig. 5). The increased EGF sensitivity of MCF-7/IRS-1 clones has been noticed before [16].

TABLE 2

Dynamics of Cell Attachment to FN

Cell line	% Nonadherent cells					
	0 h	0.5 h	1 h	2 h	6 h	24 h
MCF-7	100	74	55	8	5	2
MCF-7/SHC, 1	100	33	5	5	4	4
MCF-7/SHC, 9	100	25	6	5	2	3
MCF-7/anti-SHC, 2	100	99	100	78	80	76

Note. 0.5×10^5 cells suspended in PRF–SFM were plated into 60-mm plates coated with 50 μg/ml FN as described under Materials and Methods. At the time of plating (0 h) and at 0.5, 1, 2, 6, and 24 h after plating, the floating cells were collected and counted. The values represent the percentages of cells floating vs cells originally plated and are averages from three experiments.

DISCUSSION

SHC is a signaling substrate of most receptor-type and cytoplasmic TKs and therefore may amplify various cellular responses [2]. In consequence, the significance of SHC amplification must depend on the intracellular and extracellular cell context. Breast cancer cells, unlike normal breast epithelium, frequently overexpress TKs, such as c-Src (80%), or ERB2 (~20–30%), which may result in constitutive activation of SHC [9, 10]. The contribution of amplified SHC signaling to development and progression of breast cancer is not known. We addressed this question by examining the effects of SHC overexpression in MCF-7 cells (representing an early stage of breast cancer and characterized by moderate c-Src amplification). The major findings of this work are that unlike in fibroblasts, hyperactivation of SHC is not sufficient to provide sig-

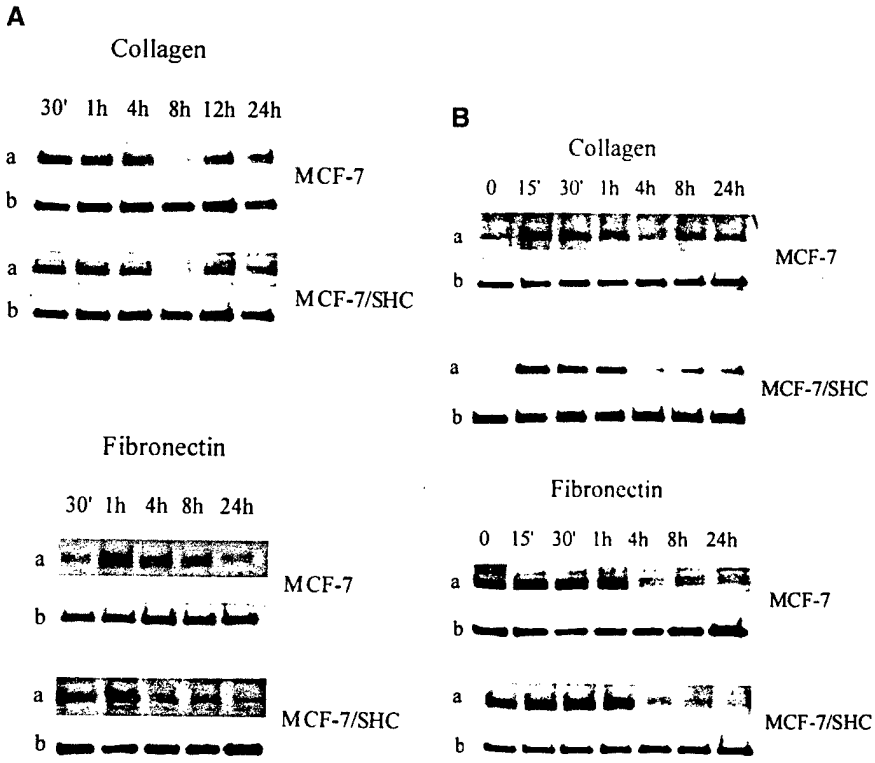

FIG. 4. Adhesion-induced (A) and EGF-dependent (B) MAPK activity in MCF-7/SHC cells. To measure adhesion-induced MAP kinase activity (A), MCF-7 and MCF-7/SHC cells were plated on COL IV or FN. The cells were lysed at the indicated times after plating. The phosphorylated forms of p42 and p44 MAPK were determined as described under Materials and Methods. EGF-induced MAP kinase activity (B) was determined in MCF-7 and MCF-7/SHC cells. The cells were plated on COL IV or FN, allowed to attach for 1 h, and then treated with 10 ng/ml EGF. The cells were lysed at different times (0–24 h) of the treatment. In (A) and (B), panels (a) represent phosphorylated MAPK, panels (b) total cellular levels of MAPK. The representative results demonstrating MAPK response in MCF-7 cells and MCF-7/SHC, clone 1, are shown; results with MCF-7/SHC, clone 9, were analogous to that obtained in clone 1.

nificant growth or transforming advantage in breast cancer cells. High levels of SHC, however, increase cell connections with FN and modulate cell growth and migration on this substrate, which may have consequences in cell spread and metastasis.

TABLE 3

Growth of MCF-7/SHC Cells on FN

Cell line	Cell number		
	5% CS	5% CS + EGF	5% CS + IGF-I
MCF-7	2.2×10^5	2.2×10^5	2.4×10^5
MCF-7/SHC, 1	1.1×10^5	1.0×10^5	1.3×10
MCF-7/SHC, 9	0.9×10^5	0.8×10^5	1.1×10^5

Note. The growth of cells on FN in normal growth medium (DMEM:F12 + 5% CS) or growth medium containing EGF (100 ng/ml) or IGF-I (100 ng/ml) was tested as described under Materials and Methods. The cells were plated at the concentration 0.5×10^5 cells/ml and counted after 4 days of culture. The values represent cell numbers/ml and are average results from three independent experiments.

SHC in epithelial cell growth and transformation. In mouse fibroblasts, overexpression of SHC resulted in increased SHC tyrosine phosphorylation, augmented EGF-, or IGF-I-dependent MAPK response, accelerated cell cycle progression through G1 phase in the absence of growth factors, and enhanced anchorage-independent growth in soft agar and tumorigenicity in nude mice [1, 6, 24]. Increased levels of SHC also potentiated growth factor response in myeloid and A549 adenocarcinama cells [3, 5]. Consistent with these findings are our previous data demonstrating that downregulation of SHC results in reduced sensitivity to mitogenic action of EGF and IGF-I and growth inhibition in breast cancer cells [16]. The present studies indicated that in SHC overexpressing epithelial cells, like in fibroblasts, basal and growth-factor-induced SHC tyrosine phosphorylation was increased, and cell responsiveness to IGF-I and EGF was moderately augmented in monolayer culture on plastic. However, amplification of SHC did not potentiate MAPK activity or proliferation of cells in complete serum-containing medium. This, again, was consistent with

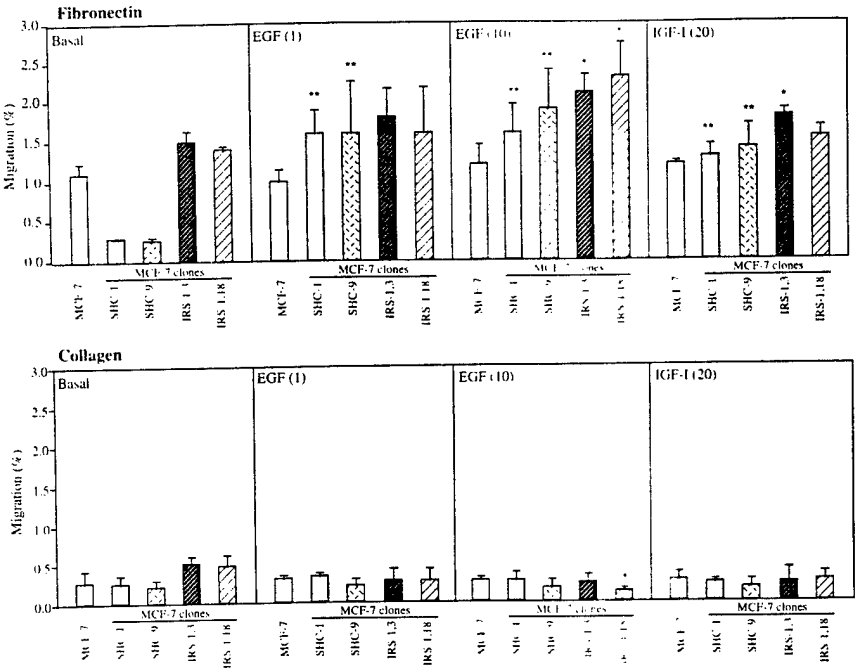

FIG. 5. Motility of MCF-7/SHC cells in FN or COL inserts. The motility of MCF-7/SHC cells and several control cell lines with normal SHC levels was tested as described under Materials and Methods. The upper and lower chambers contained PRF–SFM. Growth-factor-induced motility was assessed by supplementing PRF–SFM in lower chambers with either EGF (1 or 10 ng/ml) or IGF-I (20 ng/ml). The percentage of cells that migrated to the underside of inserts (relative to the number of cells plated) is shown. The experiments were repeated four times. Average values are given. Asterisks indicate statistically significant ($^*P < 0.05$, $^{**}P \leq 0.01$) differences between the basal and growth factor induced migration of a given cell line.

the effects observed in SHC overexpressing NIH 3T3 fibroblasts [6].

Note that high levels of SHC did not promote transformation of MCF-7 cells, whereas overexpression (at a similar level) of another signaling substrate IRS-1 markedly augmented anchorage-independent growth [32]. Since anchorage-independent growth reflects tumorigenic potential of breast cancer cells [36] and other cell types [1], our results indicate that, unlike in NIH 3T3 cells, SHC is not oncogenic in MCF-7 cells. This may reflect differences between pathways controlling transformation in fibroblasts and epithelial cells.

SHC in cell adhesion and motility. In contrast with the minimal impact of SHC overexpression on growth and transforming processes, high levels of SHC significantly modulated cell interactions with ECM in breast epithelial cells. SHC was found associated with $\alpha5\beta1$ integrin, the FN receptor, and $\alpha5\beta1$/SHC complexes were more abundant in SHC overexpressing cells than in other cell lines with SHC normal levels. The increased SHC/$\alpha5\beta1$ binding in MCF-7/SHC cells was paralleled by accelerated cell attachment to FN, reduced basal motility, abbreviated adhesion-mediated MAPK activity, and inhibited proliferation on the substrate. These effects were absent on COL (whose receptor does not bind SHC in MCF-7 cells), which suggests a specific role of SHC-$\alpha5\beta1$ interactions in the above processes.

The association of SHC with certain classes of integrins has been noted in several other cell systems. In A431 cells and other cell lines, binding and tyrosine phosphorylation of SHC to $\beta1$ integrin was induced by cell contact with ECM or by integrin cross-linking with a specific antibody [18]. Similarly, an association of SHC with $\alpha6\beta4$ integrin was observed in attached, but not suspended, A431 cells [34]. In several cell types, ligation of SHC-binding integrins, but not other integrins, has been reported to enhance cell cycle progression [18]. In our cell system, however, the increased association of SHC with $\alpha5\beta1$ integrin and the enhanced attachment to FN coincided with growth inhibition. Consistent with these findings are the observations of Wang *et al.*, who reported that in MCF-7 cells, $\alpha5\beta1$ integrin overexpression and improved interactions of cells with FN resulted in reduced proliferation on the substrate and impaired tumorigenicity *in vivo* [30].

Cell growth and survival on ECM are reflected by enhanced MAPK activity [18, 19, 35]. This pathway is induced by various integrin-associate TKs (e.g., c-Src-like TKs or FAK) and often involves activation of the SHC–GRB2–Ras pathway [19–21]. We found that the

amplification of SHC corresponded to the reduced duration of adhesion-mediated MAPK response on FN but not on COL. Note that, in mouse fibroblasts, an early decline of MAPK activity coincided with growth inhibition, whereas a prolonged activity marked cell cycle progression [37]. Thus, the abbreviated MAPK response in MCF-7/SHC cells may reflect their significantly slower proliferation on FN. In our experiments, treatment of cells spread on FN with EGF induced MAPK but did not stimulate cell growth, which confirms that MAPK signaling is required but not sufficient for the proliferation of MCF-7 cells [38].

Reduced growth and better attachment to FN in MCF-7/SHC cells were also associated with significantly reduced basal migration. However, EGF or IGF-I induced motility of MCF-7/SHC clones more strongly than other control cell lines when tested in FN-coated inserts. Such an enhancement of growth-factor-induced migration in SHC overexpressing cell lines has been reported before [5]. The increased chemotaxis was probably mediated by pathways other than MAPK, since MAPK activities were similar in MCF-7 and MCF-7/SHC cells treated with EGF.

In summary, in MCF-7 cells, the impact of the amplified SHC on cell growth and transformation is not significant; however, SHC plays an important role in the regulation of cell adhesion and motility on FN through its interaction with $\alpha 5\beta 1$ integrin. The significance of SHC-mediated interactions with FN in breast cancer metastasis is not known and will be pursued in an animal model.

This work was supported by the following grants and awards: NIH Grant DK 48969 to E.S.; U.S. Department of Defense Grant DAMD17-96-1-6250 to E.S., and DAMD Grant 17-97-1-7211 to M.A.G.; CNR Italy fellowships to D.S. and M.S., University of Calabria Postdoctoral Fellowship in Animal Biology to L.M., and POP 98 Grant from Regione Calabria to S.A.

REFERENCES

1. Pelicci, G., Lafrancone, L., Grignani, F., McGlade, J., Cavallo, F., Forni, G., Nicoletti, I., Grignani, F., Pawson, T., and Pelicci, P. G. (1992). A novel transforming protein (SHC) with an SH2 domain is implicated in mitogenic signal transduction. *Cell* **70,** 93–104.
2. Pelicci, G., Lafrancone, L., Salcini, A. E., Romano, A., Mele, S., Borrello, M. G., Segatto, O., Di Fiore, P. P., and Pelicci, P. G. (1995a). Constitutive phosphorylation of Shc proteins in human tumors. *Oncogene* **11,** 899–907.
3. Lafrancone, L., Pelicci, G., Brizzi, M. F., Aronica, M. G., Casciari, C., Giuli, S., Pegoraro, L., Pawson, T., and Pelicci, P. G. (1995). Overexpression of Shc proteins potentiates the proliferative response to the granulocyte-macrophage colony-stimulating factor and recruitment of Grb2/SoS and Grb2/p140 complexes to the beta receptor subunit. *Oncogene* **10,** 907–917.
4. Rozakis-Adcock, M., McGlade, J., Mbamalu, G., Pelicci, G., Daly, R., Li, W., Batzer, A., Thomas, S., Brugge, J., and Pelicci, P. G., *et al.* (1992). Association of the Shc and Grb2/Sem5 SH2-containing proteins is implicated in activation of the Ras pathway by tyrosine kinases. *Nature* **360,** 689–692.
5. Pelicci, G., Giordano, S., Zhen, Z., Salcini, A. E., Lafrancone, L., Bardeli, A., Panayotou, G., Waterfield, M. D., Ponzetto, C., Pelicci, P. G., and Comoglio, P. M. (1995b). The motogenic and mitogenic responses to HGF are amplified by the Shc adaptor protein. *Oncogene* **10,** 1631–1638.
6. Salcini, A. E., McGlade, J., Pelicci, G., Nicoletti, I., Pawson, T., and Pelicci, P. G. (1994). Formation of Shc-Grb2 complexes is necessary to induce neoplastic transformation by overexpression of Shc proteins. *Oncogene* **9,** 2827–2836.
7. Migliaccio, E., Mele, S., Salcini, A. E., Pelicci, G., Lai, K. M., Supreti-Furga, G., Pawson, T., Di Fiore, P. P., Lafrancone, L., and Pelicci, P. G. (1997). Opposite effects of the p52shc/p46shc and p66shc splicing isoforms on the EGF receptor-MAP kinase-fos signaling pathway. *EMBO J.* **16,** 706–716.
8. Okada, S., Kao, A. W., Ceresa, B. P., Blaikie, P., Margolis, B., and Pessin, J. E. (1997). The 66-kDa Shc isoform is a negative regulator of the epidermal growth factor-stimulated mitogen-activated protein kinase pathway. *J. Biol. Chem.* **272,** 28042–28049.
9. Biscardi, J. S., Belsches, A. P., and Pearsons, S. J. (1998). Characterization of human epidermal growth factor receptor and c-Src interactions in human breast tumor cells. *Mol. Carcinogen.* **21,** 261–272.
10. Stevenson, L. E., and Frackelton, A. R. (1998). Constitutively tyrosine phosphorylated p52shc in breast cancer cells-correlation with ERB2 and p66shc expression. *Breast Cancer Res. Treatm.* **49,** 119–128.
11. Matsuda, M., Ota, S., Tanimura, R., Nakamura, H., Matuoka, K., Takenawa, T., Nagashima, K., and Kurata, T. (1996). Interactions between the amino-terminal SH3 domain of CRK and its natural target proteins. *J. Biol. Chem.* **271,** 14468–14472.
12. Stein, D., Wu, J., Fuqua, S. A., Roonprapunt, C., Yajnik, V., D'Eustachio, P., Moskow, J. J., Buchberg, A. M., Osborne, K., and Margolis, B. (1994). The SH2 domain protein GRB-7 is co-amplified, overexpressed and in a tight complex with HER2 in breast cancer. *EMBO J.* **13,** 1331–1340.
13. Liu, L., Damen, J. E., Cutler, R. L., and Krystal, G. (1994). Multiple cytokines stimulate the binding of a common 145-kilodalton protein to Shc at the Grb2 recognition site of Shc. *Mol. Cell. Biol.* **14,** 6926–6935.
14. Kavanaugh, W. M., and Williams, L. T. (1994). An alternative to SH2 domains for binding tyrosine-phosphorylated proteins. *Science* **266,** 1862–1865.
15. Habib, T., Herrera, R., and Decker, S. J. (1994). Activators of protein kinase C stimulate association of Shc and the PEST tyrosine phosphatase. *J. Biol. Chem.* **269,** 25243–25246.
16. Nolan, M., Jankowska, L., Prisko, M., Xu, S., Guvakova, M., and Surmacz, E. (1997). Differential roles of IRS-1 and SHC signaling pathways in breast cancer cells. *Int. J. Cancer* **72,** 828–834.
17. Sachs, M., Weidner, K. M., Brinkmann, V., Walther, I., Obermeier, A., Ullrich, A., and Birchmeier, W. (1996). Motogenic and morphogenic activity of epithelial receptor tyrosine kinases. *J. Cell Biol.* **133,** 1095–1107.
18. Wary, K. K., Mainiero, F., Isakoff, S. J., Marcantonio, E. E., and Giancotti, F. G. (1996). The adaptor protein Shc couples a class of integrins to the control of cell cycle progression. *Cell* **87,** 733–743.
19. Wary, K. K., Mariotti, A., Zurzolo, C., and Giancotti, F. G. (1998). A requirement for caveolin-1 and associated kinase Fyn in integrin signaling and anchorage-dependent cell growth. *Cell* **94,** 625–634.

Experimental Cell Research 251, 244–255 (1999)
Article ID excr.1999.4566, available online at http://www.idealibrary.com on IDEAL®

The Activated Insulin-Like Growth Factor I Receptor Induces Depolarization in Breast Epithelial Cells Characterized by Actin Filament Disassembly and Tyrosine Dephosphorylation of FAK, Cas, and Paxillin

Marina A. Guvakova[1] and Ewa Surmacz

Kimmel Cancer Institute, Thomas Jefferson University, 233 South 10th Street, B.L.S.B. 606, Philadelphia, Pennsylvania 19107

Insulin-like growth factor I (IGF-I) promotes the motility of different cell types. We investigated the role of IGF-I receptor (IGF-IR) signaling in locomotion of MCF-7 breast cancer epithelial cells overexpressing the wild-type IGF-IR (MCF-7/IGF-IR). Stimulation of MCF-7/IGF-IR cells with 50 ng/ml IGF-I induced disruption of the polarized cell monolayer followed by morphological transition toward a mesenchymal phenotype. Immunofluorescence staining of the cells with rhodamine–phalloidin revealed rapid disassembly of actin fibers and development of a cortical actin meshwork. Activation of phosphatidylinositol (PI)3-kinase downstream of the IGF-IR was necessary for this process, as blocking PI 3-kinase activity with the specific inhibitor LY 294002 at 10 μM prevented disruption of the filamentous actin. In parallel, IGF-IR activation induced rapid and transient tyrosine dephosphorylation of focal adhesion proteins p125 focal adhesion kinase (FAK), p130 Crk-associated substrate (Cas), and paxillin. This process required phosphotyrosine phosphatase (PTP) activity, since pretreatment of the cells with 5 μM phenylarsine oxide (PAO), an inhibitor of PTPs, rescued FAK and its associated proteins Cas and paxillin from IGF-I-induced dephosphorylation. In addition, PAO-pretreated cells were refractory to IGF-I-induced morphological transition. Thus, our findings reveal a new function of the IGF-IR, the ability to depolarize epithelial cells. In MCF-7 cells, mechanisms of IGF-IR-mediated cell depolarization involve PI 3-kinase signaling and putative PTP activities.

Key Words: **insulin-like growth factor I receptor signaling; F-actin; phosphatidylinositol 3-kinase; focal adhesion; phosphotyrosine phosphatase.**

INTRODUCTION

Differentiated epithelial cells form tightly adherent polarized sheets with a full complement of specific adhesive junctions that stably link cells together and to the underlying biological substratum [1]. In the cell interior, various membrane junctions are connected by the cytoskeletal network, providing the strength and architecture required for the proper physiological function of the epithelial sheet [2]. Normal epithelial cells move as a coherent sheet in which each cell keeps contacts with its neighboring cells as well as with extracellular matrix [3]. The ability of cells to move individually appears to be an exclusive attribute of carcinoma cells. At present, however, little is known about how depolarization of epithelial cells is accomplished and regulated and what signals trigger this process.

The studies on chemotaxis and cell spreading suggest that insulin-like growth factor I (IGF-I) is a regulator of motility in normal and tumor cells [4–7]. In breast cancer cells, IGF-I-induced chemotactic migration has been reported to occur through the IGF-I receptor (IGF-IR) [8, 9]. Importantly, IGF-IR expression is 14 times higher and IGF-IR kinase activity is significantly increased in malignant compared with normal breast tissue. Furthermore, ligands of the IGF-IR, IGF-I, and IGF-II, are secreted by the surrounding mammary epithelium stromal cells [10]. The possibility that IGF-IR overexpression promotes depolarization and locomotive functions in breast epithelial cells has not been investigated.

The IGF-IR belongs to the tyrosine kinase receptor superfamily and is known to play an important role in normal and abnormal growth [11]. Ligand binding stimulates autophosphorylation of the IGF-IR β subunit, elevates its kinase activity, and leads to a recruitment of multiple signaling molecules: insulin receptor substrates 1 and 2 (IRS-1 and IRS-2), Shc, Crk, Gab1, Grb10, the p85 regulatory subunit of phosphatidylinositol 3-kinase (PI 3-kinase) [12]. Many of the known IGF-IR pathways convey mitogenic stimuli. IRS-1 molecule, for example, via its multiple tyrosine phosphorylation sites, recruits secondary signaling proteins containing Src-homology 2 (SH2) domains such as PI

[1] To whom reprint requests should be addressed. Fax: (215) 923–0249. E-mail: Marina.Guvakova@mail.tju.edu.

0014-4827/99 $30.00

3-kinase, phosphotyrosine phosphatase 1D (PTP1D/SH-PTP2/Syp), and Src-family kinase Fyn, as well as adapter proteins Grb-2, Crk, and Nck that participate in the mitogenic Ras/Raf/MAPK (mitogen-activated protein kinase) cascade [13]. It still remains unknown whether IGF-IR signaling pathways controlling epithelial cell motility are similar to or different from those required for cell proliferation.

The structure of the epithelial cell monolayer is supported by the integrity of the actin-enriched cytoskeleton, and its reorganization is critical for regulating cell motility [14]. Previous studies have described two types of IGF-IR effects on the actin cytoskeleton: the appearance of actin-enriched circular ruffles along the margins of KB epidermoid carcinoma cells [15, 16], and the development of an actin meshwork in the extended neurites of neuronal cells [17]. In breast epithelial cells, the relationship between the IGF-IR and the actin cytoskeleton has not been defined.

In polarized epithelial cells, focal adhesion proteins are localized to the termini of the stress fiber-like actin filaments as well as to cell–cell junctions adjacent to circumferential actin bundles [18]. Hence, reorganization of the actin network may affect the dynamics of focal adhesion assembly and lead to modulation of cell–substratum interaction, cellular shape, and consequently cell motility. In different cell types, IGF-I has been shown to positively or negatively modulate tyrosine phosphorylation of focal adhesion proteins such as FAK, Cas, and paxillin [17, 19, 20]. However, in these studies the link between IGF-I modulation of focal adhesion protein phosphorylation and cell motility was not established. Whether IGF-IR signaling regulates activity of focal adhesion proteins in breast epithelial cells, what the mechanism of the regulation might be, and how it relates to cell motility remain unexplored.

In work presented here, we analyzed the effect of IGF-IR activation on locomotion of MCF-7-derived breast epithelial cells organized in a monolayer with particular focus on elucidation of IGF-IR signaling promoting cell motility.

MATERIALS AND METHODS

Cell culture and chemicals. MCF-7 human breast epithelial cells overexpressing the IGF-IR were derived by stable transfection with pcDNA3/IGF-IR plasmid [21]. All MCF-7-derived cells were grown in DMEM:F12 (1:1) containing 5% calf serum. To starve the cells of serum, they were incubated in phenol red-free, serum-free Dulbecco's modified Eagle's medium (DMEM) containing 0.5 mg/ml bovine serum albumin (BSA), 1 μM $FeSO_4$, and 2 mM L-glutamine (SFM) for 24 h.

BSA, phenylarsine oxide (PAO), cytochalasin D (CD), and tetramethylrhodamine B isothiocyanate (TRITC)-conjugated phalloidin were purchased from Sigma. LY 294002 was from Calbiochem. Human recombinant IGF-I was purchased from Bachem.

Immunofluorescence light microscopy. Subconfluent cells grown on a glass coverslip were fixed with 3.7% formaldehyde in PBS for 15 min and permeabilized with 0.2% Triton X-100 in PBS for 5 min. To visualize actin filaments (F-actin) cells were stained with TRITC-conjugated phalloidin (1 μg/ml) for 30 min and examined with a Zeiss Axiophot microscope. Changes in the intracellular distribution of FAK, Cas, and paxillin were assessed by labeling with the primary antibodies: anti-FAK (A-17) pAb (Santa Cruz Biotechnology), a mixture of anti-Cas B and F pAbs (gift of Dr. A. H. Bouton, University of Virginia), or anti-paxillin mAb (Transduction Laboratories) for 60 min. In some experiments, subcellular localization of FAK was visualized with the 2A7 mAb raised against C terminus of pp125 FAK (gift of Dr. J. T. Parsons, University of Virginia). Primary antibody detection was performed with lissamine rhodamine (LRSC)-conjugated goat anti-rabbit IgG (Jackson ImmunoResearch Laboratories) or fluorescein isothiocyanate (FITC)-conjugated goat anti-mouse IgG (Calbiochem). In controls, the primary antibody was omitted. Some samples were examined using the Zeiss Axiovert 100 MRC 600 confocal laser scanning (Bio-Rad) immunofluorescence microscope. Optical sections were taken at the ventral plane.

Immunoprecipitation and immunoblotting. Cells were lysed in protein lysis buffer (50 mM Hepes pH 7.5, 150 mM NaCl, 1.5 mM $MgCl_2$, 1 mM EGTA, 10% glycerol, 1% Triton X-100, 20 μg/ml aprotinin, 2 mM Na orthovanadate, 1 mM phenylmethylsulfonyl fluoride). FAK, Cas, and paxillin were precipitated from the cell lysates (500 μg of total protein) with specific antibodies: anti-FAK (A-17) polyclonal antibody (pAb) (Santa Cruz Biotechnology), anti-Cas monoclonal antibody mAb (Transduction Laboratories), and anti-paxillin mAb (Transduction Laboratories), respectively. Protein–antibody complexes were collected with either protein A– or anti-mouse IgG–agarose beads overnight. The precipitates were washed with HNTG buffer (20 mM Hepes pH 7.5, 150 mM NaCl, 0.1% Triton X-100, 10% glycerol), resolved by sodium dodecyl sulfate (SDS)–polyacrylamide gel electrophoresis, and transferred to nitrocellulose. Tyrosine phosphorylation and protein levels of FAK, Cas, and paxillin were assessed by immunoblotting with anti-phosphotyrosine mAb (PY-20) (Santa Cruz Biotechnology) or the specific antibodies as used for precipitations. The proteins were visualized by enhanced chemiluminescence detection (Amersham).

RESULTS

Activation of the IGF-IR Induces Depolarization of MCF-7 Cells

Serum-starved MCF-7 cells expressing moderate levels of the endogenous IGF-IR (6×10^4 receptors/cell) and MCF-7/IGF-IR cells with an 18-fold overexpression of wild-type IGF-IR both displayed a characteristic epithelial morphology with apicobasal polarity. The basal cell surfaces were adherent to the substratum, while lateral membranes of adjacent cells were attached to each other (Figs. 1A, 1B). In response to addition of 5–50 ng/ml IGF-I the cell monolayers underwent a dose-related morphological reorganization (data not shown). The most drastic changes occurred in 50 ng/ml IGF-I and were characterized by disruption of the epithelial sheet, loss of cell polarity, and development of a fibroblast-like phenotype by the majority of cells (Figs. 1C, 1D). Within 15 min cell–cell contacts loosened. By 60 min the cells partially detached from the plastic surface and rounded up slightly. Between 1 and 4 h of continuous IGF-I exposure the cells devel-

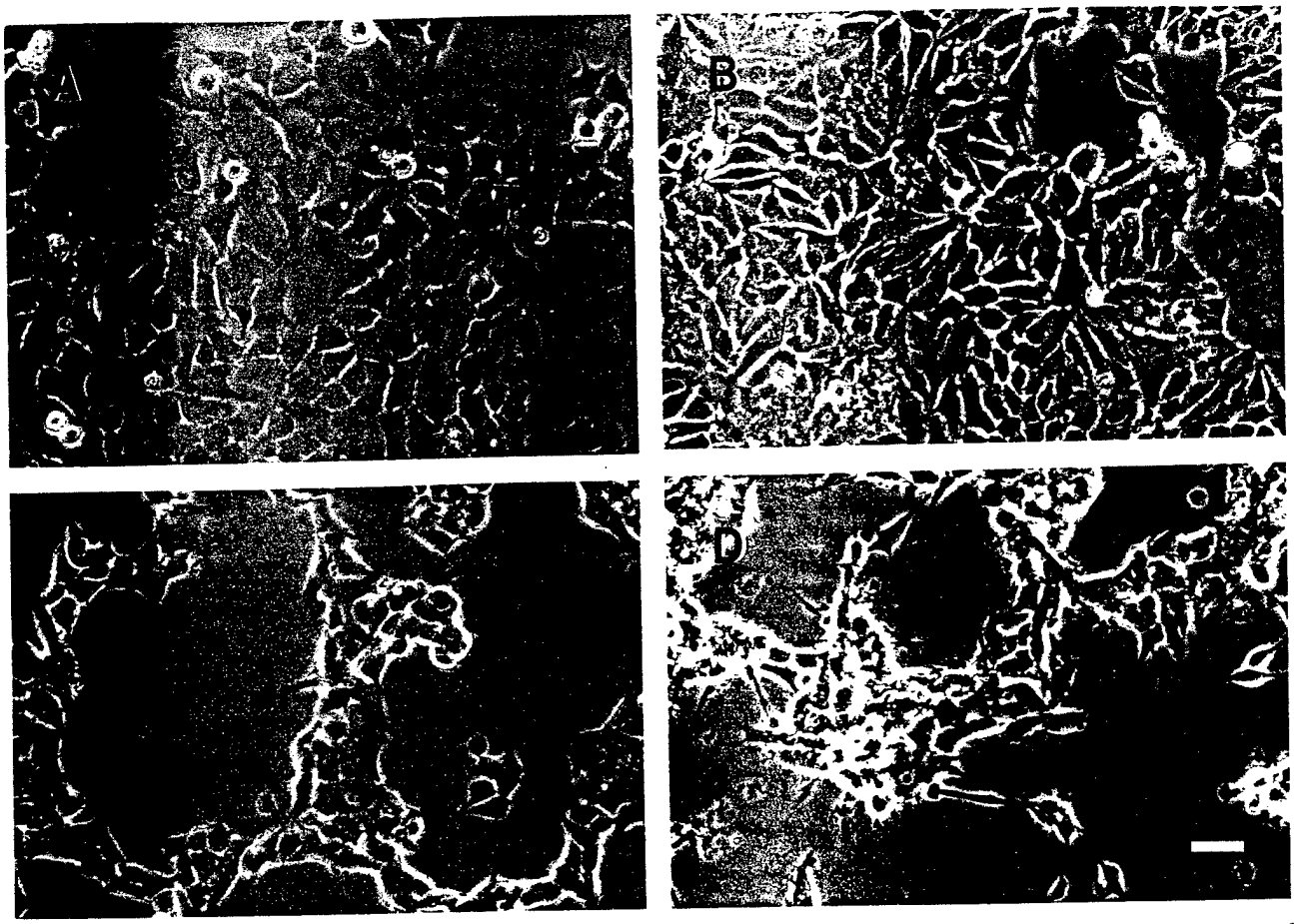

FIG. 1. IGF-IR activation stimulates depolarization and morphological transition in MCF-7-derived cells. The representative phase-contrast micrographs show the morphology of serum-starved MCF-7 (A) and MCF-7/IGF-IR (B) cells. In (C), MCF-7 and in (D), MCF-7/IGF-IR serum-starved cells were stimulated with 50 ng/ml IGF-I for 4 h. Bar = 100 μm.

oped multiple lamellipodial structures, which are characteristics of motile cells. Both control and IGF-IR-overexpressing cells were affected by IGF-I; however, the extent of the modifications was more pronounced in MCF-7/IGF-IR than MCF-7 cells (compare Figs. 1C and 1D). Therefore, IGF-IR-overexpressing cells were chosen for analysis in all subsequent experiments.

IGF-IR Activation Induces PI 3-Kinase-Dependent Disassembly of the Actin Filaments

To determine if IGF-IR activation induces reorganization of the actin cytoskeleton, F-actin was visualized in serum-starved MCF-7/IGF-IR cells treated with 50 ng/ml IGF-I for various times (Figs. 2A–2D). Within 5 min, the IGF-I effect on the actin cytoskeleton was detected as a disappearance of circumferential actin bundles, disassembly of stress fiber-like filaments, and development of a widespread cortical actin meshwork (Fig. 2B). After approximately 15 min, accumulation of F-actin was observed at the cell margins within structures resembling microspikes or small membrane ruffles (Figs. 2C, 2E). Between 1 and 4 h, the cells developed multiple extended protrusions, and fine long actin filaments reappeared, traversing cytoplasm and terminating in the veil-like lamellipodia (Fig. 2D).

Activation of PI 3-kinase has been implicated in restructuring of the actin cytoskeleton in other cell types [18, 26]. We investigated the role of PI 3-kinase in IGF-IR-induced modification of F-actin using a synthetic compound LY 294002 that blocks PI 3-kinase specifically (IC_{50} = 1.4 μM) and does not affect the activity of either IGF-IR or IRS-1 at concentrations up to 20 μM (data not shown). When MCF-7/IGF-IR cells pretreated with 10 μM LY 294002 for 30 min were stimulated with 50 ng/ml IGF-I for 30 min in the presence of the inhibitor, F-actin disassembly was prevented completely (compare Figs. 2E and 2F). The appearance of short actin bundles in membrane ruffles also was blocked. The actin cytoskeleton remained intact even 1 h after addition of IGF-I (data not shown).

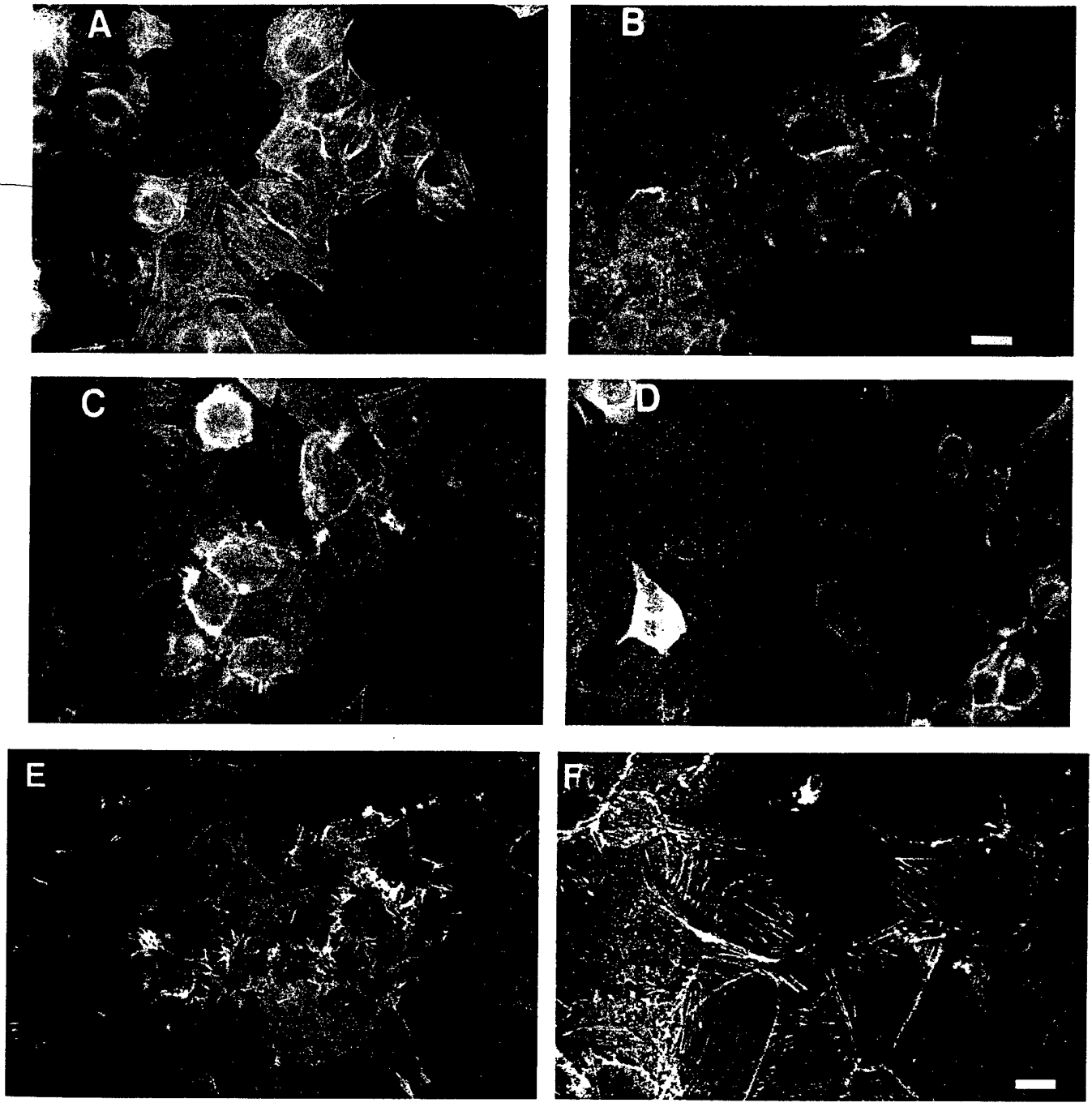

FIG. 2. IGF-I stimulation rapidly changes F-actin pattern in MCF-7/IGF-IR cells. The representative images of the selected time points show MCF-7/IGF-IR cells in which F-actin was visualized with TRITC-labeled phalloidin. Serum-starved cells (A); serum-starved cells stimulated with 50 ng/ml IGF-I for 5 min (B), 15 min (C), 30 min (E), and 4 h (D). (F) The cells were pretreated with 10 μM LY 294002 for 30 min, followed by stimulation with 50 ng/ml IGF-I for 30 min. Bar = 20 μm.

These results indicate that IGF-IR-activated PI 3-kinase signaling is critical for the initial step of IGF-IR-induced F-actin reorganization, namely, for the transient breakdown of actin filaments, as well as for subsequent F-actin rearrangement related to membrane protrusion.

The Activated IGF-IR Promotes Restructuring of Focal Adhesion Contacts

To investigate the relationship between changes in the actin filament network and organization of focal adhesions, conventional immunofluorescence light mi-

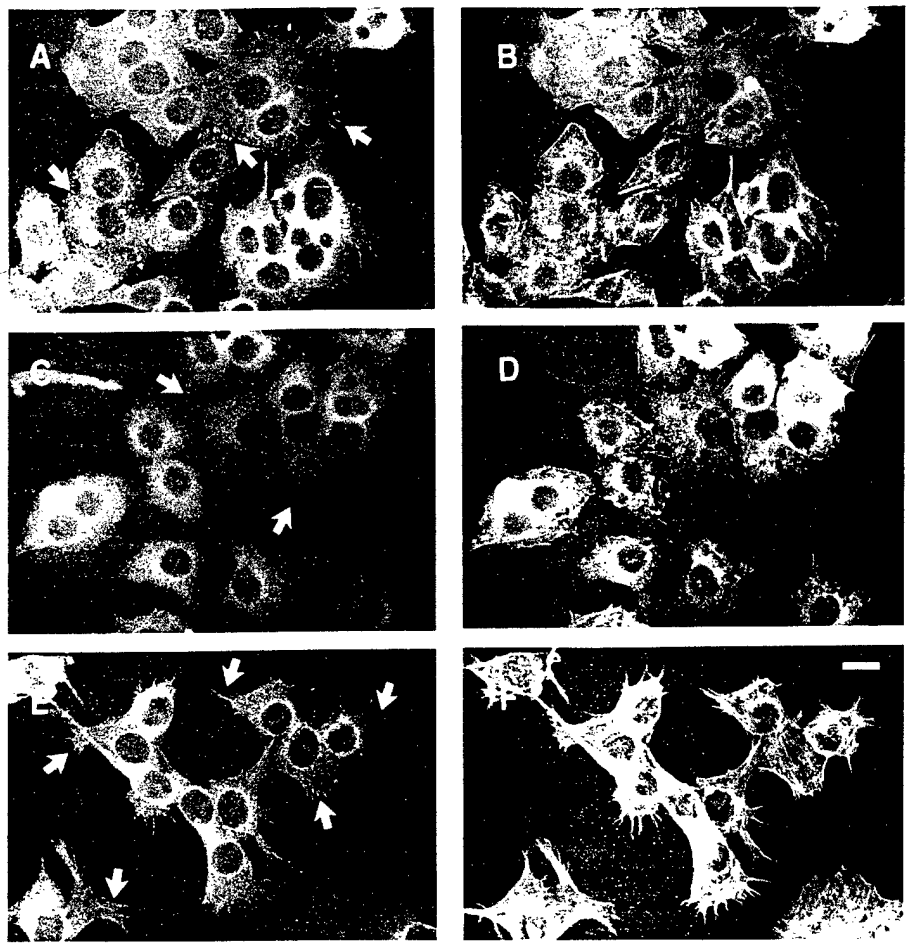

FIG. 3. Actin cytoskeleton reorganization is accompanied by redistribution of paxillin in IGF-I-stimulated MCF-7/IGF-IR cells. The representative images show cells costained with an anti-paxillin mAb (A, C, E) and TRITC-phalloidin (B, D, F). Serum-starved cells (A, B). Serum-starved cells treated with 50 ng/ml IGF-I for 5 min (C, D) and 60 min (E, F). Arrows in (A), (C), and (E) point to the position of the paxillin accumulations in membrane protrusions. Bar = 20 μm.

croscopy was used. MCF-7/IGF-IR cells stimulated with 50 ng/ml IGF-I for various times were examined (Figs. 3A–3F). Costaining of F-actin and paxillin, a marker of focal adhesions, revealed that "arrowhead"-shaped paxillin clusters disappeared, along with actin filament disassembly, within 5 min of IGF-I stimulation (compare Figs. 3A, 3B and 3C, 3D). Approximately 1 h after IGF-I addition, when the fine actin filaments reappeared, elongated streaks of paxillin staining were observed in numerous membrane protrusions (Figs. 3E, 3F).

To investigate whether changes in paxillin localization paralleled redistribution of two other focal adhesion-associated proteins, FAK and Cas, MCF-7/IGF-IR cells were doubly stained with anti-paxillin mAb [Figs. 4A(a)–4F(a)] and either anti-FAK (A-17) [Figs. 4A(b), 4C(b), 4E(b)] or anti-Cas [Figs. 4B(b), 4D(b), 4F(b)] pAbs. In fully spread, serum-starved cells, FAK and Cas partially colocalized with paxillin in punctate arrays of dots along cell edges and in fine clusters distributed over the ventral surface of cells (Figs. 4A, 4B). Within 15 min of IGF-I stimulation, FAK, Cas, and paxillin were all stained in the cytoplasm. At this time point the cells were slightly rounded up and had only a few paxillin-positive focal contacts (Figs. 4C, 4D). After 1–4 h, FAK and Cas could not be detected clearly in membrane protrusions where paxillin streaks were abundant [Figs. 4E(b), 4F(b)]. Similar results with respect to the intracellular redistribution of FAK were observed with both the A-17 and 2A7 anti-FAK antibodies.

Activation of the IGF-IR Induces Rapid Tyrosine Dephosphorylation of Focal Adhesion Proteins: FAK, Cas, and Paxillin

Actin fiber disassembly was shown to correlate with a reduction of FAK tyrosine phosphorylation in CHO cells [22]. We examined the time course and extent of the FAK tyrosine phosphorylation in MCF-7/IGF-IR

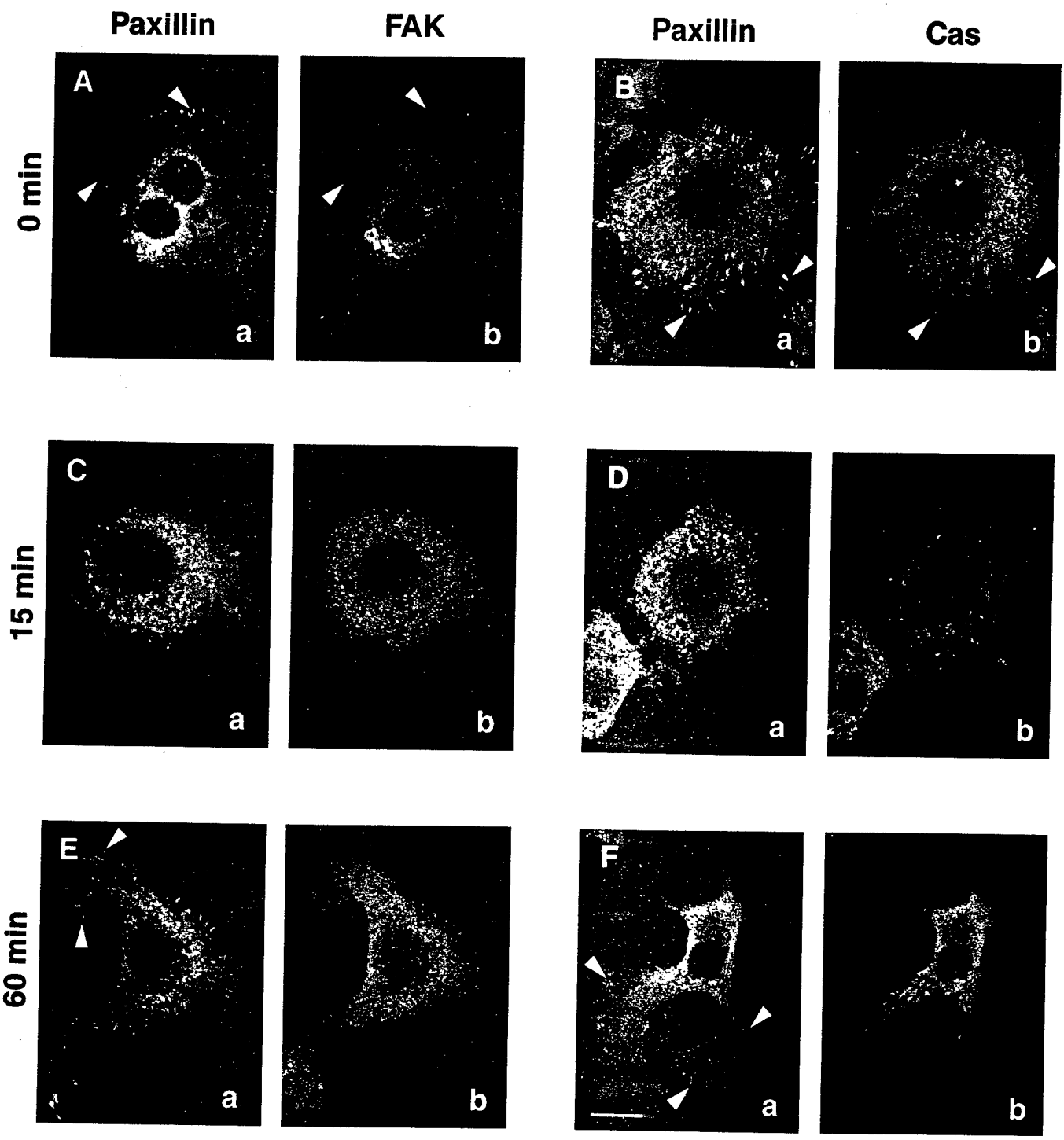

FIG. 4. IGF-I stimulation changes intracellular localization of FAK and Cas along with paxillin in MCF-7/IGF-IR cells. The representative confocal microscopy images demonstrate cells colabeled with anti-paxillin mAb [A(a), C(a), E(a)] and anti-FAK (N-17) pAb [A(b), C(b), E(b)]; cells colabeled with anti-paxillin mAb [B(a), D(a), F(a)] and a mixture of anti-Cas B and anti-Cas F pAbs [B(b), D(b), F(b)]. Serum-starved cells (A, B); serum-starved cells treated with 50 ng/ml IGF-I for 15 min (C, D) and 60 min (E, F). The representative areas of coincidental staining of paxillin with either FAK or Cas are marked by arrowheads in (A) and (B), respectively. In (E) and (F), arrowheads indicate the accumulation of paxillin in prolonged streaks localized to membrane protrusions. Bar = 20 μm.

cells stimulated with IGF-I. In serum-starved cells, FAK was prominently tyrosine phosphorylated (Fig. 5A′). Within 5 min of IGF-I treatment, FAK became dephosphorylated by 50% (Fig. 5A). The level of FAK phosphorylation remained low for at least 15 min, then was elevated almost to basal level by 1 h (Figs. 5A and

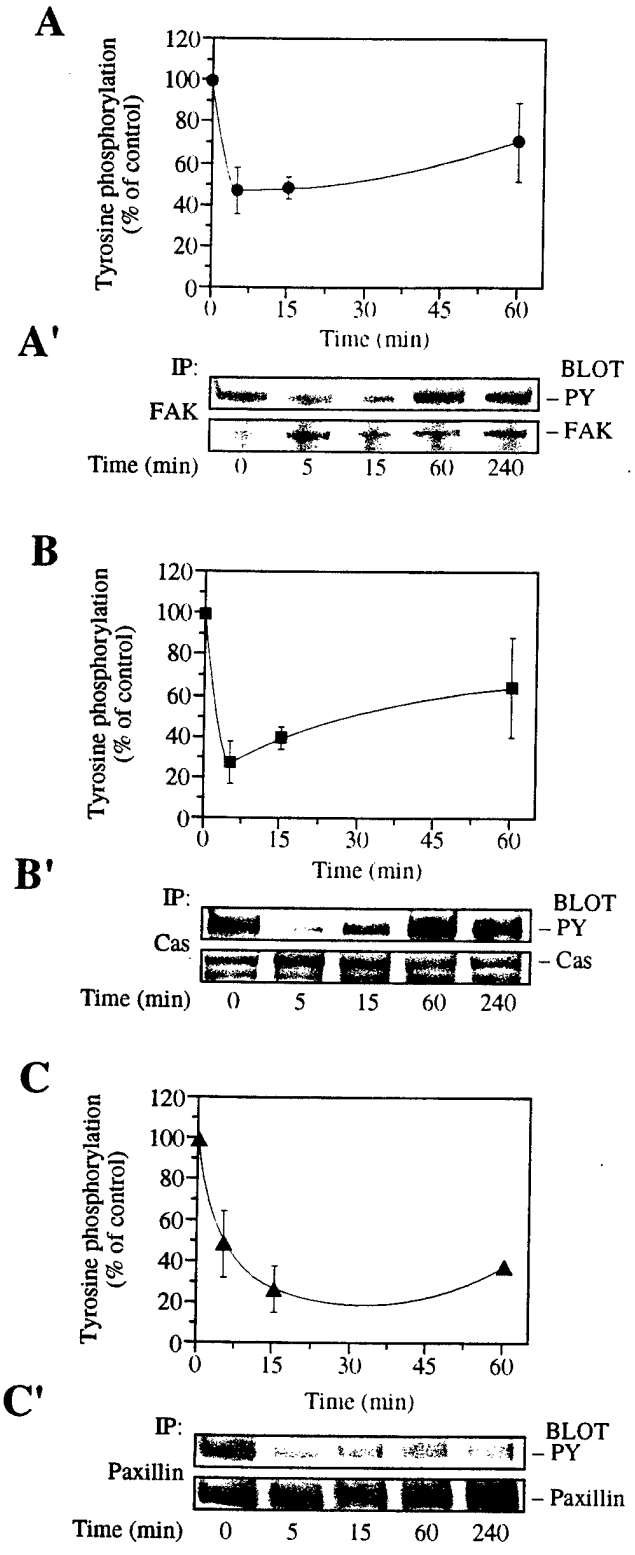

FIG. 5. IGF-IR activation induces rapid tyrosine dephosphorylation of FAK, Cas, and paxillin in MCF-7/IGF-IR cells. (A, B, C) Time courses of the relative tyrosine phosphorylation of FAK, Cas, and paxillin in response to 50 ng/ml IGF-I, correspondingly. The intensity of the bands of the phosphorylated proteins was measured by laser scanning densitometry. The value of tyrosine phosphorylation for each protein in serum-starved cells (time point 0 min) was taken as 100%. Error bars show SEM, $n = 4$. (A', B', C') Representative blots demonstrate the various levels of the tyrosine phosphorylated FAK, Cas, and paxillin (upper panels) and the comparable amounts of these proteins in the correspondent samples (lower panels) before and after IGF-I stimulation at the indicated time points. In the lower panels of (A'), (B'), and (C'), the anti-phosphotyrosine blots were stripped and reprobed with the indicated antibodies.

5A', upper panel). To test the possibility that tyrosine dephosphorylation of FAK affected the phosphotyrosine content of FAK targets such as Cas and paxillin, we immunoprecipitated both these proteins from the same lysates as FAK.

In control serum-starved cells, the tyrosine phosphorylation level of Cas and paxillin was high (Figs. 5B', 5C', upper panels). After 5 min of IGF-I stimulation, the Cas tyrosine phosphorylation was reduced by more than 70% of the control level. Tyrosine dephosphorylation of Cas was transient, since within 15 min of IGF-I addition its phosphorylation was elevated, and by 1 h it almost reverted to the basal level (Figs. 5B, 5B'). Within 5 min of IGF-I stimulation, tyrosine phosphorylation of paxillin was reduced by 50%, and over the next 10 min it declined further to 30–40% of basal phosphorylation, remaining at this level for at least 4 h (Fig. 5C).

In the absence of IGF-I stimulation, the basal level of tyrosine phosphorylation of FAK, Cas, and paxillin in the parental MCF-7 cells was comparable to that in MCF-7/IGF-IR cells. However, no significant changes in tyrosine phosphorylation status of focal adhesion-associated proteins FAK, Cas, and paxillin were observed in MCF-7 cells treated with 50 ng/ml IGF-I for up to 4 h (data not shown).

PAO Prevents Tyrosine Dephosphorylation of FAK, Cas, and Paxillin and Inhibits Membrane Protrusion in IGF-I-Stimulated MCF-7/IGF-IR Cells

To investigate whether protein tyrosine phosphatase activity was required for the reduced tyrosine phosphorylation of FAK, Cas, and paxillin in response to IGF-I stimulation of MCF-7/IGF-IR cells, we attempted to block a putative IGF-IR-activated PTP. The trivalent arsenical compound PAO was selected for this purpose. PAO is a membrane-permeable PTP inhibitor that blocks tyrosine phosphatase activity in insulin signaling and upregulates tyrosine phosphorylation of FAK and paxillin in fibroblasts at concentrations of 1–5 μM [23, 24].

In a series of control experiments we established that 5 μM PAO had no effect on IGF-I-induced tyrosine phosphorylation of either the IGF-IR β subunit or IRS-1 (data not shown). Subsequently, we examined

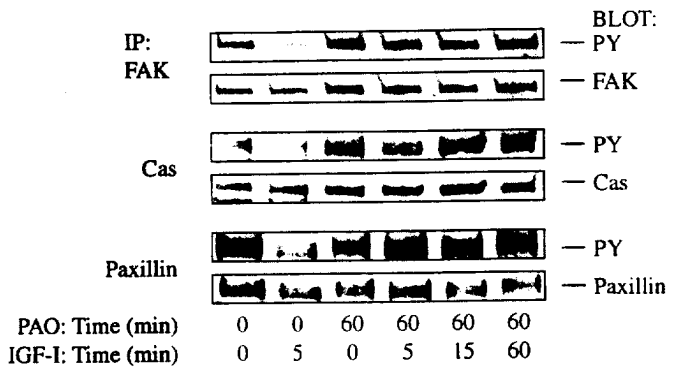

FIG. 6. PAO prevents tyrosine dephosphorylation of focal adhesion proteins in cells stimulated with IGF-I. Western blots show tyrosine phosphorylation and protein levels of the immunoprecipitated FAK, Cas, and paxillin in samples of serum-starved cells, serum-starved cells stimulated with 50 ng/ml IGF-I for 5 min, and serum-starved cells pretreated with 5 μM PAO for 60 min and then stimulated with 50 ng/ml IGF-I for the time indicated.

the effect of PAO on IGF-I-induced dephosphorylation of focal adhesion proteins FAK, Cas, and paxillin (Fig. 6). Preincubation with PAO for 60 min resulted in slightly increased basal tyrosine phosphorylation only of FAK and Cas. The following stimulation of PAO-treated cells with IGF-I for up to 60 min did not reduce tyrosine phosphorylation of FAK, Cas, and paxillin, indicating that PTP activity is required for IGF-IR-mediated dephosphorylation of these molecules.

We further investigated whether PAO rescue of the focal adhesion proteins from IGF-I-induced dephosphorylation influenced IGF-IR-mediated changes in cell morphology. MCF-7/IGF-IR cells were incubated in either 5 μM PAO in SFM or SFM alone for 60 min (Figs. 7A and 7D, respectively). Next, both cell monolayers were stimulated with 50 ng/ml IGF-I, and cell morphology was recorded after 15 and 60 min (Figs. 7B, E and 7C, F). After 60 min, PAO-treated cells formed lobopodium-like membrane advances resembling those displayed by serum-starved cells in response to a 15-min treatment with IGF-I (compare Figs. 7C and 7E). The outward extensions of lamellipodia typically seen in control cells after 60 min of IGF-I addition appeared to be blocked in PAO-pretreated cells, thereby suggesting at least a partial inhibition of morphological transition toward the motile phenotype.

DISCUSSION

The structural organization of a normal polarized epithelium restricts the separation and movement of individual cells. However, at early stages of malignant progression loss of epithelial polarity can promote cell motility and facilitate dissemination of cancer cells from epithelial tissue, thereby increasing the chance of a metastatic spread [25].

The increased level and enhanced autophosphorylation of the IGF-IR observed in malignant versus normal human breast tissues [10], as well as association of the IGF-IR with cell migration *in vitro* [8, 9], prompted our current investigations on the cellular and molecular mechanisms governing IGF-IR-mediated motility in breast cancer cells.

In the present work, we assessed the effects of IGF-IR overexpression on the events related to motility of MCF-7 breast epithelial cells. For the first time, we demonstrated that activation of the overexpressed IGF-IR causes depolarization of an epithelial cell monolayer. The magnitude of IGF-IR signaling as determined by the number of activated IGF-IRs appears critical for converting epithelial cells from a polarized to a motile phenotype, since a more striking morphological transformation occurred in MCF-7/IGF-IR (1.1×10^5 receptors/cell) than in the parental MCF-7 (6.0×10^4 receptors/cell) cells.

The drastic changes in morphology of IGF-I-stimulated MCF-7/IGF-IR cells point to the involvement of cytoskeleton restructuring in cell depolarization. In this study we analyzed reorganization of the actin cytoskeleton in MCF-7/IGF-IR cells stimulated with IGF-I for 4 h, and identified three distinct phases of F-actin reorganization: (1) actin filament disassembly followed by (2) accumulation of condensed short actin bundles along the cell periphery, and (3) reassembly of the long F-actin bundles.

We have demonstrated that disruption of circumferential and stress fiber-like actin bundles as well as cortical actin filaments—the cytoskeletal structures responsible for the architecture and strength of the multicellular epithelial sheet—is an early event associated with IGF-IR-induced depolarization. Disassembly of actin filamentous network appeared to be transient (5–15 min). How does the activated IGF-IR cause F-actin disassembly? One possibility is that the rapid breakdown of the actin filaments is caused by the activation of actin-severing proteins, like gelsolin, whose stimulation, in turn, requires the transient increase in intracellular Ca^{2+} [26]. In some cell types, IGF-I stimulates phosphatidylinositide turnover and intracellular Ca^{2+} release [27]. Whether a rise in Ca^{2+} and stimulation of the actin-severing proteins occur following IGF-IR activation in MCF-7 cells remains to be determined.

Another possibility might be an IGF-IR-mediated activation of the small GTP-binding protein Rac as well as other members of the Rho family. Recently, microinjection studies on Rho D, Rho G, TC10, Rnd 1, and Rnd 3 (RhoE) demonstrated that these proteins cause breakdown of the stress fibers and associated loss of cell adhesion in fibroblasts [28]. In mammary epithelial cells, Cdc42- and Rac-mediated actin reorganization has been disrupted by inhibition of the PI 3-kinase

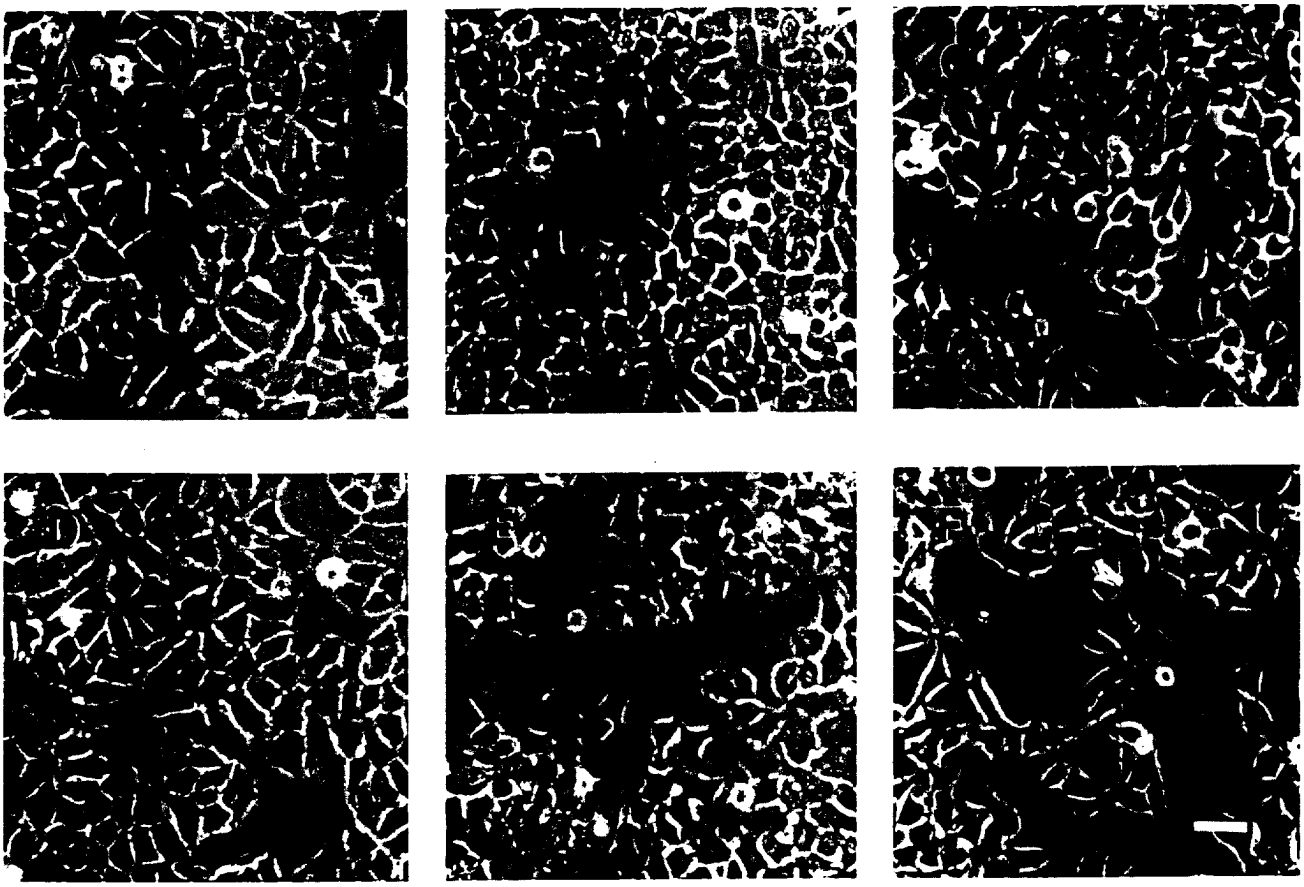

FIG. 7. PAO blocks morphological transitions in MCF-7/IGF-IR cells stimulated with IGF-I. The representative phase-contrast micrographs show the morphology of MCF-7/IGF-IR cells under different conditions. Serum-starved cells were pretreated with 5 μM PAO in SFM for 60 min (A) and then stimulated with 50 ng/ml IGF-I for either 15 min (B) or 60 min (C). In parallel, serum-starved cells (D) were stimulated with 50 ng/ml IGF-I for either 15 min (E) or 60 min (F). Bar = 100 μm.

[29]. In fibroblasts expressing the Ras oncogene, active PI 3-kinase has been implicated in the disruption of actin stress fibers via dissociation of cortactin, an F-actin crosslinking protein, from the actin–myosin II complex [30]. According to our previous data, the amount and activity of IRS-1-associated PI 3-kinase are higher in MCF-7/IGF-IR than in MCF-7 cells stimulated with IGF-I [21, 31]. In the study reported here, we tested the involvement of the PI 3-kinase in F-actin rearrangements in MCF-7/IGF-IR cells. Preincubation of the cells with the specific PI 3-kinase inhibitor LY 294002 abrogated IGF-I-induced F-actin disassembly, suggesting that IGF-IR/PI 3-kinase-dependent signaling triggers the rapid F-actin breakdown in MCF-7/IGF-IR cells.

The second phase of IGF-IR modulation of the actin cytoskeleton lasted approximately 1 h and was characterized by organization of the short F-actin bundles into microspike-like structures along the cell periphery. We speculate that IGF-IR regulation of actin-binding/bundling proteins is involved in microspike formation, which in turn might facilitate cell depolarization. This hypothesis is being tested currently.

The reappearance of the long actin filaments in the nascent lamellipodia apparently required actin polymerization, since addition of IGF-I along with cytochalasin, the drug that caps the plus end of actin filament and blocks actin polymerization, prevented lamellipodial extension (Guvakova, unpublished data). In many cell types, actin polymerization is closely linked with PI 3-kinase signaling [32], which also is required for lamellipodium formation and membrane ruffling [33]. Accordingly, we demonstrated that a block of PI 3-kinase activity inhibited IGF-I-induced membrane protrusion. This, however, does not rule out the possibility that the blockade of membrane extension is a secondary event, since the inhibition of PI 3-kinase also prevented F-actin disassembly, and the latter preceded lamellipodial protrusion in MCF-7/IGF-IR cells.

Previous studies have revealed that the breakdown of cell–cell adhesions plays an important role in epithelial–mesenchymal transition induced by different

growth factors [34, 35]. However, morphological cell transformation from polarized to nonpolarized phenotype is certainly related to modulation of cell–substratum interaction, and, therefore, mechanisms must exist to regulate the assembly and disassembly of cell–matrix junctions. We have shown here that IGF-IR activation induces rapid reorganization of focal adhesions. In response to IGF-I, "arrowhead"-shaped paxillin clusters in the static cell transformed into elongated streaks of paxillin at the periphery of membrane protrusions. The latter might function similarly to "transient focal contacts" of slowly moving cells described by Couchman and Rees [36]. Paxillin possesses multiple protein–protein interaction motifs [37] and, in contrast to FAK and Cas, is prominent in membrane protrusions. It is tempting to speculate that an exchange in paxillin molecular partners plays a key role in IGF-IR-mediated turnover of focal adhesions.

The effect of IGF-I on the tyrosine phosphorylation status of the focal adhesion proteins has been investigated in various cell models, and the reported influence of IGF-I on either FAK or paxillin appeared to be contrasting in different cells [17, 19, 20]. Recently, it was demonstrated that in IGF-I-stimulated Swiss 3T3 fibroblasts expressing very low levels of the IGF-IR there was an increase in FAK, Cas, and paxillin tyrosine phosphorylation [38]. In contrast to MCF-7 cells, however, serum-starved Swiss 3T3 cells lose their stress fibers and associated focal adhesions as well as tyrosine phosphorylation of FAK and paxillin [39]. Therefore, the contrasted cellular context and varying levels of IGF-IR expression in different cellular systems make it difficult to compare the results.

To clarify the relationship between IGF-IR stimulation, focal adhesion protein activity, and cell locomotion, we analyzed the time course of tyrosine phosphorylation of FAK, Cas, and paxillin in MCF-7 and MCF-7/IGF-IR cells exposed to IGF-I. In the MCF-7 parental cells, the relatively high basal phosphorylation of FAK, Cas, and paxillin was not reduced notably on IGF-I stimulation, whereas in MCF-7/IGF-IR cells, stronger IGF-IR activation triggered an acute tyrosine dephosphorylation of FAK and Cas. The kinetic profiles of FAK and Cas dephosphorylation were similar, consistent with the regulatory role of FAK in direct or indirect (via the activation of Src-family kinases) tyrosine phosphorylation of Cas [40, 41]. Alternatively, the activated IGF-IR might stimulate a PTP controlling the function of FAK, Cas, or Src-family proteins. In this respect it is interesting that a newly discovered dual-specificity phosphatase PTEN (MMAC1) interacts with FAK and reduces tyrosine phosphorylation of this kinase as well as Cas [42]. The SH3 domain of Cas also directly binds to proline-rich region of the cytoplasmic PTP1B [43] whose role in IGF-IR signaling remains obscure. In the present study, we found that another FAK-associated phosphoprotein, paxillin, underwent tyrosine dephosphorylation in response to IGF-I. The recent discovery of the physical association between a nonreceptor PTP–PEST and paxillin suggests that paxillin itself or paxillin-binding partners, including FAK, might serve as PTP–PEST substrates [44]. Another enticing candidate for a role in IGF-IR-regulated PTP activity is PTP1D (also known as Shp2/SH-PTP2/Syp). This cytoplasmic PTP is activated by direct binding to the phosphorylated insulin receptor (IR), IGF-IR or IRS-1 [45], and is known to mediate insulin-induced dephosphorylation of FAK and paxillin in CHO cells overexpressing the IR [46]. Recent studies identified an important role for PTP1D in regulating cell spreading, migration, and cytoskeletal architecture in fibroblasts, presumably via control of FAK [47].

Despite the unknown identity of IGF-IR-activated PTP in our cell model, the experiments with PAO, a phosphotyrosine phosphatase inhibitor, support the idea that induction of a PTP is critical for depolarization in MCF-7/IGF-IR cells. PAO rescue of FAK, Cas, and paxillin, from IGF-I-induced tyrosine dephosphorylation was sufficient to block development of the motile membrane protrusions. Collectively, our findings suggest the IGF-IR as an upstream regulator of a PAO-sensitive PTP, which either directly or indirectly dephosphorylates FAK, Cas, and paxillin and disrupts focal contacts.

In summary, we have established that activation of the overexpressed IGF-IR in MCF-7 cells results in a loss of epithelial cell polarity associated with acute disassembly of the actin filaments, subcellular reorganization of paxillin-enriched focal contacts, and rapid tyrosine dephosphorylation of FAK, Cas, and paxillin. Both PI 3-kinase and PTP activities are required for the depolarization of MCF-7 breast cancer cells. Taken together, these results suggest that IGF-IR overexpression in mammary epithelial cells may have a significant impact in stimulating tumor cell motility.

We are grateful to Dr. Joseph A. DePasquale for valuable discussions during the work, to Dr. Karen Knudsen and Dr. Carol Marshall for the critical comments on the manuscript, to Todd Sargood and Dawn Fowler for help with image processing, and to Priya K. Hingorani for the expert assistance with confocal microscopy. We thank Dr. Amy H. Bouton and Dr. J. Thomas Parsons for the generous gift of the antibodies. M.A.G. is a recipient of a fellowship from the U.S. Army (DAMD 17-97-1-7211). This work was in part supported by NIH Grant DK48969 (E.S.)

REFERENCES

1. Davies, J. A., and Garrod, D. R. (1997). Molecular aspects of the epithelial phenotype. *BioEssays* **19,** 699–704.
2. Gumbiner, B. (1996). Cell adhesion: The molecular basis for tissue architecture and morphogenesis. *Cell* **84,** 345–357.
3. Danjo, Y., and Gipson, I. K. (1998). Actin 'purse string' filaments are anchored by E-cadherin-mediated adherens junc-

tions at the leading edge of the epithelial wound, providing coordinated cell movement. *J. Cell Sci.* **111,** 3323–3331.

4. Ando, Y., and Jensen, P. J. (1993). Epidermal growth factor and insulin-like growth factor I enhance keratinocyte migration. *J. Invest. Dermatol.* **100,** 633–639.
5. Leventhal, P. S., and Feldman, E. L. (1997). Insulin-like growth factors as regulators of cell motility: Signaling mechanisms. *Trends Endocrinol. Metab.* **8,** 1–6.
6. Brooks, P. C., Klemke, R. L., Schön, S., Lewis, J. M., Schwartz, M. A., and Cheresh, D. A. (1997). Insulin-like growth factor receptor cooperates with integrin $\alpha_v\beta5$ to promote tumor cell dissemination in vivo. *J. Clin. Invest.* **99,** 1390–1398.
7. Henricks, D. M., Kouba, A. J., Lackey, B. R., Boone, W. R., and Gray, S. L. (1998). Identification of insulin-like growth factor I in bovine seminal plasma and its receptor on spermatozoa: Influence on sperm motility. *Biol. Reprod.* **59,** 330–337.
8. Kohn, E. C., Francis, E. A., Liotta, L. A., and Schiffmann, E. (1990). Heterogeneity of the motility responses in malignant tumor cells: A biological basis for the diversity and homing of metastatic cells. *Int. J. Cancer* **46,** 287–292.
9. Doerr, M. E., and Jones, J. I. (1996). The roles of integrins and extracellular matrix proteins in the insulin-like growth factor I-stimulated chemotaxis of human breast cancer cells. *J. Biol. Chem.* **271,** 2443–2447.
10. Resnik, J. L., Reichart, D. B., Huey, K., Webster, N. J. G., and Seely, B. L. (1998). Elevated insulin-like growth factor I receptor autophosphorylation and kinase activity in human breast cancer. *Cancer Res.* **58,** 1159–1164.
11. Baserga, R. (1998). The IGF-I receptor in normal and abnormal growth. *In* "Hormones and Growth Factors in Development and Neoplasia" (R. B. Dickson and D. S. Salomon, Eds.), pp. 269–287. Wiley–Liss, New York.
12. Sepp-Lorenzino, L. (1998). Structure and function of the insulin-like growth factor I receptor. *Breast Cancer Res. Treat.* **47,** 235–253.
13. Yenush, L., and White, M. F. (1997). The IRS-1-signaling system during insulin and cytokine action. *BioEssays* **19,** 491–500.
14. Yonemura, S., Itoh, M., Nagafuchi, A., and Tsukita, S. (1995). Cell-to-cell adherens junction formation and actin filament organization: Similarities and differences between non-polarized fibroblasts and polarized epithelial cells. *J. Cell Sci.* **108,** 127–142.
15. Kadowaki, T., Koyasu, S., Nishida, E., Sakai, H., Takaku, F., Yahara, I., and Kasuga, M. (1986). Insulin-like growth factors, insulin, and epidermal growth factor cause rapid cytoskeletal reorganization in KB cells. *J. Biol. Chem.* **261,** 16141–16147.
16. Izumi, T., Saeki, Y., Akanuma, Y., Takaku, F., and Kasuga, M. (1988). Requirement for receptor-intrinsic tyrosine kinase activities during ligand-induced membrane ruffling of KB cells. *J. Biol. Chem.* **263,** 10386–10393.
17. Leventhal, P. S., Shelden, E. A., Kim, B., and Feldman, E. L. (1997). Tyrosine phosphorylation of paxillin and focal adhesion kinase during insulin-like growth factor-I-stimulated lamellipodia advance. *J. Biol. Chem.* **272,** 5214–5218.
18. Jones, J. L., Royall, J. E., Critchley, D. R., and Walker, R. A. (1997). Modulation of myoepithelial-associated $\alpha6\beta4$ integrin in a breast cancer cell line alters invasive potential. *Exp. Cell Res.* **235,** 325–333.
19. Konstantopoulos, N., and Clark, S. (1996). Insulin and insulin-like growth factor-1 stimulate dephosphorylation of paxillin in parallel with focal adhesion kinase. *Biochem. J.* **314,** 387–390.
20. Baron, V., Calléja, V., Ferrari, P., Alengrin, F., and van Obberghen, E. (1998). $p125^{Fak}$ focal adhesion kinase is a substrate for the insulin and insulin-like growth factor-I tyrosine kinase receptors. *J. Biol. Chem.* **273,** 7162–7168.
21. Guvakova, M. A., and Surmacz, E. (1997a). Overexpressed IGF-I receptors reduce estrogen growth requirements, enhance survival, and promote E-cadherin-mediated cell–cell adhesion in human breast cancer cells. *Exp. Cell Res.* **231,** 149–162.
22. Knight, J. B., Yamauchi, K., and Pessin, J. E. (1995). Divergent insulin and platelet-derived growth factor regulation of focal adhesion kinase ($pp125^{FAK}$) tyrosine phosphorylation, and rearrangement of actin stress fibers. *J. Biol. Chem.* **270,** 10199–10203.
23. Noguchi, T., Matozaki, T., Horita, K., Fujioka, Y., and Kasuga, M. (1994). Role of SH-PTP2, a protein–tyrosine phosphatase with Src homology 2 domains, in insulin-stimulated Ras activation. *Mol. Cell. Biol.* **14,** 6674–6682.
24. Retta, S. F., Barry, S. T., Critchley, D. R., Defilippi, P., Silengo, L., and Tarone, G. (1996). Focal adhesion and stress fiber formation is regulated by tyrosine phosphatase activity. *Exp. Cell Res.* **299,** 307–317.
25. Kohn, E. C., and Liotta, L. A. (1995). Molecular insights into cancer invasion: Strategies for prevention and intervention. *Cancer Res.* **55,** 1856–1862.
26. Burtnick, L. D., Koepf, E. K., Grimes, J., Jones, E. Y., Stuart, D. I., McLaughlin, P. J., and Robinson, R. C. (1997). The crystal structure of plasma gelsolin: Implication for actin severing, capping, and nucleation. *Cell* **90,** 661–670.
27. Bornfeldt, K. E., Raines, E. W., Nakano, T., Graves, L. M., Krebs, E. G., and Ross, R. (1994). Insulin-like growth factor-I and platelet-derived growth factor-BB induce directed migration of human arterial smooth muscle cells via signaling pathways that are distinct from those of proliferation. *J. Clin. Invest.* **93,** 1266–1274.
28. Aspenström, P. (1999). The Rho GTPases have multiple effects on the actin cytoskeleton. *Exp. Cell Res.* **246,** 20–25.
29. Keely, P. J., Westwick, J. K., Whitehead, I. P., Der, C. J., and Parise, L. V. (1997). Cdc42 and rac1 induce integrin-mediated cell motility and invasiveness through PI(3)K. *Nature* **390,** 632–636.
30. He, H., Watanabe, T., Zhan, X., Huang, C., Schuuring, E., Fukami, K., Takenawa, T., Kumar, C. C., Simpson, R. J., and Maruta, H. (1998). Role of phosphatidylinositol 4,5-bisphosphate in Ras/Rac-induced disruption of the cortactin–actomyosin II complex and malignant transformation. *Mol. Cell. Biol.* **18,** 3829–3837.
31. Guvakova, M. A., and Surmacz, E. (1997b). Tamoxifen interferes with the insulin-like growth factor I receptor (IGF-IR) signaling pathway in breast cancer cells. *Cancer Res.* **57,** 2606–2610.
32. Lange, K., Brandt, U., Gartzke, J., and Bergmann, J. (1998). Action of insulin on the surface morphology of hepatocytes: Role of phosphatidylinositol 3-kinase in insulin-induced shape change of microvilli. *Exp. Cell Res.* **239,** 139–151.
33. Wennström, S., Hawkins, P., Cooke, F., Hara, K., Yonezawa, K., Kasuga, M., Jackson, T., Claesson-Welsh, L., and Stephens, L. (1994). Activation of phosphoinositide 3-kinase is required for PDGF-stimulated membrane ruffling. *Curr. Biol.* **4,** 385–393.
34. Boyer, B., Dufour, S., and Thiery, J. P. (1992). E-cadherin expression during the acidic FGF-induced dispersion of a rat bladder carcinoma cell line. *Exp. Cell Res.* **201,** 347–357.
35. Potempa, S., and Ridley, A. J. (1998). Activation of both MAP kinase and phosphatidylinositide 3-kinase by Ras is required for hepatocyte growth factor/scatter factor-induced adherens junction disassembly. *Mol. Biol. Cell* **9,** 2185–2200.

36. Couchman, J. R., and Rees, D. A. (1979). The behaviour of fibroblasts migrating from chick heart explants: Changes in adhesion, locomotion and growth, and in the distribution of actomyosin and fibronectin. *J. Cell Sci.* **39,** 149–165.

37. Turner, C. E., and Miller, J. T. (1994). Primary sequence of paxillin contains putative SH2 and SH3 domain binding motifs and multiple LIM domains: Identification of a vinculin and pp125Fak-binding region. *J. Cell Sci.* **107,** 1583–1591.

38. Casamassima, A., and Rozengurt, E. (1998). Insulin-like growth factor I stimulates tyrosine phosphorylation of p130' ", focal adhesion kinase, and paxillin. *J. Biol. Chem.* **273,** 26149–26156.

39. Machesky, L. M., and Hall, A. (1996). Rho: a connection between membrane receptor signalling and the cytoskeleton. *Trends Cell Biol.* **6,** 304–310.

40. Polte, T. R., and Hanks, S. K. (1997). Complexes of focal adhesion kinase (FAK) and Crk-associated substrate (p130 (Cas)) are elevated in cytoskeleton-associated fractions following adhesion and Src transformation: Requirements for Src kinase activity and FAK proline-rich motifs. *J. Biol. Chem.* **272,** 5501–5509.

41. Tachibana, K., Urano, T., Fujita, H., Ohashi, Y., Kamiguchi, K., Iwata, S., Hirai, H., and Morimoto, C. (1997). Tyrosine phosphorylation of Crk-associated substrates by focal adhesion kinase. *J. Biol. Chem.* **272,** 29083–29090.

42. Tamura, M., Gu, J., Matsumoto, K., Aota, S.-I., Parsons, R., and Yamada, K. M. (1998). Inhibition of cell migration, spreading, and focal adhesions by tumor suppressor PTEN. *Science* **280,** 1614–1617.

43. Liu, F., Hill, D. E., and Chernoff, J. (1996). Direct binding of the proline-rich region of protein tyrosine phosphatase 1B to the Src homology 3 domain of p130 (Cas). *J. Biol. Chem.* **271,** 31290–31295.

44. Shen, Y., Schneider, G., Cloutier, J.-F., Veillette, A., and Schaller, M. D. (1998). Direct association of protein–tyrosine phosphatase PTP-PEST with paxillin. *J. Biol. Chem.* **273,** 6474–6481.

45. Rocchi, S., Tartare-Deckert, S., Sawka-Verhelle, D., Gamha, A., and van Obberghen, E. (1996). Interaction of SH2-containing protein tyrosine phosphatase 2 with the insulin receptor and the insulin-like growth factor-I receptor: Studies of the domains involved using the yeast two-hybrid system. *Endocrinology* **137,** 4944–4952.

46. Ouwens, D. M., Mikkers, H. M. M., van der Zon, G. C. M., Stein-Gerlach, M., Ullrich, A., and Maassen, J. A. (1996). Insulin-induced tyrosine dephosphorylation of paxillin and focal adhesion kinase requires active phosphotyrosine phosphatase 1D. *Biochem. J.* **318,** 609–614.

47. Yu, D-H., Qu, C-K., Henegariu, O., Lu, X., and Feng, G-S. (1998). Protein–tyrosine phosphatase Shp-2 regulates cell spreading, migration, and focal adhesion. *J. Biol. Chem.* **273,** 21125–21131.

Received February 11, 1999
Revision received May 21, 1999

Int. J. Cancer: **81**, 299–304 (1999)

Publication of the International Union Against Cancer
Publication de l'Union Internationale Contre le Cancer

INSULIN RECEPTOR SUBSTRATE 1 IS A TARGET FOR THE PURE ANTIESTROGEN ICI 182,780 IN BREAST CANCER CELLS

Michele SALERNO[1,2], Diego SISCI[1,2], Loredana MAURO[1,2], Marina A. GUVAKOVA[1], Sebastiano ANDO[2,3] and Ewa SURMACZ[1]*

[1]*Kimmel Cancer Center, Thomas Jefferson University, Philadelphia, PA, USA*
[2]*Department of Cellular Biology, University of Calabria, Cosenza, Italy*
[3]*Faculty of Pharmacy, University of Calabria, Cosenza, Italy*

The pure antiestrogen ICI 182,780 inhibits insulin-like growth factor (IGF)-dependent proliferation in hormone-responsive breast cancer cells. However, the interactions of ICI 182,780 with IGF-I receptor (IGF-IR) intracellular signaling have not been characterized. Here, we studied the effects of ICI 182,780 on IGF-IR signal transduction in MCF-7 breast cancer cells and in MCF-7-derived clones overexpressing either the IGF-IR or its 2 major substrates, insulin receptor substrate 1 (IRS-1) or src/collagen homology proteins (SHC). ICI 182,780 blocked the basal and IGF-I-induced growth in all studied cells in a dose-dependent manner; however, the clones with the greatest IRS-1 overexpression were clearly least sensitive to the drug. Pursuing ICI 182,780 interaction with IRS-1, we found that the antiestrogen reduced IRS-1 expression and tyrosine phosphorylation in several cell lines in the presence or absence of IGF-I. Moreover, in IRS-1-overexpressing cells, ICI 182,780 decreased IRS-1/p85 and IRS-1/GRB2 binding. The effects of ICI 182,780 on IGF-IR protein expression were not significant; however, the drug suppressed IGF-I-induced (but not basal) IGF-IR tyrosine phosphorylation. The expression and tyrosine phosphorylation of SHC as well as SHC/GRB binding were not influenced by ICI 182,780. In summary, downregulation of IRS-1 may represent one of the mechanisms by which ICI 182,780 inhibits the growth of breast cancer cells. Thus, overexpression of IRS-1 in breast tumors could contribute to the development of antiestrogen resistance. *Int. J. Cancer* 81:299–304, 1999.
© *1999 Wiley-Liss, Inc.*

ICI 182,780, an alpha-alkylsulfinylamide, is a new-generation pure antiestrogen (Wakeling *et al.*, 1991). The drug has shown great promise as a second-line endocrine therapy agent in patients with advanced breast cancer resistant to the non-steroidal antiestrogen tamoxifen (Tam). Indeed, in several *in vitro* and *in vivo* studies, the antitumor effects of ICI 182,780 were greater than those of Tam (Nicholson *et al.*, 1996; Osborne *et al.*, 1995; de Cupis *et al.*, 1995; Chander *et al.*, 1993; Wakeling *et al.*, 1991). Moreover, unlike Tam, ICI 182,780 lacks agonist (estrogenic) activity and its administration does not appear to be associated with deleterious side effects such as induction of endometrial cancer or retinopathy (Osborne *et al.*, 1995; Chander *et al.*, 1993). ICI 182,780 antagonizes multiple cellular effects of estrogens by impairing the dimerization of the estrogen receptor (ER) and by reducing ER half-life (de Cupis and Favoni, 1997; Chander *et al.*, 1993). ICI 182,780 also interferes with growth factor-induced growth, but it is not clear whether this activity is mediated exclusively through the ER, or if some ER-independent mechanism is implicated (de Cupis *et al.*, 1995). Despite their great antitumor effects, pure antiestrogens do not circumvent the development of antiestrogen resistance, as most breast tumor cells initially sensitive to ICI 182,780 eventually become unresponsive to the drug (de Cupis and Favoni, 1997; Pavlik *et al.*, 1996; Nicholson *et al.*, 1995). The mechanism of this resistance is not clear, but it has been suggested that both mutations of the ER as well as alterations in growth factor-dependent mitogenic pathways may be involved (de Cupis and Favoni, 1997; Larsen *et al.*, 1997; Pavlik *et al.*, 1996; Wiseman *et al.*, 1993).

The insulin-like growth factor (IGF) system [IGFs, IGF-I receptor (IGF-IR) and IGF binding proteins (IGFBP)] plays a critical role in the pathobiology of hormone-responsive breast cancer (reviewed in Surmacz *et al.*, 1998). In the experimental setting, IGF-IR has been shown to stimulate growth and transformation, improve survival, as well as regulate cell-cell and cell-substrate interactions in breast cancer cells (Surmacz *et al.*, 1998). Moreover, overexpression of different elements of the IGF system, such as IGF-II, IGF-IR or insulin receptor substrate 1 (IRS-1), provides breast cancer cells with growth advantage and reduces or abrogates estrogen growth requirements (Surmacz *et al.*, 1998). On the other hand, downregulation of IGF-IR expression, inhibition of IGF-IR signaling and reduced bioavailability of the IGFs have all been demonstrated to block proliferation and survival as well as to interfere with motility or intercellular adhesion in breast cancer cells (Surmacz *et al.*, 1998).

Clinical studies confirm the role of the IGF-I system in breast cancer development. First, IGF-IR has been found to be up to 14-fold overexpressed in breast cancer compared with its levels in normal mammary epithelium (Surmacz *et al.*, 1998; Resnik *et al.*, 1998; Turner *et al.*, 1997). Moreover, cellular levels of IGF-IR or its substrate IRS-1 correlate with cancer recurrence at the primary site (Rocha *et al.*, 1997; Turner *et al.*, 1997). The ligands of IGF-IR, IGF-I and IGF-II, are often present in the epithelial and/or stromal component of breast tumors, indicating that an autocrine or a paracrine IGF-IR loop may be operative and involved in the neoplastic process (Surmacz *et al.*, 1998). In addition, endocrine IGFs probably also contribute to breast tumorigenesis since the levels of circulating IGF-I correlate with breast cancer risk in premenopausal women (Hankinson *et al.*, 1998).

ICI 182,780 interferes with the IGF-I system in breast cancer cells. The antiestrogen has been shown to attenuate IGF-I-stimulated growth, modulate expression of IGFBPs and downregulate IGF binding sites (Surmacz *et al.*, 1998; de Cupis and Favoni, 1997; de Cupis *et al.*, 1995). The interactions of ICI 182,780 with the IGF-IR signaling pathways, however, have not been characterized.

Our previous work demonstrated that in breast cancer cells, Tam interferes with the IGF-IR signaling acting upon IGF-IR substrates IRS-1 and src/collagen homology proteins (SHC) (Guvakova and Surmacz, 1997). Normally, activation of IGF-IR results in the recruitment and tyrosine phosphorylation of IRS-1 and SHC, followed by their association with several downstream effector proteins and induction of various signaling pathways (Surmacz *et al.*, 1998). For instance, association of either IRS-1 or SHC with GRB-2/SOS complexes activates the Ras/MAP pathway, whereas binding of IRS-1 with p85 stimulates PI-3 kinase. Tam treatment blocks IGF-dependent growth, which coincides with decreased tyrosine phosphorylation of IRS-1 and IGF-IR and with hyperphos-

Grant sponsor: NIH; Grant number: DK 48969; Grant sponsor: U.S. Department of Defense; Grant numbers: DAMD 17-96-1-6250 and DAMD 17-97-1-7211; Grant sponsors: NCR Italy, M.U.R.S.T. Italy 60% and P.O.P. 1998, Italy.

*Correspondence to: Kimmel Cancer Center, Thomas Jefferson University, 233 S. 10th Street, BLSB 606, Philadelphia, PA 19107, USA. Fax: (215) 923-0249. E-mail: surmacz1@jeflin.tju.edu.

Received 17 August 1998; revised 5 November 1998

phorylation of SHC (Guvakova and Surmacz, 1997). Here, we demonstrate the interactions of ICI 182,780 with IGF-IR signaling and discuss the relevant similarities and differences in the modes of action of the 2 antiestrogens.

MATERIAL AND METHODS

Cell lines and cell culture conditions

We used MCF-7 cells and several MCF-7-derived clones overexpressing either IGF-IR (MCF-7/IGF-IR cells), IRS-1 (MCF-7/IRS-1 cells) or SHC (MCF-7/SHC cells). MCF-7/IGF-IR clone 17 and MCF-7/IRS-1 clones 9, 3 and 18 were developed by stable transfection of MCF-7 cells with expression vectors encoding either IGF-IR or IRS-1 and have been characterized previously (Guvakova and Surmacz, 1997; Surmacz and Burgaud, 1995). MCF-7/SHC cells are MCF-7-derived cells transfected with the plasmid pcDNA3/SHC; compared with MCF-7 cells, the level of $p55^{SHC}$ and $p47^{SHC}$ overexpression in MCF-7/SHC cells is approximately 5-fold (data not shown). The above MCF-7-derived clones express ERs and respond to E2, similar to MCF-7 cells (Guvakova and Surmacz, 1997; Surmacz and Burgaud, 1995). The levels of IRS-1 in MCF-7/IGF-IR and MCF-7/SHC cells are similar to those in MCF-7 cells (see Fig. 2*b* and data not shown).

MCF-7 cells were grown in DMEM:F12 (1:1) containing 5% calf serum (CS). MCF-7-derived clones were maintained in DMEM:F12 plus 5% CS plus 200 μg/ml G418. In the experiments requiring E2-free conditions, the cells were cultured in phenol red-free DMEM containing 0.5 mg/ml BSA, 1 μM $FeSO_4$ and 2 mM L-glutamine (PRF-SFM) (Guvakova and Surmacz, 1997; Surmacz and Burgaud, 1995).

Cell growth assay

Cells were plated at a concentration 2×10^5 in 6-well plates in a growth medium; the following day (day 0), the cells were shifted to PRF-SFM containing different doses of ICI 182,780 (1–300 nM) with or without 50 ng/ml IGF-I and incubated for 4 days. The increase in cell number from day 0 to day 4 in PRF-SFM was designated as 100% growth increase.

IP and WB

The expression and tyrosine phosphorylation of IGF-I signaling proteins were measured by IP and WB, as described previously (Guvakova and Surmacz, 1997; Surmacz and Burgaud, 1995). Protein lysates (500 μg) were immunoprecipitated with the following antibodies (Abs): for the IGF-IR: anti-IGF-IR monoclonal Ab (MAb) alpha-IR3 (Oncogene Science, Cambridge, MA); for IRS-1: anti-C-terminal IRS-1 polyclonal Ab (pAb) (UBI, Lake Placid, NY); for SHC: anti-SHC pAb (Transduction Laboratories, Lexington, KY). Tyrosine phosphorylation was probed by WB with an antiphosphotyrosine MAb PY20 (Transduction Laboratories). The levels of IRS-1, IGF-IR and SHC expression were determined by stripping the phosphotyrosine blots and reprobing them with the following Abs: for IRS-1: anti-IRS-1 pAb (UBI); for IGF-IR: anti-IGF-IR mAb (Santa Cruz Biotechnology, Santa Cruz, CA); for SHC: anti-SHC MAb (Transduction Laboratories). The association of GRB2 or p85 with IRS-1 or SHC was visualized in IRS-1 or SHC blots using an anti-GRB2 MAb (Transduction Laboratories) or an anti-p85 MAb (UBI), respectively. The intensity of bands was measured by laser densitometry scanning.

Northern blotting

The levels of IRS-1 mRNA were detected by Northern blotting in 20 μg of total RNA using a 631 bp probe derived from a mouse IRS-1 cDNA (nt 1351–2002). This fragment (99.8% homology with the human IRS-1 sequence) hybridizes with both human and mouse IRS-1 mRNA (Nishiyama and Wands, 1992).

Statistical analysis

The results in cell growth experiments were analyzed by analysis of variance (ANOVA) or Student's *t*-test, where appropriate.

RESULTS

ICI 182,780 inhibits growth of MCF-7 cells with amplified IGF-IR signaling. Sensitivity to ICI 182,780 is determined by the cellular levels of IRS-1

All cell lines used in this study secrete autocrine IGF-I-like mitogens and are able to proliferate in PRF-SFM (Guvakova and Surmacz, 1997; Surmacz and Burgaud, 1995). The basal (autocrine) growth of the cells was enhanced in the presence of IGF-I (Fig. 1*a,b*). Short (1–2 days) treatments with ICI 182,780 were not sufficient to inhibit cell growth (data not shown), but a 4-day culture in the presence of the antiestrogen produced evident cytostatic effects (Fig. 1*a,b*). In general, the response to ICI 182,780 was dose dependent (Fig. 1*a,b*), however, compared with the other cell lines, the cells highly overexpressing IRS-1 (MCF-7/IRS-1 clones 3 and 18) were more resistant to the drug (Fig. 1*b,c*). Specifically, 1 nM ICI 182,780 inhibited the basal growth by 80, 55 and 50% in MCF-7, MCF-7/IGF-IR and MCF-7/SHC cells, respectively, but the same dose produced only a 20–30% growth inhibition in MCF-7/IRS-1 clones 3 and 18 (Fig. 1*a,b*). Higher concentrations of ICI 182,780 (10 and 100 nM) effectively suppressed the autocrine growth, or even induced cell death in all cell lines, except MCF-7/IRS-1 clone 18, where the maximal reduction (32%) of the basal growth occurred with a 100 nM dose (Fig. 1*b*).

In the presence of IGF-I, the effects of ICI 182,780 were attenuated: 1 nM ICI 182,780 was never cytostatic (data not shown), while the 10 and 100 nM doses inhibited (by 30–50% and 47–78%, respectively) IGF-I-dependent proliferation of cells with low IRS-1 levels (Fig. 1*a,b*). The same doses, however, were less efficient in MCF-7/IRS-1 clones 3 and 18, where growth reduction was 20–25% for 10 nM and 41–47% for 100 nM. Similarly, 300 nM ICI 182,780 produced a prominent cytostatic effect in all cell lines with low IRS-1 expression, but was less active in the clones highly overexpressing IRS-1 (70–93% *vs.* 45–60% growth inhibition) (Fig. 1*a–c*).

The above results suggested that IRS-1 may be an important target for ICI 182,780 action. Consequently, in the next set of experiments we studied the effects of ICI 182,780 on the expression and function of IRS-1.

ICI 182,780 reduces IRS-1 levels and impairs IRS-1 signaling in MCF-7/IRS-1, MCF-7 and MCF-7/IGF-IR cells

In MCF-7/IRS-1 cells grown under basal conditions, IRS-1 was tyrosine phosphorylated for up to 4 days (Fig. 2*a*). IGF-I induced a rapid and marked (5-fold) increase of IRS-1 phosphorylation which persisted for up to 1 day and declined thereafter reaching close to the basal phosphorylation status at day 4. A short (≤1 day) treatment with ICI 182,780 had no consequences on IRS-1 expression or tyrosine phosphorylation. (Fig. 2*a*, panels a and b). However, p85/IRS-1 association was approximately 30% reduced under the basal conditions at day 1 of the treatment (Fig. 2*a*, panel c).

The evident effect of ICI 182,780 action on IRS-1 expression and signaling occurred at day 4, and was especially pronounced in the absence of IGF-I. Specifically, without IGF-I, the drug suppressed IRS-1 protein expression by 60%, which was paralleled by a 60% reduction of IRS-1 tyrosine phosphorylation, and coincided with an almost complete (approximately 95%) inhibition of p85/IRS-1 and GRB2/IRS-1 binding. The addition of IGF attenuated ICI 182,780 action, however, the effects of the treatment remained well detectable: IRS-1 levels were downregulated by 30%, IRS-1 tyrosine phosphorylation by 20% and p85/IRS-1 binding by 30%. Under IGF-I conditions, GRB2/IRS-1 binding was not appreciably affected (Fig. 2*a*, panels a–d).

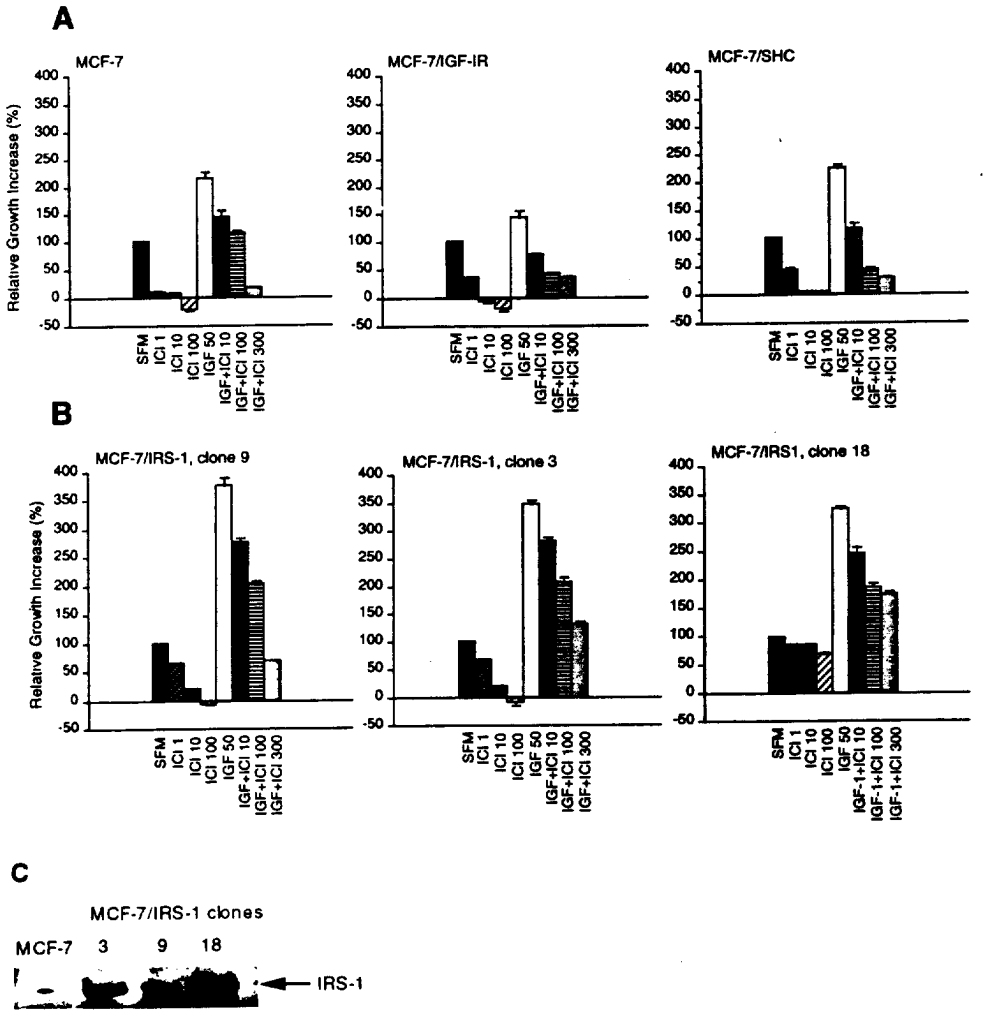

FIGURE 1 – ICI 182,780 inhibits the growth of MCF-7 cells overexpressing different elements of IGF-IR signaling. IRS-1 levels determine ICI 182,780 sensitivity. *(a)* ICI 182,780-induced growth inhibition in the parental MCF-7 cells (8×10^4 IGF-IR/cell), MCF-7/IGF-IR clone 17 (1×10^6 IGF-IR/cell) and MCF-7/SHC (5-fold SHC overexpression over the level in MCF-7 cells). *(b)* Growth reduction in MCF-7/IRS-1 clone 9 (3-fold IRS-1 overexpression over the levels in MCF-7 cells), clone 3 (7-fold overexpression) and clone 18 (9-fold overexpression). The cells were treated with different doses of ICI 182,780 in the presence or absence of 50 ng/ml IGF-I, as described in Material and Methods. The increase in cell number between day 0 and day 4 is taken as 100%. The results are means from at least 4 experiments. Bars indicate standard error. *(c)* Levels of IRS-1 protein in different MCF-7/IRS-1 cell lines. IRS-1 levels were determined by IP and WB as described in Material and Methods. Representative results from 3 experiments are shown.

Importantly, analogous action of ICI 182,780 on IRS-1 expression and tyrosine phosphorylation was seen in other cell lines studied (Fig. 2*b*). In both MCF-7/IGF-IR and MCF-7 cells containing only endogenous IRS-1, ICI 182,780 inhibited the IRS-1 expression under basal conditions by approximately 60%, which was paralleled by the reduced IRS-1 tyrosine phosphorylation (by approximately 90–95%). In the presence of IGF-I, the antiestrogen suppressed the IRS-1 levels by approximately 50% and IRS-1 tyrosine phosphorylation by approximately 40%.

ICI 182,780 attenuates IRS-1 mRNA expression

ICI 182,780 reduced the levels of 5 kb IRS-1 mRNA (Nishiyama and Wands, 1992) in MCF-7 and MCF-7/IGF-IR cells in the absence or presence of IGF-I, by 50 and 70%, respectively (Fig. 3). Moreover, the 5 kb message transcribed from the CMV-IRS-1 plasmid was downregulated (by approximately 70%) in MCF-7/IRS-1 cells treated with both IGF-I and ICI 182,780 (data not shown).

ICI 182,780 inhibits IGF-I-induced but not basal tyrosine phosphorylation of IGF-IR

In MCF-7/IGF-IR cells, IGF-I moderately increased the expression of IGF-IR. This effect was slightly (by 20%) blocked in the presence of ICI 182,780. Under the same conditions, the drug significantly (by 80%) reduced tyrosine phosphorylation of IGF-IR (Fig. 4). ICI 182,780 had no effect on the basal expression of IGF-IR, however, it produced a 30% increase in the basal tyrosine phosphorylation of IGF-IR (Fig. 4). The latter peculiar effect of the antiestrogen occurred in several repeat experiments. Short treatments with ICI 182,780 ($\leq$1 day) were not associated with any significant changes in IGF-IR expression (data not shown).

Long-term ICI 182,780 treatment does not affect SHC signaling

In the presence of IGF-I, SHC tyrosine phosphorylation was moderately induced, with the maximum seen at 1 hr upon stimulation. On the other hand, GRB2/SHC binding peaked at 15 min after IGF-I addition and declined thereafter with the minimal

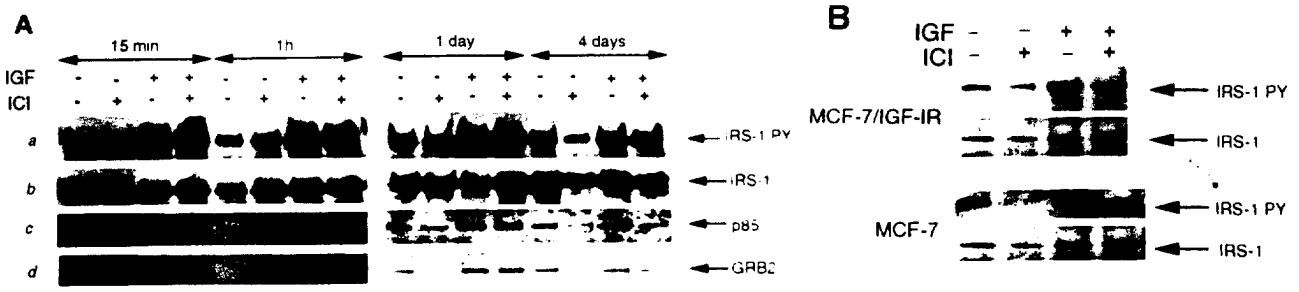

FIGURE 2 – ICI 182,780 inhibits IRS-1-mediated signaling. *(a)* Effects of ICI 182,780 in MCF-7/IRS-1 clone 3. IRS-1 tyrosine phosphorylation (IRS-1 PY) (panel a), protein levels (IRS-1) (panel b), as well as IRS-1-associated p85 of PI-3 kinase (panel c) and GRB2 (panel d) were determined in cells treated for 15 min, 1 hr, 1 day or 4 days with 100 nM ICI 182,780 in the presence or absence of 50 ng/ml IGF-I. In the 1 hr treatment, lane IGF (−) ICI (−) is underloaded. Representative results from 5 experiments are shown. *(b)* Effects of ICI 182,780 on IRS-1 in MCF-7/IGF-IR and MCF-7 cells. IRS-1 tyrosine phosphorylation (IRS-1 PY) and protein levels (IRS-1) were examined in cells treated with 100 nM ICI 182,780 for 4 days. Representative blots of 5 experiments are shown.

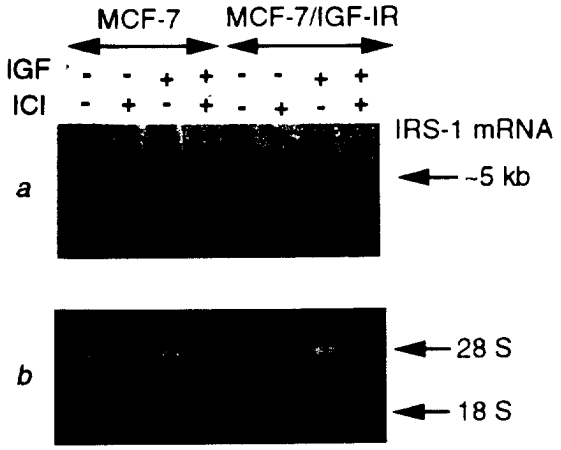

FIGURE 3 – ICI 182,780 attenuates the expression of IRS-1 mRNA levels in MCF-7 and MCF-7/IGF-IR cells. The expression of IRS-1 mRNA was determined in cells treated with 100 nM ICI 182,780 for 4 days in the presence or absence of IGF-I. Panel *a*. IRS-1 mRNA of approximately 5 kb. Panel *b*. Control RNA loading: 28S and 18S RNA in the same blot.

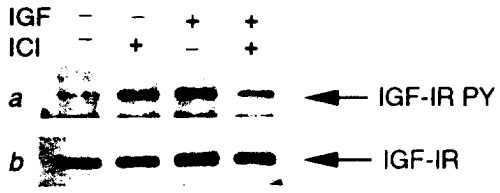

FIGURE 4 – Effects of ICI 182,780 on IGF-IR. IGF-IR tyrosine phosphorylation (IGF-IR PY) (panel *a*) and protein levels (IGF-IR) (panel *b*) in MCF-7/IGF-IR clone 17 treated for 4 days with 100 nM ICI 182,780 in the presence or absence of 50 ng/ml IGF-I. Representative results of 3 different experiments are shown.

binding found at day 4 (Fig. 5). ICI 182,780 treatment, in the presence or absence of IGF-I, failed to induce significant changes in the levels or tyrosine phosphorylation of SHC proteins, except a transient stimulation of the basal SHC tyrosine phosphorylation at 15 min (Fig. 5). Importantly, at all time points, SHC/GRB2 association was not influenced by the drug.

Interestingly, at day 4, SHC tyrosine phosphorylation and SHC/GRB2 binding were suppressed in the presence of IGF-I (Fig. 5). This characteristic regulation of SHC by IGF-I, documented by us previously in MCF-7 cells and MCF-7-derived clones, was not affected by ICI 182,780 (Guvakova and Surmacz, 1997).

Similar lack of ICI 182,780 effects on SHC expression and signaling was noted in MCF-7 and MCF-7/IGF-IR cells (data not shown).

DISCUSSION

Pure antiestrogens have been shown to interfere with one of the most important systems regulating the biology of hormone-dependent breast cancer cells, namely, the IGF-I system (de Cupis and Favoni, 1997; Nicholson *et al.*, 1996). The compounds inhibit IGF-induced proliferation, which is associated with, *i.e.*, downregulation of IGF binding sites and reduction of IGF availability. Similar action has been ascribed to non-steroidal antiestrogens such as Tam or 4-OH-Tam (Chander *et al.*, 1993).

The effects of pure antiestrogens on the IGF signal transduction have been unknown. Here, we studied if and how ICI 182,780 modulates the IGF-IR intracellular pathways in breast cancer cells. We focused on the relationship between drug efficiency and signaling capacities of IGF-IR or IRS-1 since these molecules appear to control proliferation and survival in breast cancer cells (Surmacz *et al.*, 1998; Rocha *et al.*, 1997; Turner *et al.*, 1997).

Previously we found that the cytostatic action of Tam involves its interference with IGF signaling pathways. In particular, Tam suppressed tyrosine phosphorylation of IRS-1 and caused hyperphosphorylation of SHC (Guvakova and Surmacz, 1997). The most important conclusion of the present work is that inhibition of IRS-1 expression is an important element of ICI 182,780 mode of action. The first observation was that amplification of IGF signaling did not abrogate sensitivity to ICI 182,780. Next, ICI 182,780 appeared to affect a specific IGF signaling pathway, as the efficiency of the drug was dictated by the cellular levels of IRS-1, but not that of SHC or IGF-IR. For instance, MCF-7/IGF-IR clone 17 was very sensitive to ICI 182,780 despite a 12-fold IGF-IR overexpression, whereas MCF-7/IRS-1 clones 3 and 18 (7- and 9-fold IRS-1 overexpression, respectively) were quite resistant to the drug (Fig. 1). Moreover, ICI 182,780 reduced IRS-1 levels and tyrosine phosphorylation in several cell lines in the presence or absence of IGF-I, while its action on IGF-IR was limited to the inhibition of IGF-I-induced tyrosine phosphorylation and its effects on SHC were none.

The reduction of IRS-1 expression by ICI 182,780 occurred in all cell lines studied, however, it was clearly more pronounced in the cells expressing lower (endogenous) levels of the substrate (*i.e.*, MCF-7 and MCF-7/IGF-IR cells) (Fig. 2). This suggests that downregulation of IRS-1 by ICI 182,780 is a saturable process, and overexpression of IRS-1 may provide resistance to the drug. Indeed, although we did not notice a strict correlation between

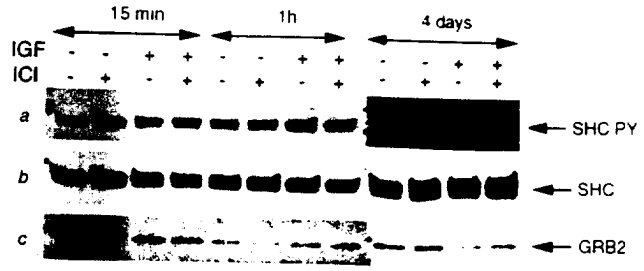

FIGURE 5 – Effects of ICI 182,780 on SHC signaling. SHC tyrosine phosphorylation (SHC PY) (panel *a*), protein levels (SHC) (panel *b*) and SHC-associated GRB2 (panel *c*) were studied in MCF-7/SHC cells treated for 4 days with 100 nM ICI 182,780 in the presence or absence of 50 ng/ml IGF-I. Representative results of 5 experiments are shown.

IRS-1 levels or IRS-1 tyrosine phosphorylation and ICI 182,780-dependent growth inhibition. IRS-1-overexpressing cells tended to be more resistant to the cytostatic action of the antiestrogen (Fig. 1). Interestingly, overexpression of IRS-1 clearly had a greater impact on the response to high doses of ICI 182,780 (≥100 nM) than on the effects of low drug concentrations. This suggests that ICI 182;780 action is multiphased, with the initial inhibition being IRS-1 independent (but perhaps, ER-dependent) and the strong growth reduction associated with the blockade of IRS-1 function (Figs. 1, 2).

ICI 182,780 affected IRS-1 expression not only on the level of protein but also on the level of mRNA. In our experiments, the antiestrogen reduced the expression of IRS-1 mRNA in the presence or absence of IGF-I. However, the mechanism by which ICI 182,780 interferes with IRS-1 mRNA expression was not studied here and it remains speculative. Regarding transcriptional regulation, no estrogen-responsive elements have been mapped in the IRS-1 promoter, but it cannot be ruled out that ICI 182,780 acts indirectly through some other regulatory sequences in the 5' untranslated region of *IRS-1* gene, such as AP1, AP2, Sp1, C/EBP, E box (Araki *et al.*, 1995; Matsuda *et al.*, 1997). A post-transcriptional component may be argued by the fact that the inhibition of IRS-1 mRNA by ICI 182,780 was evident in IGF-I-treated MCF-7/IRS-1 cells, in which the majority of IRS-1 message originated from the expression plasmid devoid of any IRS-1 promoter sequences (CMV-driven IRS-1 cDNA) (Surmacz and Burgaud, 1995) (data not shown). In addition, the finding that ICI 182,780 similarly inhibited IRS-1 mRNA levels under the basal and IGF-I conditions, but IRS-1 protein was significantly more reduced in the absence of IGF-I (Fig. 3 *vs.* Fig. 2*a*) could suggest that the drug acts upon some IGF-I-dependent mechanism controlling mRNA stability, translation, or post-translational events. In fact, in other experimental systems, IGF-I or insulin regulated various messages, including IRS-1 mRNA, on the post-transcriptional level (Araki *et al.*, 1995).

In its action on IRS-1, ICI 182,780 appeared more potent than Tam, which decreased tyrosine phosphorylation of IRS-1 but did not cause any detectable changes in IRS-1 expression. Our results with Tam suggested that this antiestrogen may influence the activity of tyrosine phosphatases (PTPases) (Guvakova and Surmacz, 1997). Indeed, both Tam and ICI 182,780 interfere with IGF-I-dependent growth by upregulating PTPases LAR and FAP-1 (Freiss *et al.*, 1998). In the present work, ICI 182,780 effects on phosphatases acting on IRS-1 were impossible to assess, since the drug also affected IRS-1 expression (Fig. 3). However, some interference of ICI 182,780 with the phosphorylation/dephosphorylation events could be indicated, for instance, by our experiments with IGF-IR, where, under basal conditions, the compound induced IGF-IR phosphorylation without evident modifications of the receptor expression (Fig. 4).

Other important observations stemming from our results concern similarities and differences between the effects of ICI 182,780 and Tam on the IGF-IR and SHC. While Tam did not modulate the expression of IGF-IR protein (Guvakova and Surmacz, 1997), ICI 182,780 moderately decreased IGF-IR levels in the presence of IGF-I. The action of ICI 182,780 and Tam on IGF-IR tyrosine phosphorylation was similar, namely, both compounds inhibited IGF-I-induced but not basal tyrosine phosphorylation of IGF-IR. The effects of ICI 182,780 and Tam on SHC were different. With Tam, we observed elevated tyrosine phosphorylation of SHC proteins and increased SHC/GRB2 binding in growth-arrested cells, while ICI 182,780 did not affect SHC phosphorylation or expression (Guvakova and Surmacz, 1997). Thus, induction of non-mitogenic SHC signaling is a peculiarity of Tam but not a ICI 182,780 mechanism of action.

In summary, cytostatic effects of ICI 182,780, similar to Tam, are associated with the inhibition of IGF-IR signaling. The mitogenic/survival IRS-1 pathway is a target for both antiestrogens. Both drugs reduce the levels of tyrosine phosphorylated IRS-1, but only ICI 182,780 clearly inhibits expression of the substrate. High cellular levels of IRS-1 hinder the response to higher doses of ICI 182,780, thus overexpression of IRS-1 in breast tumors may represent an important mechanism of antiestrogen resistance.

ACKNOWLEDGEMENTS

This work was supported by NIH grant DK 48969 to E.S., U.S. Department of Defense grants DAMD 17-96-1-6250 to E.S. and DAMD 17-97-1-7211 to M.A.G., NCR Italy grants to D.S. and M.S., a M.U.R.S.T. Italy 60% grant to M.S. and a P.O.P. 1998, Italy grant to S.A. ICI 182,780 used in this project was generously provided by Dr. A. Wakeling (ZENECA, Macclesfield, UK).

REFERENCES

ARAKI, E., HAAG, B.L., MATSUDA, K., SHICHIRI, M. and KAHN, C.R., Characterization and regulation of the mouse insulin receptor substrate gene promoter. *Mol. Endocrinol.*, **9**, 1367–1379 (1995).

CHANDER, S.K., SAHOTA, S.S., EVANS, T.R.J. and LUQMANI, Y.A., The biological evaluation of novel antiestrogens for the treatment of breast cancer. *Crit. Rev. Oncol. Hematol.*, **15**, 243–269 (1993).

DE CUPIS, A. and FAVONI, R.E., Oestrogen/growth factor cross-talk in breast carcinoma: a specific target for novel antiestrogens. *Trends Pharmacol. Sci.*, **18**, 245–251 (1997).

DE CUPIS, A., NOONAN, D., PIRANI, P., FERRERA, A., CLERICO, L. and FAVONI, R.E., Comparison between novel steroid-like and conventional nonsteroidal antioestrogens in inhibiting oestradiol- and IGF-I-induced proliferation of human breast cancer-derived cells. *Brit. J. Pharmacol.*, **116**, 2391–2400 (1995).

FREISS, G., PUECH, C. and VIGNON, F., Extinction of insulin-like growth factor-I mitogenic signaling by antiestrogen-stimulated FAS-associated protein tyrosine phosphatase-1 in human breast cancer cells. *Mol. Endocrinol.*, **12**, 568–579 (1998).

GUVAKOVA, M.A. and SURMACZ, E., Tamoxifen interferes with the insulin-like growth factor I receptor (IGF-IR) signaling pathway in breast cancer cells. *Cancer Res.*, **57**, 2606–2610 (1997).

HANKINSON, S., WILLET, W.C., COLDITZ, G., HUNTER, D.J., MICHAUD, D.S., DEROO, B., ROSNER, B., SPEIZER, F. and POLLAK, M., Circulating concentrations of insulin-like growth factor I and risk of breast cancer. *Lancet*, **351**, 1393–1396 (1998).

LARSEN, S.S., MADSEN, M.W., JENSEN, B.L. and LYKKESFELDT, A.E., Resistance of human breast cancer cells to the pure steroidal antiestrogen ICI 182,780 is not associated with a general loss of estrogen-receptor expression or lack of estrogen responsiveness. *Int. J. Cancer*, **72**, 1129–1136 (1997).

MATSUDA, K., ARAKI, E., YOSHIMURA, R., TSURUZOE, K., FURUKAWA, N., KANEKO, K., MOTOSHIMA, H., YOSHIZATO, K., KISHIKAWA, K. and SHICHIRI, M., Cell-specific regulation of IRS-1 gene expression: role of E box and

C/EBP binding site in HepG2 cells and CHO cells. *Diabetes*, **46**, 354–362 (1997).

NICHOLSON, R.I., GEE, J.M., BRYANT, S., FRANCIS, A.B., MCCLELLAND, R.A., KNOWLDEN, J., WAKELING, A.E. and OSBORNE, C.K., Pure antiestrogens. The most important advance in the endocrine therapy of breast cancer since 1896. *Ann. N.Y. Acad. Sci.*, **784**, 325–335 (1996).

NICHOLSON, R.I., GEE, J.M., MANNING, D.L., WAKELING, A.E., MONTANO, M.M. and KATZENELLENBOGEN, B.S., Responses to pure antiestrogens (ICI 164,384, ICI 182,780) in estrogen-sensitive and -resistant experimental and clinical breast cancer. *Ann. N.Y. Acad. Sci.*, **761**, 148–163 (1995).

NISHIYAMA, M. and WANDS, J.R., Cloning and increased expression of an insulin receptor substrate 1-like gene in human hepatocellular carcinoma. *Biochem. biophys. Res. Comm.*, **183**, 280–285 (1992).

OSBORNE, C.K., CORONADO-HEINSOHN, E.B., HILSENBECK, S.G., MCCUE, B.L., WAKELING, A.E., MCCLELLAND, R.A., MANNING, D.L. and NICHOLSON, R.I., Comparison of the effects of a pure antiestrogen with those of tamoxifen in a model of human breast cancer. *J. nat. Cancer Inst.*, **87**, 746–750 (1995).

PAVLIK, E.J., NELSON, K., SRINIVVASAN, S., DEPRIEST, P.D. and KENADY, D.E., Antiestrogen resistance in human breast cancer. *In* E.J. Pavlik (ed.), *Estrogens, progestins, and their antagonists*, Vol. **1**, pp. 116–159, Birkhauser, Boston (1996).

RESNIK, J.L., REICHART, D.B., HUEY, K., WEBSTER, N.J.G. and SEELY, B.L., Elevated insulin-like growth factor I receptor autophosphorylation and kinase activity in human breast cancer. *Cancer Res.*, **58**, 1159–1164 (1998).

ROCHA, R.L., HILSENBECK, S.G., JACKSON, J.G. and YEE, D., Insulin-like growth factor binding protein-3 (IGFBP3) and insulin receptor substrate (IRS1) in primary breast cancer: correlation with clinical parameters and disease-free survival. *Clin. Cancer Res.*, **3**, 103–109 (1997).

SURMACZ, E. and BURGAUD, J.-L., Overexpression of insulin receptor substrate 1 (IRS-1) in the human breast cancer cell line MCF-7 induces loss of estrogen requirements for growth and transformation. *Clin. Cancer Res.*, **1**, 1429–1436 (1995).

SURMACZ, E., GUVAKOVA, M.A., NOLAN, M.K., NICOSIA, R. and SCIACCA, L., Type I insulin-like growth factor receptor function in breast cancer. *Breast Cancer Res. Treat.*, **47**, 255–267 (1998).

TURNER, B.C., HAFFTY, B.G., NAYARANNAN, L., YUAN, J., HAVRE, P.A., GUMBS, A., KAPLAN, L., BURGAUD, J.-L., CARTER, D., BASERGA, R. and GLAZER, P., IGF-IR and cyclin D1 expression influence cellular radiosensitivity and local breast cancer recurrence after lumpectomy and radiation. *Cancer Res.*, **57**, 3079–3083 (1997).

WAKELING, A.E., DUKES, M. and BOWLER, J., A potent specific pure antiestrogen with clinical potential. *Cancer Res.*, **51**, 3867–3873 (1991).

WISEMAN, L.R., JOHNSON, M.D., WAKELING, A.E., LYKKESFELDT, A.E., MAY, F.E. and WESTLEY, B.R., Type I IGF receptor and acquired tamoxifen resistance in oestrogen-responsive human breast cancer. *Europ. J. Cancer*, **29A**, 2256–2264 (1993).